The Anatomical Record
Advances in Integrative Anatomy and Evolutionary Biology

WILEY

Deconstructing the Gestalt: New concepts and tests of homology, as exemplified by a re-conceptualization of "microstomy" in squamates

Catherine R. C. Strong[1] | Mark D. Scherz[2] | Michael W. Caldwell[1,3]

[1]Department of Biological Sciences, University of Alberta, Edmonton, Alberta, Canada

[2]Institute for Biochemistry and Biology, University of Potsdam, Potsdam, Germany

[3]Department of Earth and Atmospheric Sciences, University of Alberta, Edmonton, Alberta, Canada

Correspondence
Catherine R. C. Strong, Department of Biological Sciences, University of Alberta, CW-405 Biological Sciences Building, Edmonton, Alberta T6G 2E9, Canada.
Email: crstrong@ualberta.ca

Abstract

Snakes—a subset of lizards—have traditionally been divided into two major groups based on feeding mechanics: "macrostomy," involving the ingestion of proportionally large prey items; and "microstomy," the lack of this ability. "Microstomy"—considered present in scolecophidian and early-diverging alethinophidian snakes—is generally viewed as a symplesiomorphy shared with non-snake lizards. However, this perspective of "microstomy" as plesiomorphic and morphologically homogenous fails to recognize the complexity of this condition and its evolution across "microstomatan" squamates. To challenge this problematic paradigm, we formalize a new framework for conceptualizing and testing the homology of overall character complexes, or "morphotypes," which underlies our re-assessment of "microstomy." Using micro-computed tomography (micro-CT) scans, we analyze the morphology of the jaws and suspensorium across purported "microstomatan" squamates (scolecophidians, early-diverging alethinophidians, and non-snake lizards) and demonstrate that key components of the jaw complex are not homologous at the level of primary character state identity across these taxa. Therefore, rather than treating "microstomy" as a uniform condition, we instead propose that non-snake lizards, early-diverging alethinophidians, anomalepidids, leptotyphlopids, and typhlopoids each exhibit a unique and nonhomologous jaw morphotype: "minimal-kinesis microstomy," "snout-shifting," "axle-brace maxillary raking," "mandibular raking," and "single-axle maxillary raking," respectively. The lack of synapomorphy among scolecophidians is inconsistent with the notion of scolecophidians representing an ancestral snake condition, and instead reflects a hypothesis of the independent evolution of fossoriality, miniaturization, and "microstomy" in each scolecophidian lineage. We ultimately emphasize that a rigorous approach to comparative anatomy is necessary in constructing evolutionary hypotheses that accurately reflect biological reality.

KEYWORDS
ancestral state reconstruction, functional morphology, homology, skull anatomy, snake evolution

wileyonlinelibrary.com/journal/ar **1**

1 | INTRODUCTION

Scolecophidians ("blindsnakes") are a distinctive group of snakes, comprised of three major lineages: Anomalepididae, Leptotyphlopidae, and Typhlopoidea, the latter of which is further subdivided into three families, Typhlopidae, Gerrhopilidae, and Xenotyphlopidae (Figures 1 and 2). However, due in part to their small size and reclusive life habits, many aspects of scolecophidian anatomy and evolution remain understudied (Kley, 2006; Kley & Brainerd, 1999). As scolecophidians have traditionally played a key role in our understanding of the origin of snakes (e.g., Bellairs & Underwood, 1951; Miralles et al., 2018; Rieppel, 2012), it is of critical importance that these knowledge gaps continue to shrink; central among these, and the focus of this study, is the role of scolecophidians in informing our understanding of the evolution of feeding mechanisms in squamates.

Most extant snakes—including booids, pythonoids, and caenophidians (Figures 1 and 2)—exhibit macrostomy, the ability to consume prey items with a disproportionately large cross-sectional area (Rieppel, 1988, 2012; Scanferla, 2016). Other squamates—including non-snake lizards, as well as "anilioid" (uropeltoid and amerophidian) and scolecophidian snakes—lack this ability, and have thus been termed "microstomatan" (Miralles et al., 2018; Rieppel, 1988). The presence of microstomy in non-snake lizards and several phylogenetically basal snake lineages has traditionally led to the conclusion that the microstomatan condition in "anilioids" and scolecophidians is a plesiomorphic retention of the ancestral snake condition (e.g., Bellairs & Underwood, 1951; Rieppel, 2012). This hypothesis ties into a broader perspective in which scolecophidians are considered a largely "primitive" lineage, retaining several features not just of the ancestor of snakes, but of nonsnake lizards more broadly (e.g., List, 1966).

However, several authors have cautioned that, because the scolecophidian skull is highly autapomorphic, it is therefore largely uninformative regarding the ancestral snake anatomy (e.g., Caldwell, 2019; Chretien, Wang-Claypool, Glaw, & Scherz, 2019; Hsiang et al., 2015; Kley, 2001; Kley & Brainerd, 1999). In particular, the combined influences of fossoriality, miniaturization, and heterochrony (evolutionary changes in the rate or timing of developmental events; McNamara, 1986) have greatly affected the evolution of the scolecophidian skull (Chretien et al., 2019; Harrington & Reeder, 2017; Kley, 2006; Palci et al., 2016; Strong, Palci, & Caldwell, 2021).

Despite these cautions, though, recent analyses have continued to treat scolecophidian microstomy as a plesiomorphic retention of the nonophidian squamate condition, particularly via ancestral state reconstructions (ASRs) which codify "microstomy" as a single, morphologically homogenous condition (e.g., Harrington & Reeder, 2017; Miralles et al., 2018). This perspective on scolecophidian anatomy has therefore been central in formulating higher-order hypotheses of snake phylogeny and origins, including reconstructions of the ancestral morphology and ecology of snakes (e.g., Harrington & Reeder, 2017; Miralles et al., 2018). In order to fully evaluate such hypotheses, a close analysis of the validity of this characterization of scolecophidian jaw anatomy is essential.

A re-assessment of this anatomy is also important in evaluating the phylogenetic relationships among scolecophidians. Although morphology-based phylogenies generally recover scolecophidians as monophyletic (e.g., Garberoglio et al., 2019; Gauthier, Kearney, Maisano, Rieppel, & Behlke, 2012; Hsiang et al., 2015), molecular-based phylogenies tend to recover this group as paraphyletic (e.g., Burbrink et al., 2020; Figueroa, McKelvy, Grismer, Bell, & Lailvaux, 2016; Miralles et al., 2018; Pyron, Burbrink, & Wiens, 2013; Zheng & Wiens, 2016). Recent authors have further suggested that, based on the highly autapomorphic nature of scolecophidians relative not only to other squamates but also relative to each other, scolecophidians may even represent completely convergent lineages (Caldwell, 2019; Chretien et al., 2019; Harrington & Reeder, 2017), rendering this group potentially polyphyletic (Caldwell, 2019). This phylogenetic hypothesis derives largely from the unique jaw structure exhibited by each major scolecophidian clade, as well as a recognition of the role of fossoriality and miniaturization in giving rise to convergent morphotypes (Caldwell, 2019; Chretien et al., 2019; Harrington & Reeder, 2017). Although this hypothesis has only recently been advocated, it presents an intriguing possibility warranting further analysis.

In light of these questions surrounding scolecophidian evolution—primarily regarding whether the scolecophidian jaw anatomy is plesiomorphic and whether "microstomy" is morphologically homogenous among "microstomatan" taxa—we herein present an assessment of the jaws and suspensorium of scolecophidians in comparison to other snakes and to nonophidian squamates (Figure 1). We address three major questions related to the scolecophidian jaw complex. First, can this morphofunctional system be considered homologous among the three main scolecophidian clades? Second, is this jaw structure homologous to the condition in nonophidian squamates? And ultimately, how do the answers to these questions affect higher-level evolutionary hypotheses, such as phylogenetic analyses or ASRs?
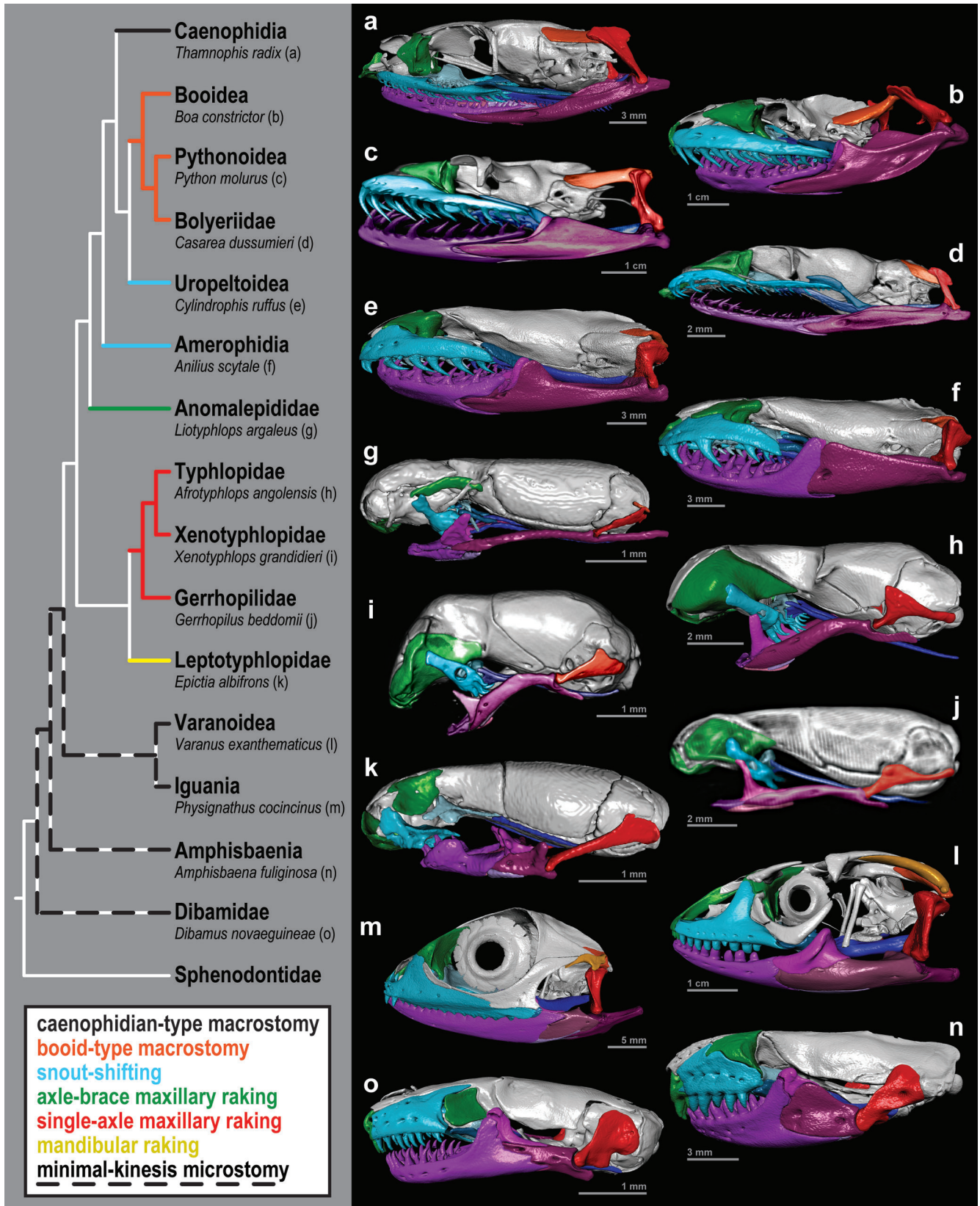
FIGURE 1 Overview of jaw evolution in squamates. Coloured branches reflect the proposed jaw morphotype for each major squamate clade (see legend, Figures 12–14, and main text). Relevant skull elements are highlighted in an exemplar specimen from each group (colouration as in Figures 3–11). See Table 2 for specimen numbers. MCZ scan data used by permission of the Museum of Comparative Zoology, Harvard University
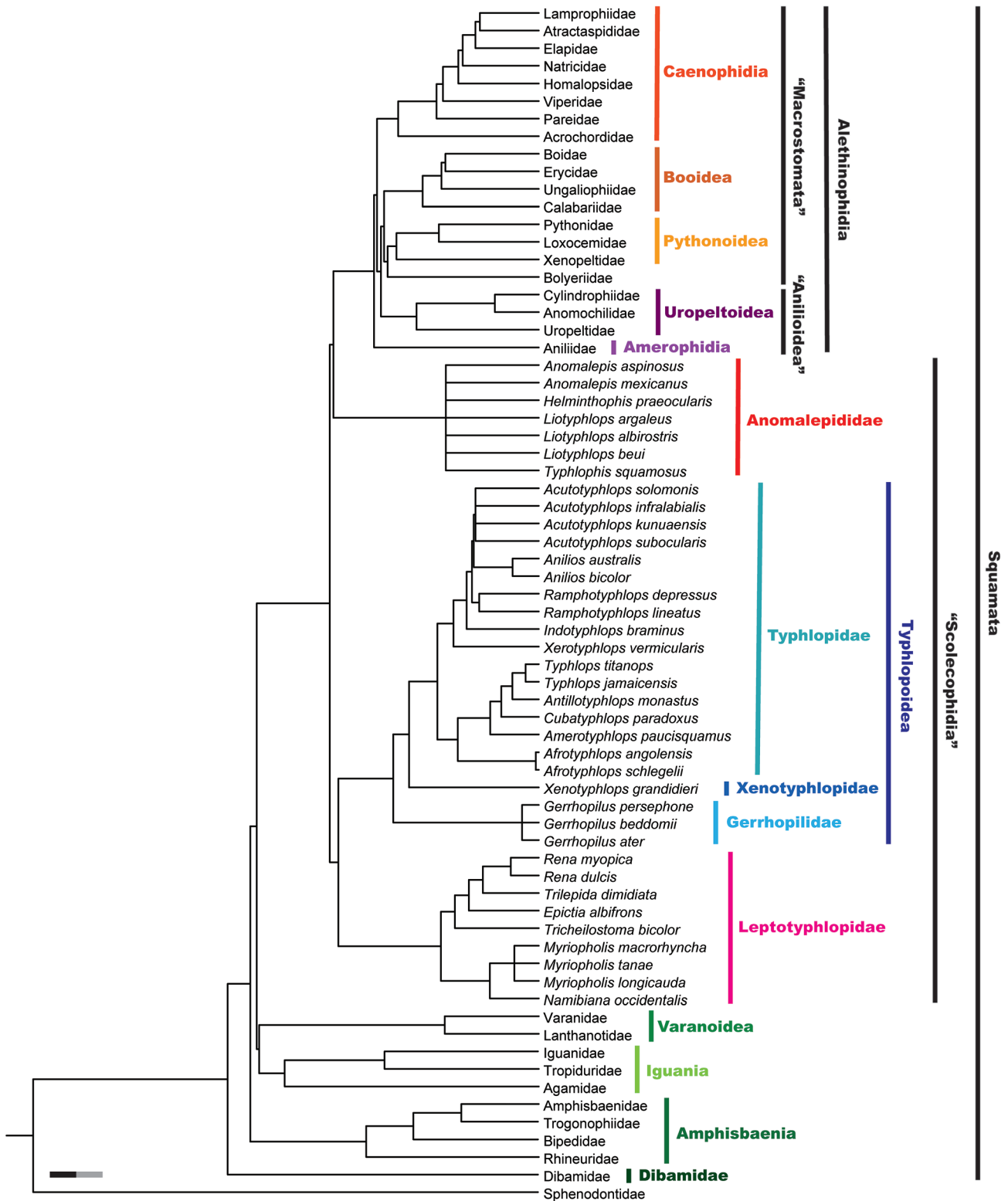
FIGURE 2 Phylogenetic context of taxa examined herein. Relationships are provided at the species level for scolecophidians and at the family level for other taxa. Relevant higher taxa are indicated in colour, with broader groups labelled in black. Branch lengths represent divergence time, with the scale bar measuring 30 million years. See Section 2 for phylogeny construction, including relevant literature sources

To examine these questions, we begin with comparative descriptions reviewing the jaw structures of various squamates. We then discuss the homology of these conditions and implications for the scolecophidian phylogeny. Finally, we use ASRs to illustrate the impact that different homology concepts can have on hypotheses of squamate evolution.

On a taxonomic note, all references to scolecophidians throughout this study employ the classical definition of this group—that is, comprising all major lineages, as outlined above (Figure 2)—rather than the restricted, clade-based definition of "Scolecophidia *sensu stricto*" as employed by some other authors (e.g., Miralles et al., 2018). References to "anilioids" similarly evoke the classical definition of this group as an informal grade of basally-diverging alethinophidians, with the recognition that this group is likely polyphyletic (e.g., Burbrink et al., 2020) and composed of at least two distinct lineages: Amerophidia (Aniliidae and Tropidophiidae) and Uropeltoidea (Cylindrophiidae, Uropeltidae, and Anomochilidae; Figures 1 and 2; taxonomy from Burbrink et al., 2020).

2 | MATERIALS AND METHODS

2.1 | Institutional abbreviations

Institutional abbreviations of specimens examined in this study are provided in Table 1.

2.2 | Comparative specimens

Various micro-computed tomography (micro-CT) scans of squamate skulls were observed for this study, as listed in Table 2. For consistency, nomenclature follows the Reptile Database (http://reptile-database.reptarium.cz/) as of October 2020. Among non-snake lizards, our sampling strategy focused on phylogenetic breadth rather than completeness, with an emphasis on taxa typically recovered or hypothesized as closely related to snakes. Among snakes, our sampling strategy focused on "microstomatan" taxa, including several representatives of each major "microstomatan" group.

MCZ scans were conducted by C. R. C. S (see Section 2.3) and will be made available on MorphoSource.org. Information regarding *Xenotyphlops grandidieri*, *Gerrhopilus persephone*, and *Cenaspis aenigma* was derived from the figures and supporting information of Chretien et al. (2019), Kraus (2017), and Campbell, Smith, and Hall (2018), respectively. Information regarding the sources of the other scans is provided in the Acknowledgments.

2.3 | Scanning protocols and visualization

All MCZ specimens observed herein were scanned using a Nikon Metrology X-Tek HMXST225 micro-CT scanner at the Harvard University Center for Nanoscale Systems. Exact scanning parameters varied among specimens, though generally employed the

TABLE 1 Institutional abbreviations of specimens examined in this study

Abbreviation	Institution	Location
AMS	Australian Museum	Sydney, Australia
CAS	California Academy of Sciences	San Francisco, USA
FMNH	Field Museum of Natural History	Chicago, USA
FRIM	Forest Research Institute Malaysia	Kuala Lumpur, Malaysia
KUH	University of Kansas Biodiversity Institute and Natural History Museum	Lawrence, USA
MCZ	Museum of Comparative Zoology, Harvard University	Cambridge, USA
QM	Queensland Museum	South Brisbane, Australia
SAMA	South Australian Museum	Adelaide, Australia
TCWC	Biodiversity Research and Teaching Collections, Texas A&M University	College Station, USA
TNHC	Texas Natural History Collections, Texas Memorial Museum of Science and History, University of Texas at Austin	Austin, USA
TMM	Texas Memorial Museum of Science and History, University of Texas at Austin	Austin, USA
UAMZ	University of Alberta Museum of Zoology	Edmonton, Canada
UF	Florida Museum of Natural History, University of Florida	Gainesville, USA
UMMZ	University of Michigan Museum of Zoology	Ann Arbor, USA
UTA	University of Texas at Arlington	Arlington, USA
YPM	Yale Peabody Museum	New Haven, USA
ZSM	Zoologische Staatssammlung München	Munich, Germany

TABLE 2 List of specimens observed for this study

Higher taxon			Species	Specimen number
Alethinophidia	"Anilioidea"	Amerophidia	_Anilius scytale_	USNM 204078 KUH 125976
		Uropeltoidea	_Anomochilus leonardi_	FRIM 0026
			Cylindrophis ruffus	UMMZ 201901 FMNH 60958
			Uropeltis melanogaster	FMNH 167048
			Uropeltis woodmasoni	TMM M-10006
	Bolyeriidae		_Casarea dussumieri_	UMMZ 190285
	Booidea	Boidae	_Boa constrictor_	FMNH 31182
		Calabariidae	_Calabaria reinhardtii_	FMNH 117833
		Erycidae	_Eryx colubrinus_	FMNH 63117
		Ungaliophiidae	_Ungaliophis continentalis_	UTA 50569
	Caenophidia	Acrochordidae	_Acrochordus arafurae_	QM J11033
			Acrochordus granulatus	MCZ R-146128
		Atractaspididae	_Atractaspis irregularis_	FMNH 62204
		Elapidae	_Naja naja_	FMNH 22468
		Homalopsidae	_Homalopsis buccata_	FMNH 259340
		Lamprophiidae	_Boaedon fuliginosus_	FMNH 62248
			Lycophidion capense	FMNH 58322
		Natricidae	_Afronatrix anoscopus_	FMNH 179335
			Natrix natrix	FMNH 30522
			Thamnophis radix	UAMZ R636
		Pareidae	_Pareas hamptoni_	FMNH 128304
		Viperidae	_Bothrops asper_	FMNH 31162
	Pythonoidea	Loxocemidae	_Loxocemus bicolor_	FMNH 104800
		Pythonidae	_Python molurus_	TNHC 62769
			Python regius	UAMZ R381
		Xenopeltidae	_Xenopeltis unicolor_	FMNH 148900
"Scolecophidia"	Anomalepididae		_Anomalepis aspinosus_	MCZ R-14782
			Anomalepis mexicanus	MCZ R-191201
			Helminthophis praeocularis	MCZ R-17960
			Liotyphlops albirostris	FMNH 216257
			Liotyphlops argaleus	MCZ R-67933
			Liotyphlops beui	SAMA 40142
			Typhlophis squamosus	MCZ R-145403
	Leptotyphlopidae		_Epictia albifrons_	MCZ R-2885
			Myriopholis longicauda	MCZ R-184447
			Myriopholis macrorhyncha	MCZ R-9650
			Myriopholis tanae	MCZ R-40099
			Namibiana occidentalis	MCZ R-193094
			Rena dulcis	TNHC 60638 UAMZ R335
			Rena myopica	MCZ R-45563
			Tricheilostoma bicolor	MCZ R-49718
			Trilepida dimidiata	SAMA 40143

TABLE 2 (Continued)

Higher taxon			Species	Specimen number
	Typhlopoidea	Gerrhopilidae	*Gerrhopilus ater*	MCZ R-33505
			Gerrhopilus beddomii	MCZ R-22372
			Gerrhopilus persephone	UMMZ 242536
		Typhlopidae	*Acutotyphlops infralabialis*	AMS R.77116
			Acutotyphlops kunuaensis	AMS R.12305
			Acutotyphlops solomonis	AMS R.11452
			Acutotyphlops subocularis	SAMA R64770
			Afrotyphlops angolensis	MCZ R-170385
			Afrotyphlops schlegelii	MCZ R-190405
			Amerotyphlops paucisquamus	MCZ R-147336
			Anilios australis	SAMA R26901
			Anilios bicolor	SAMA 60626 SAMA 62252
			Antillotyphlops monastus	MCZ R-81112
			Cubatyphlops paradoxus	MCZ R-92993
			Indotyphlops braminus	UAMZ R363
			Ramphotyphlops depressus	AMS R.129537
			Ramphotyphlops lineatus	MCZ R-37751
			Typhlops jamaicensis	USNM 12378
			Typhlops titanops	MCZ R-68571
			Xerotyphlops vermicularis	MCZ R-56477
		Xenotyphlopidae	*Xenotyphlops grandidieri*	ZSM 2194/2007 ZSM 2213/2007 ZSM 2216/2007
"Non-snake lizards"	Amphisbaenia	Amphisbaenidae	*Amphisbaena alba*	FMNH 195924
			Amphisbaena fuliginosa	FMNH 22847
		Bipedidae	*Bipes biporus*	CAS 126478
			Bipes canaliculatus	CAS 134753
		Rhineuridae	*Rhineura floridana*	FMNH 31774
		Trogonophiidae	*Agamodon anguliceps*	FMNH 264702
			Trogonophis wiegmanni	FMNH 109462
	Dibamidae		*Anelytropsis papillosus*	TCWC 45501
			Dibamus leucurus	UMMZ 174763
			Dibamus novaeguineae	UF 33488 CAS 26937
	Iguania	Agamidae	*Physignathus cocincinus*	YPM 14378
		Iguanidae	*Dipsosaurus dorsalis*	YPM 14376
			Sauromalus ater	TNHC 18483
		Tropiduridae	*Uranoscodon superciliosus*	YPM 12871
	Varanoidea	Lanthanotidae	*Lanthanotus borneensis*	FMNH 148589 YPM 6057
		Varanidae	*Varanus exanthematicus*	FMNH 58299

Note: See Table 1 for institutional abbreviations.

following settings: detector dimensions, 2,000 × 2,000 pixels; projections, 3,142; maximum voltage, 65–80 kV; maximum current output, 116–130 μA. A 0.5 mm aluminum filter was used for MCZ R-33505, R-2885, R-14782, R-92993, R-68571, and R-40099. Exact settings for all specimens are available upon request. Slices were reconstructed using the bundled vendor software CT Pro 3D and exported as VGL files, which were loaded in VG Studio Max and exported as TIFF files.

Brightness and contrast for all scans were adjusted in ImageJ. All scans were visualized in Dragonfly 4.0 (Object Research Systems, 2019), with the Threshold tool used to digitally remove soft tissues and the Manual Segmentation tool used to digitally isolate each skull element for key taxa (Figures 3–11).

2.4 | Phylogeny construction

The phylogeny used for the ASRs was constructed using a "super-tree" approach, that is, compiling dated finer-scale phylogenies into a higher-level phylogenetic framework. Other ASRs have used a similar approach in assessing a variety of other animal groups (e.g., Asplen, Whitfield, de Boer, & Heimpel, 2009; Finarelli & Flynn, 2006).

Relationships among families and higher clades are based on Burbrink et al. (2020), with the placement of Rhineuridae and Lanthanotidae derived from Pyron et al. (2013). Species-level phylogenetic relationships are derived from Burbrink et al. (2020) for Anomalepididae, Amphisbaenia, and Iguania, from
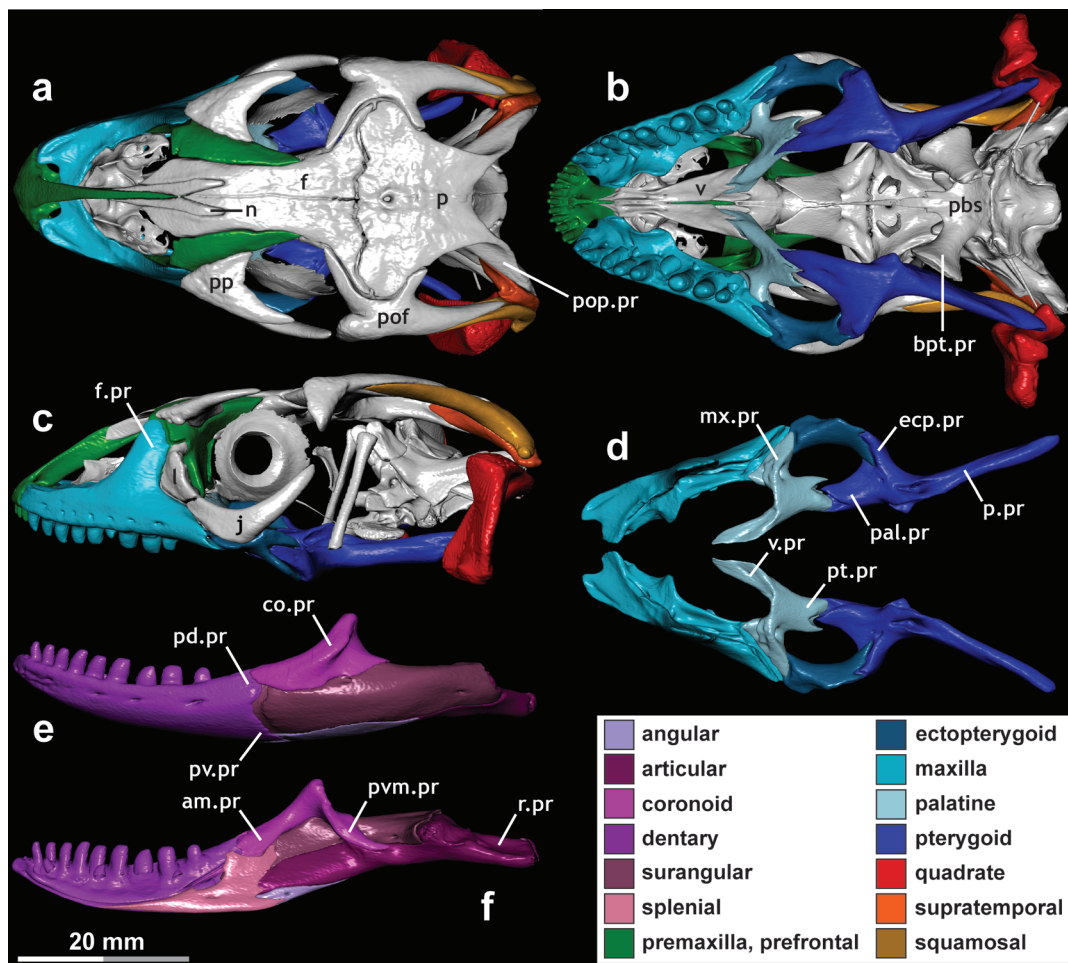

FIGURE 3 Skull of _Varanus exanthematicus_ (FMNH 58299), exemplifying "minimal-kinesis microstomy." Key elements related to feeding are highlighted. In this morphotype, these elements are robust and solidly braced (see text for details). (a–c) Skull, with mandibles digitally removed, in (a) dorsal, (b) ventral, and (c) lateral view. (d) Palatomaxillary arch in dorsal view. (e,f) Mandible in (e) lateral and (f) medial view. am.pr, anteromedial process; bpt.pr, basipterygoid process; co.pr, coronoid process; ecp.pr, ectopterygoid process; f, frontal; f.pr, facial process; j, jugal; l, lacrimal; mx.pr, maxillary process; n, nasal; p, parietal; pal.pr, palatine process; pbs, parabasisphenoid; pd.pr, posterodorsal process; pof, postorbitofrontal; pop.pr, postparietal process; pp, palpebral; p.pr, posterior process; pt.pr, pterygoid process; pvm.pr, posteroventromedial process; pv.pr, posteroventral process; r.pr, retroarticular process; v, vomer; v.pr, vomerine process
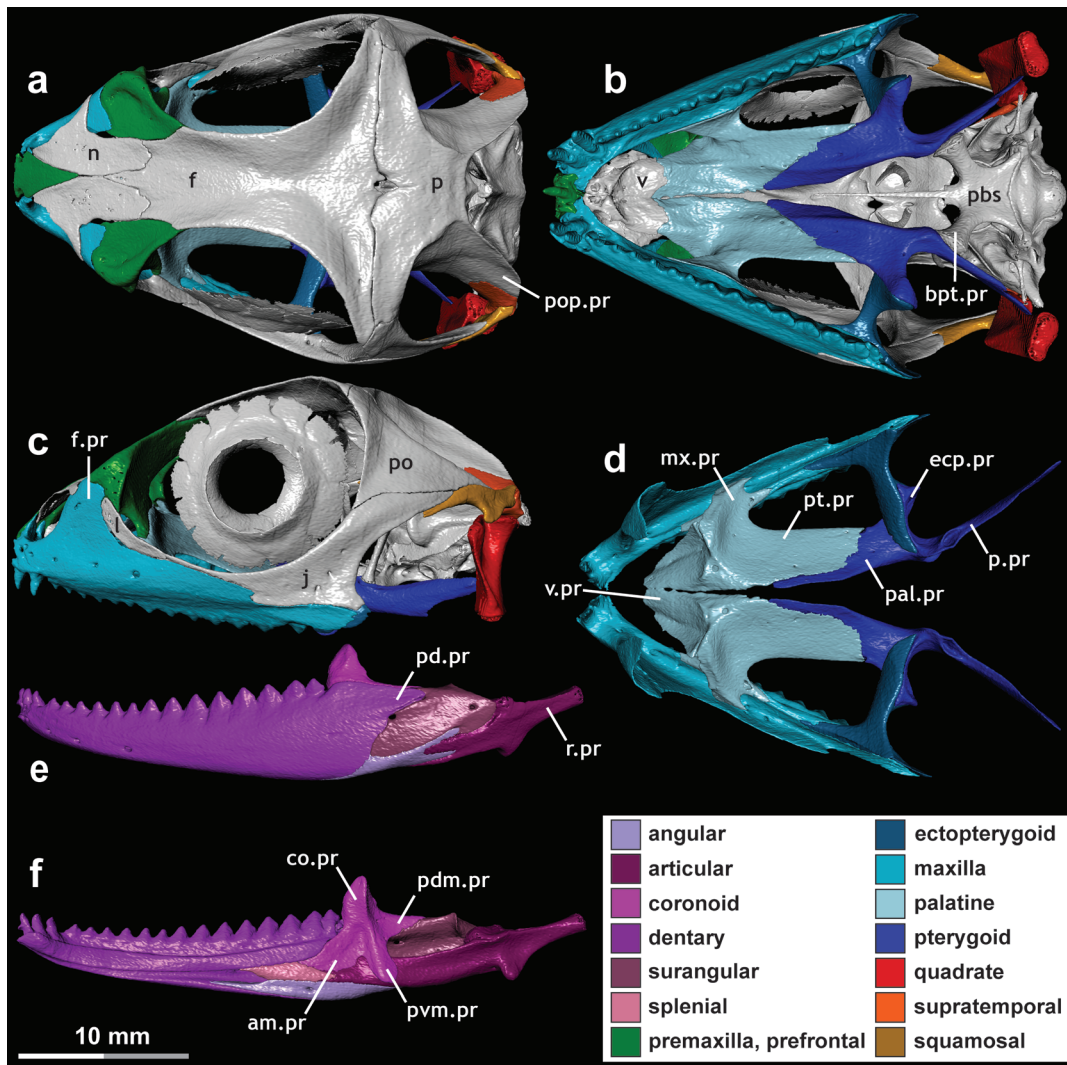
FIGURE 4 Skull of *Physignathus cocincinus* (YPM 14378), exemplifying "minimal-kinesis microstomy." Key elements related to feeding are highlighted. In this morphotype, these elements are robust and solidly braced (see text for details). (a–c) Skull, with mandibles digitally removed, in (a) dorsal, (b) ventral, and (c) lateral view. (d) Palatomaxillary arch in dorsal view. (e,f) Mandible in (e) lateral and (f) medial view. am.pr, anteromedial process; bpt.pr, basipterygoid process; co.pr, coronoid process; ecp.pr, ectopterygoid process; f, frontal; f.pr, facial process; j, jugal; l, lacrimal; mx.pr, maxillary process; n, nasal; p, parietal; pal.pr, palatine process; pbs, parabasisphenoid; pdm.pr, posterodorsomedial process; pd.pr, posterodorsal process; po, postorbital; pop.pr, postparietal process; p.pr, posterior process; pt.pr, pterygoid process; pvm.pr, posteroventromedial process; r.pr, retroarticular process; v, vomer; v.pr, vomerine process

Pyron et al. (2013) for Dibamidae and Leptotyphlopidae, and from Nagy et al. (2015) for Typhlopoidea. *Dibamus leucurus* was placed based on Greer (1985) and Pyron et al. (2013), *Agamodon anguliceps* was placed based on Kearney and Stuart (2004), *Amphisbaena alba* and *Typhlops titanops* were placed based Pyron et al. (2013), *Trilepida dimidiata* and *Rena myopica* were placed based on the location of congeneric taxa in Pyron et al. (2013), and *Amerotyphlops*, *Cubatyphlops*, and *Gerrhopilus* were placed based on the location of congeneric taxa in Nagy et al. (2015). Certain taxa (*Acutotyphlops infralabialis*, *A. solomonis*, *Anomalepis aspinosus*, *A. mexicanus*,

Helminthophis praeocularis, *Liotyphlops argaleus*, *Myriopholis tanae*, and *M. macrorhyncha*) have not been included in any prior phylogenies based on actual character data to our knowledge, so were placed in the most exclusive clade possible based on taxonomy.

Branch lengths, representing time, are derived mainly from Burbrink et al. (2020). Key nodes within Typhlopoidea were also dated using Miralles et al. (2018), and nodes involving *Lanthanotus* and *Rhineura* were dated using Simões et al. (2018). For some branches, dated phylogenies incorporating the relevant taxa were not available (often because genetic data are not available
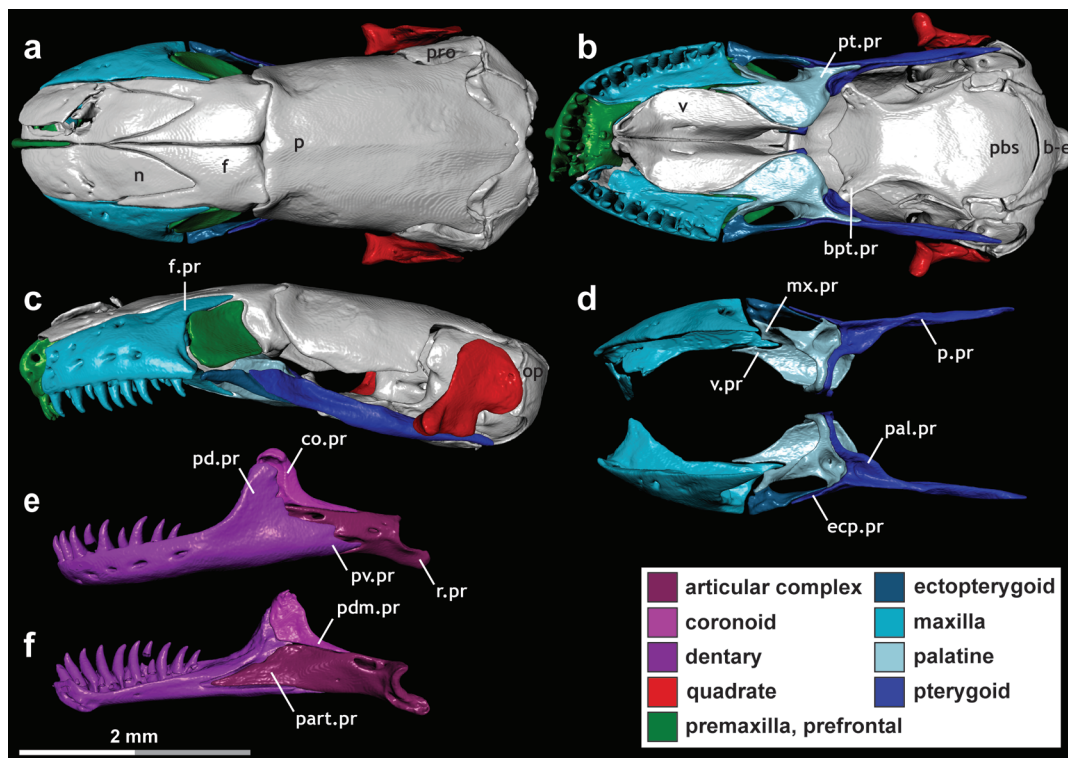
FIGURE 5 Skull of *Dibamus novaeguineae* (UF 33488), exemplifying "minimal-kinesis microstomy" in a miniaturized and fossorial non-snake lizard. Key elements related to feeding are highlighted. In this morphotype, these elements are robust and solidly braced (see text for details). (a–c) Skull, with mandibles digitally removed, in (a) dorsal, (b) ventral, and (c) lateral view. (d) Palatomaxillary arch in dorsal view. (e,f) Mandible in (e) lateral and (f) medial view. b-e, basioccipital-exoccipital; bpt.pr, basipterygoid process; ch.pr, choanal process; co.pr, coronoid process; ecp.pr, ectopterygoid process; f, frontal; f.pr, facial process; mx.pr, maxillary process; n, nasal; op, opisthotic; p, parietal; pal.pr, palatine process; part.pr, prearticular process; pbs, parabasisphenoid; pdm.pr, posterodorsomedial process; pd.pr, posterodorsal process; p.pr, posterior process; pro, prootic; pt.pr, pterygoid process; pv.pr, posteroventral process; r.pr, retroarticular process; v, vomer; v.pr, vomerine process

for those taxa), so dates for these branches were derived by evenly subdividing the distance between the closest dated nodes.

2.5 | Ancestral state reconstruction

ASRs of squamate feeding mechanisms were performed in Mesquite v. 3.61 (Maddison & Maddison, 2019) using both maximum parsimony (MP) and maximum likelihood (ML) algorithms. For the ML reconstructions, traits were mapped using the Markov k-state 1-parameter (Mk1) model, which assumes that forward and reverse changes occur at the same rate (Lewis, 2001; Maddison & Maddison, 2006). Feeding mechanisms were examined via three scoring schemes: "basic," "detailed microstomy," and "detailed microstomy and macrostomy." The more detailed scoring methods aim to reflect morphological variability more accurately within these broad categories, as described herein or as recognized by recent authors (e.g., Chretien et al., 2019; Harrington &

Reeder, 2017; Palci et al., 2016). Feeding mechanisms were scored based on personal observations of the specimens in Table 2. Nodes were considered "definitively reconstructed" when a single state was most parsimonious or when the likelihood of any state was greater than 90%. Nodes were considered "equivocal" when multiple states were equally parsimonious or when none of the states had a likelihood greater than 50%.

The "basic" character scheme scores taxa simply as "macrostomatan" or "microstomatan," reflecting a common though arguably over-simplified approach in the literature (e.g., Harrington & Reeder, 2017; Miralles et al., 2018). The "detailed microstomy" scheme divides microstomy into five morphotypes ("minimal-kinesis," "snout-shifting," "single-axle maxillary raking," "axle-brace maxillary raking," and "mandibular raking") as described below (see Sections 3 and 4); however, macrostomy remains a single state following the traditional perspective that macrostomy is a synapomorphy uniting derived alethinophidians (e.g., Miralles et al., 2018; Rieppel, 1988). The "detailed microstomy and macrostomy"
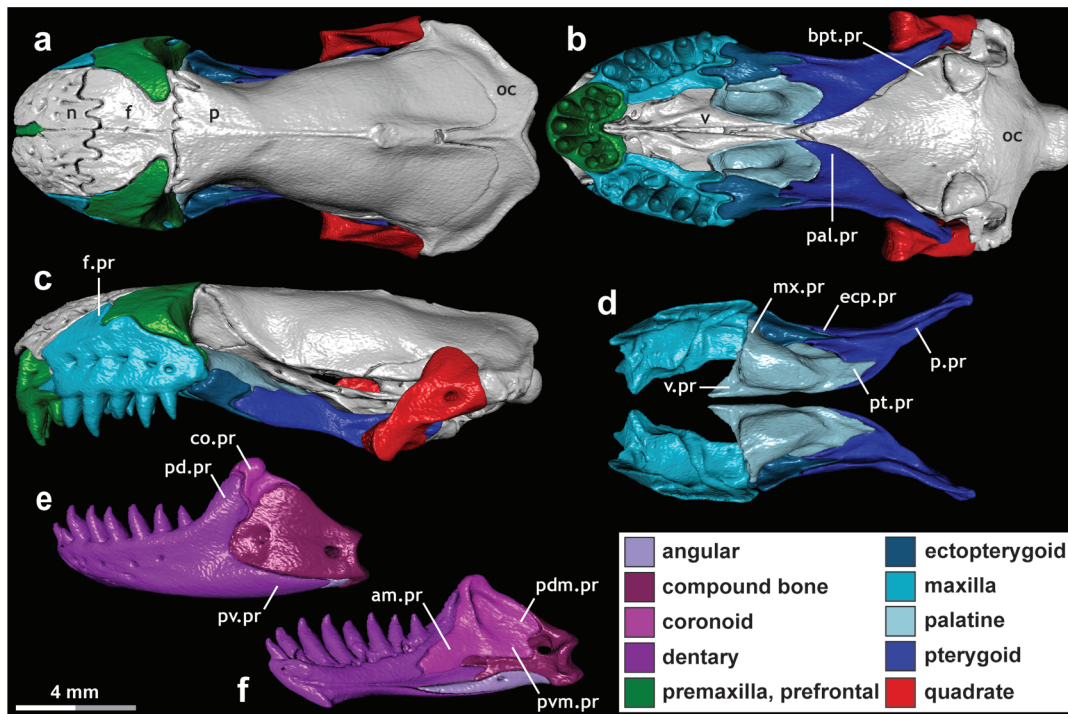
FIGURE 6 Skull of *Amphisbaena fuliginosa* (FMNH 22847), exemplifying "minimal-kinesis microstomy" in a fossorial non-snake lizard. Key elements related to feeding are highlighted. In this morphotype, these elements are robust and solidly braced (see text for details). (a–c) Skull, with mandibles digitally removed, in (a) dorsal, (b) ventral, and (c) lateral view. (d) Palatomaxillary arch in dorsal view. (e–f) Mandible in (e) lateral and (f) medial view. am.pr, anteromedial process; bpt.pr, basipterygoid process; co.pr, coronoid process; ecp.pr, ectopterygoid process; f, frontal; f.pr, facial process; mx.pr, maxillary process; n, nasal; oc, occipital complex; p, parietal; pal.pr, palatine process; pdm.pr, posterodorsomedial process; pd.pr, posterodorsal process; p.pr, posterior process; pt.pr, pterygoid process; pvm.pr, posteroventromedial process; pv.pr, posteroventral process; v, vomer; v.pr, vomerine process

scheme divides microstomy into these same five morphotypes and also divides macrostomy into two morphotypes ("booid-" and "caenophidian-type"). Because the current study is focused on microstomy, and because macrostomy is an equally complex and poorly understood condition, we do not analyze the homology of macrostomatan jaw mechanisms herein; indeed, the homology of these latter mechanisms is a topic more than expansive enough in scope to warrant a detailed treatment of its own. Instead, this latter subdivision is based on recent suggestions from ontogenetic, phylogenetic, and anatomical perspectives that "macrostomy" may have evolved independently in booid-pythonoids and caenophidians (Burbrink et al., 2020; Palci et al., 2016; Strong et al., 2019).

3 | RESULTS

We provide below a brief description of the jaw structures of select squamate taxa (Figures 1 and 3–11). Thorough descriptions of the overall cranial anatomy of these taxa have been provided by several previous authors, and so

we refer the reader throughout to the relevant literature rather than repeating those detailed efforts here. Instead, our descriptions focus on features relevant in comparing the jaw conditions among "microstomatan" squamates. These descriptions are grouped according to functional morphology, reflecting the distinct biomechanical arrangements of the jaws and suspensorium that occur in non-snake lizards, uropeltoids and amerophidians, typhlopoids, anomalepidids, and leptotyphlopids. These distinct versions of microstomy are best reflected by the anatomy and functional morphology of the palatomaxillary arch and suspensorium, though the mandible also exhibits key differences among groups. These biomechanics-based categories are discussed from an evolutionary or homology-based perspective in the Discussion.

3.1 | Non-snake lizards

As discussed by several authors (e.g., Cundall, 1995; Frazzetta, 1962), some degree of cranial kinesis occurs throughout all major lizard clades. However, this kinesis
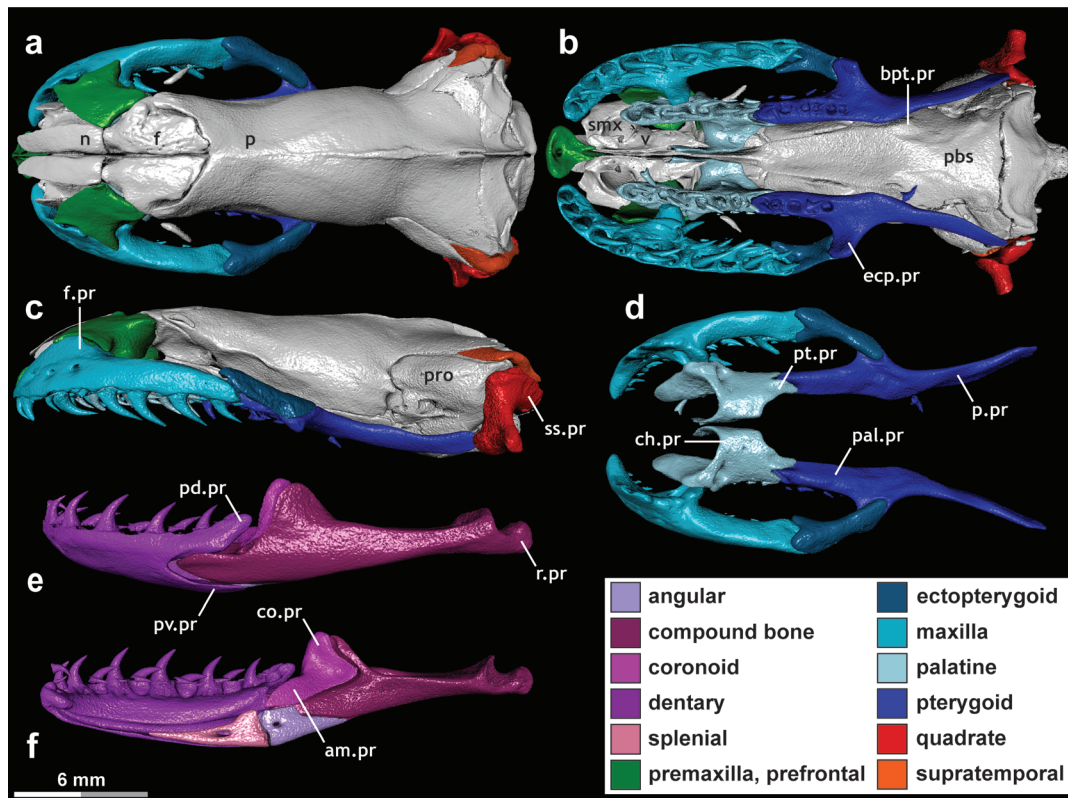
FIGURE 7 Skull of *Cylindrophis ruffus* (UMMZ 201901), exemplifying "snout-shifting" (sensu Cundall, 1995) in a uropeltoid alethinophidian. Key elements related to feeding are highlighted. In this morphotype, these elements are generally robust and well-braced; however, the maxilla-palatine joint exhibits a distinct "ball-and-socket"-like form and the vomers and septomaxillae are more loosely connected to the dorsal snout elements and to their contralaterals, thus enabling a slight degree of unilateral movement of the left and right palatomaxillary arches (see text for details). (a–c) Skull, with mandibles digitally removed, in (a) dorsal, (b) ventral, and (c) lateral view. (d) Palatomaxillary arch in dorsal view. (e,f) Mandible in (e) lateral and (f) medial view. am.pr, anteromedial process; bpt.pr, basipterygoid process; ch.pr, choanal process; co.pr, coronoid process; ecp.pr, ectopterygoid process; f, frontal; f.pr, facial process; n, nasal; p, parietal; pal.pr, palatine process; pbs, parabasisphenoid; pd.pr, posterodorsal process; p.pr, posterior process; pro, prootic; pt.pr, pterygoid process; pv.pr, posteroventral process; r.pr, retroarticular process; smx, septomaxilla; ss.pr, suprastapedial process; v, vomer

is much less pronounced in non-snake lizards than the extensive mobility—especially regarding the jaws and suspensorium—present in snakes (Cundall, 1995). References herein to the non-snake lizard skull as "minimally kinetic" thus reflect this comparison to the snake condition.

3.1.1 | Mandible

The non-snake lizard mandible is long and robust, typically equal in length to the skull (Figures 3 and 4), except in some burrowing forms (e.g., dibamids and amphisbaenians; Figures 5 and 6) in which the mandible is 60–70% of the total skull length. The dentaries are similarly long and robust, bearing multiple teeth and articulating closely with all, or almost all, other mandibular elements (Figures 3e,f, 4e,f, 5e,f, and 6e,f). Notably, the dentaries approach each other very closely at the mental

symphysis, with roughened symphyseal or articular facets for the attachment of connective tissue and cartilage (Kley, 2006). A posteroventral process is typically present on the dentary (Figures 3e, 5e, and 6e), though it is reduced or absent in some taxa (e.g., *Lanthanotus*, some iguanians; Figure 4e).

The splenial varies in size and shape among taxa, from large and plate-like in *Varanus* (Figure 3e,f), to much smaller in iguanians (Figure 4e,f), to absent in amphisbaenians (Figure 6e,f) and absent or fused to the articular complex in dibamids (Figure 5e,f; Evans, 2008). However, despite these differences in morphology, its overall role in the mandible is similar: integrating tightly with all or almost all other mandibular elements to bridge the intramandibular joint.

The coronoid varies in shape among taxa, though it plays a consistent functional role in the overall mandible. In *Varanus* (Figure 3e,f), iguanians (Figure 4e,f), and amphisbaenians (Figure 6e,f), the coronoid sits dorsally
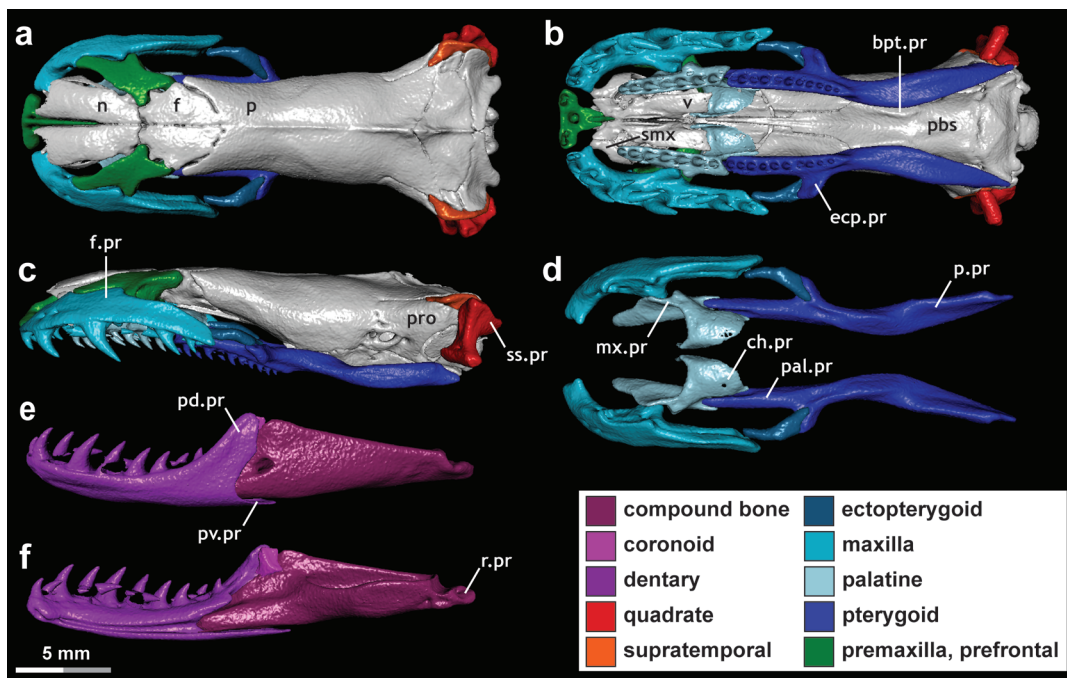
FIGURE 8 Skull of *Anilius scytale* (KUH 125976), exemplifying "snout-shifting" (sensu Cundall, 1995) in an amerophidian alethinophidian. Key elements related to feeding are highlighted. This taxon largely resembles *Cylindrophis*, though the mandibular structure differs somewhat (see Figure 7 and text for details). (a–c) Skull, with mandibles digitally removed, in (a) dorsal, (b) ventral, and (c) lateral view. (d) Palatomaxillary arch in dorsal view. (e,f) Mandible in (e) lateral and (f) medial view. bpt.pr, basipterygoid process; ch.pr, choanal process; ecp.pr, ectopterygoid process; f, frontal; f.pr, facial process; mx.pr, maxillary process; n, nasal; p, parietal; pal.pr, palatine process; pbs, parabasisphenoid; pd.pr, posterodorsal process; p.pr, posterior process; pro, prootic; pv.pr, posteroventral process; r.pr, retroarticular process; smx, septomaxilla; ss.pr, suprastapedial process; v, vomer

or dorsomedially on the mandible, extending well anteriorly and posteriorly to strongly bridge the intramandibular joint. In dibamids, the anteromedial and posteroventromedial processes of the coronoid are highly reduced or absent, though the elongate posterodorsomedial process articulates extensively with the articular complex and the coronoid process articulates closely with the dentary anterolaterally (Figure 5e,f). Therefore, despite differences in morphology among these taxa, the coronoid plays an equivalent functional role in all of them: bracing the anterior and posterior mandibular elements and bridging the intramandibular joint.

The angular is long and thin, running along the ventral or ventromedial mandible (except in dibamids and amphisbaenians; see Section 3.1.4). The angular exhibits extensive mediolateral overlap with the splenial in *Varanus* (Figure 3e,f) and extensive dorsoventral articulation with this element in iguanians (Figure 4e,f). It also articulates with the dentary in all non-snake lizards observed herein, and with the other elements of the posterior mandible (Figures 3–6). Via these articulations, the angular thus effectively bridges the intramandibular joint.

In most non-snake lizards, the articular and prearticular are fused—referred to herein as simply the

articular, following the convention of other authors such as Evans (2008) and Werneburg, Polachowski, and Hutchinson (2015)—but the surangular remains separate. Additional fusion of the posterior mandibular elements occurs in dibamids (Figure 5e,f), amphisbaenians (Figure 6e,f), and some iguanians, and so these taxa are described separately in Section 3.1.4. The surangular articulates tightly with all or most other mandibular elements, including strong articulation with the coronoid dorsally, the angular ventrally or ventrolaterally, and the articular ventrally (Figures 3e,f and 4e,f). Of particular note, it extends anteriorly across the intramandibular joint to articulate anterolaterally with the dentary (Figures 3f and 4f), as well as medially with the splenial in some taxa (e.g., *Varanus*; Figure 3f). The articular also articulates tightly with all other mandibular elements (though see Section 3.1.4 for an exception in *Lanthanotus*), except for the dentary in varanoids and some iguanians. The lower jaw bears a moderate retroarticular process, comprising approximately 25–30% of the total length of the articular (Figures 3e,f and 4e,f). This process is shorter in dibamids (comprising about 10–15% of articular complex length; Figure 5e,f), amphisbaenians (process either essentially absent or
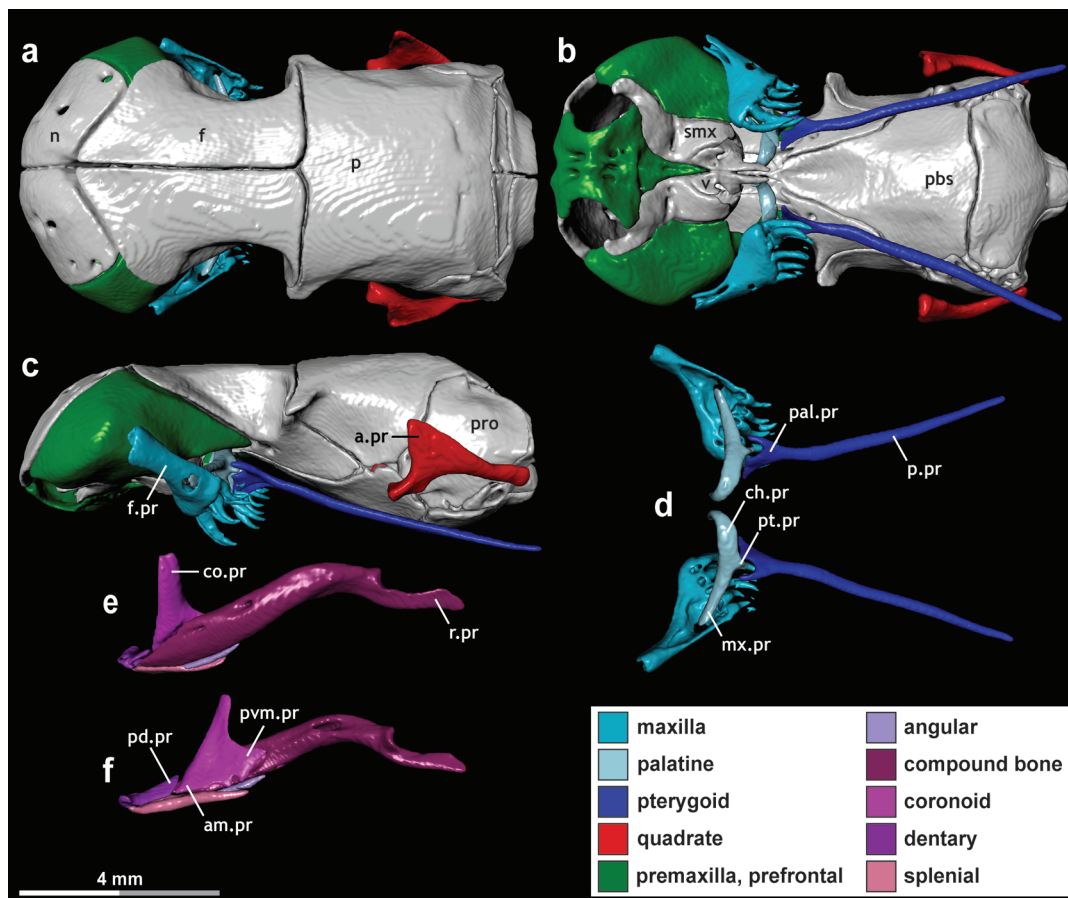
FIGURE 9 Skull of *Afrotyphlops angolensis* (MCZ R-170385), exemplifying "single-axle maxillary raking." Key elements related to feeding are highlighted. In this morphotype of microstomy, the mandible is reduced and largely akinetic, with feeding being driven by rotation of the maxilla about the elongate maxillary process of the palatine (see text for details). (a–c) Skull, with mandibles digitally removed, in (a) dorsal, (b) ventral, and (c) lateral view. (d) Palatomaxillary arch in dorsal view. (e,f) Mandible in (e) lateral and (f) medial view. am.pr, anteromedial process; a.pr, anterior process; ch.pr, choanal process; co.pr, coronoid process; f, frontal; f.pr, facial process; mx.pr, maxillary process; n, nasal; p, parietal; pal.pr, palatine process; pbs, parabasisphenoid; pd.pr, posterodorsal process; p.pr, posterior process; pro, prootic; pt.pr, pterygoid process; pvm.pr, posteroventromedial process; r.pr, retroarticular process; smx, septomaxilla; v, vomer. MCZ scan data used by permission of the Museum of Comparative Zoology, Harvard University

barely extending beyond the mandibular condyle; Figure 6e,f), and *Lanthanotus* (comprising about 15–20% of articular length; see for example, Evans, 2008: fig. 1.91).

Altogether, the intramandibular joint is typically quite tightly integrated and well braced by the mandibular elements. Almost all mandibular elements articulate closely across this joint in most non-snake lizards observed herein (Figures 3–6). Though some mandibular kinesis is possible (Cundall, 1995; Frazzetta, 1962), this is to a lesser extent and via a different configuration than in snakes, including "anilioids" (Cundall, 1995; see also Section 3.2). This, combined with the upper jaw structure (see below), represents a very different configuration of the jaw and suspensorium than in scolecophidians, thus justifying a different category for non-snake lizards from a functional perspective.

3.1.2 | Suspensorium

The non-snake lizard quadrate is stout and robust (Figures 3–6). It is typically oriented roughly vertically (Figures 3 and 4), though dibamids and amphisbaenians are exceptions to this (Figures 5 and 6; Section 3.1.4). The quadrate mainly articulates with the articular ventrally and the supratemporal and squamosal dorsally (Figures 3 and 4), with the paroccipital process of the otoccipital occasionally also contributing to this dorsal articulation (e.g., *Lanthanotus*).

The supratemporal forms a flattened rod, articulating with the squamosal laterally, the quadrate ventrally, and the postparietal process of the parietal—and paroccipital process of the otoccipital, in some taxa (e.g., *Lanthanotus*, *Sauromalus*)—medially (Figures 3 and 4). It is absent in dibamids and most amphisbaenians (Figures 5 and 6; Section 3.1.4).
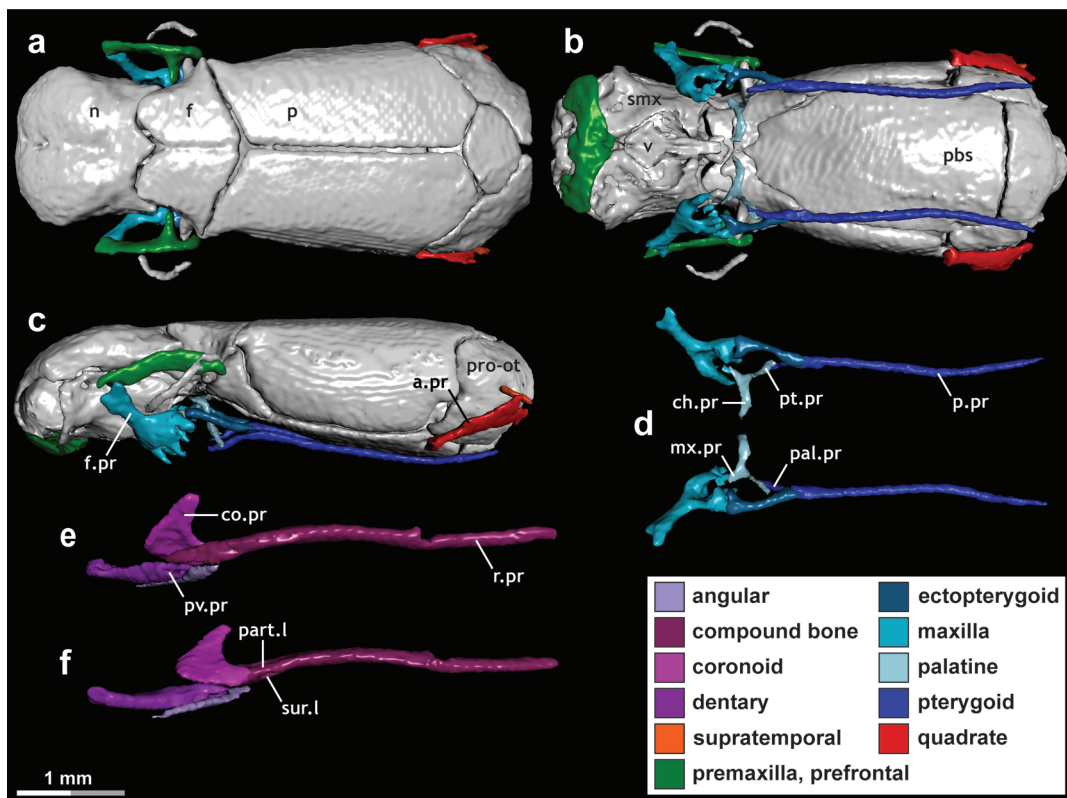
FIGURE 10 Skull of *Liotyphlops argaleus* (MCZ R-67933), exemplifying "axle-brace maxillary raking." Key elements related to feeding are highlighted. In this morphotype of microstomy, the maxilla is suspended from the mobile and highly reduced prefrontal and is braced posteriorly by the ectopterygoid. As in typhlopoids, the mandible is reduced and does not contribute to feeding (see text for details). (a–c) Skull, with mandibles digitally removed, in (a) dorsal, (b) ventral, and (c) lateral view. (d) Palatomaxillary arch in dorsal view. (e,f) Mandible in (e) lateral and (f) medial view. a.pr, anterior process; ch.pr, choanal process; co.pr, coronoid process; f, frontal; f.pr, facial process; mx.pr, maxillary process; n, nasal; p, parietal; pal.pr, palatine process; part.l, prearticular lamina; pbs, parabasisphenoid; p.pr, posterior process; pro-ot, prootic-otoccipital; pt.pr, pterygoid process; pv.pr, posteroventral process; r.pr, retroarticular process; smx, septomaxilla; sur.l, surangular lamina; v, vomer. MCZ scan data used by permission of the Museum of Comparative Zoology, Harvard University

The squamosal varies in shape among taxa, though typically consistently contributes to the jaw suspension via a ventral articulation with the quadrate (Figures 3 and 4). Its anterior terminus articulates dorsomedially with the elements bordering the posterior margin of the orbit (e.g., postorbitofrontal in *Varanus*, Figure 3; postorbital, and sometimes jugal, in iguanians, Figure 4) to form the upper temporal bar and enclose the supratemporal fenestra. The posterior terminus of the squamosal articulates medially with the supratemporal (Figures 3 and 4). The supratemporal and squamosal are somewhat reduced in *Sauromalus* and *Lanthanotus*, and absent in dibamids and most amphisbaenians (Figures 5 and 6; Section 3.1.4).

3.1.3 | Palatomaxillary arch

The key features of the palatomaxillary arch in non-snake lizards are its degree of robustness and extensive articulation among elements, resulting in minimal palatomaxillary mobility.

The non-snake lizard maxilla is generally large, robust, and toothed (Figures 3–6). The maxilla typically bears a distinct facial process, which is posteriorly angled in dibamids (Figure 5b) and amphisbaenians (Figure 6b) as a result of the "telescoping" (sensu Rieppel, 1984) of the skull as an adaptation for fossoriality. The facial process is generally tall (Figures 3–5), though it is shorter in a few taxa (e.g., *Amphisbaena* and *Anelytropsis*; Figure 6), particularly *Lanthanotus*, in which the facial process is low and broad, similar to the condition in "anilioid" snakes (e.g., see Evans, 2008, fig. 1.91). The maxilla articulates very closely with all or almost all surrounding elements, including the snout (premaxilla, septomaxilla, vomer, and nasal, the latter contact absent in varanoids), palatine, ectopterygoid, jugal, lacrimal, frontal (in dibamids and amphisbaenians), and prefrontal, when these elements are present (Figures 3–6).
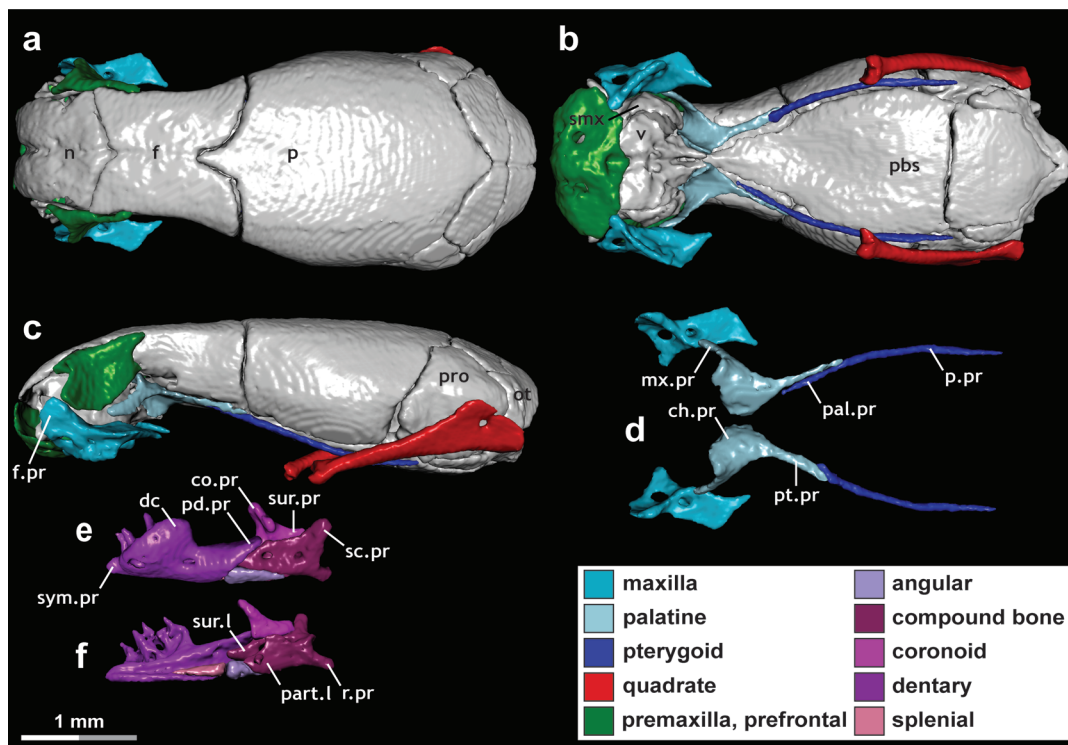
FIGURE 11 Skull of *Epictia albifrons* (MCZ R-2885), exemplifying "mandibular raking" (sensu Kley & Brainerd, 1999). Key elements related to feeding are highlighted. In this morphotype of microstomy, feeding is driven by rapid retraction of the mandibles, enabled by a flexible intramandibular joint, whereas the palatomaxillary arches are edentulous and do not contribute to feeding (see text for details). (a–c) Skull, with mandibles digitally removed, in (a) dorsal, (b) ventral, and (c) lateral view. (d) Palatomaxillary arch in dorsal view. (e,f) Mandible in (e) lateral and (f) medial view. ch.pr, choanal process; co.pr, coronoid process; dc, dental concha; f, frontal; f.pr, facial process; mx.pr, maxillary process; n, nasal; ot, otoccipital; p, parietal; pal.pr, palatine process; part.l, prearticular lamina; pbs, parabasisphenoid; pd.pr, posterodorsal process; p.pr, posterior process; pro, prootic; pt.pr, pterygoid process; r.pr, retroarticular process; sc.pr, supracotylar process; smx, septomaxilla; sur.l, surangular lamina; sur.pr, surangular process; sym.pr, symphyseal process; v, vomer. MCZ scan data used by permission of the Museum of Comparative Zoology, Harvard University

The pterygoid is large, robust, and often edentulous (Figures 3–6), though it does bear teeth in some taxa (e.g., *Lanthanotus*). It is gracile in dibamids (Figure 5), but still well-developed, like other non-snake lizards (Figures 3, 4, and 6) and unlike scolecophidians (Figures 9–11; Sections 3.4–3.6). The pterygoid articulates extensively with surrounding elements, primarily the palatine and ectopterygoid, and is further braced by the basipterygoid processes of the parabasisphenoid medially and by the quadrate posterolaterally (Figures 3–6).

The palatine is robust and edentulous, with well-developed pterygoid, maxillary, and vomerine processes (Figures 3b,d, 4b,d, 5b,d, and 6b,d). These processes articulate tightly with: the pterygoid posteriorly; the maxilla, ectopterygoid, and often the lacrimal and/or jugal laterally; and the vomer anteriorly, respectively. An additional process is present in dibamids, arching over the ventral or main shelf of the palatine in a manner analogous to the choanal process of snakes (Figure 5d).

The ectopterygoid is short and robust (Figures 3–6). Although its specific form and articulations vary slightly across taxa, it plays a consistent functional role in tightly bracing the palatopterygoid bar medially against the maxilla and certain orbital elements (e.g., jugal, prefrontal) laterally, thus supporting and helping immobilize the tightly integrated palatomaxillary arch.

The prefrontal is closely integrated with the skull (Figures 3–6), though in a manner quite different to typhlopoids and leptotyphlopids (Figures 1, 9, and 11; Sections 3.4 and 3.6). The prefrontal typically exhibits minimal to no contact with the snout, instead mainly articulating with the frontal medially and the maxilla laterally (Figures 3a,c, 4a,c, 5a,c, and 6a,c). In some taxa (e.g., many iguanians; Figure 4a), contact with the nasal can be fairly extensive, though this is of a very different nature than in any scolecophidian (Figures 9–11). The prefrontal may also articulate with other surrounding elements (e.g., the lacrimal laterally in varanoids and

iguanians, the palpebral dorsolaterally in *Varanus*, and the palatine ventrally in iguanians; Figures 3 and 4).

The premaxilla is tightly integrated with the other snout elements and the maxilla, thus playing an important role in "locking together" the left and right palatomaxillary arches (Figures 3a–c, 4a–c, 5a–c, and 6a–c). The palatomaxillary arch is often additionally braced by: the lacrimal anteriorly, at the junction between the maxilla, prefrontal, and palatine (Figures 3c and 4c); the jugal laterally, between the maxilla, ectopterygoid, and sometimes palatine (Figures 3c and 4c); the vomer anteriorly (Figures 3b, 4b, 5b, and 6b); the basipterygoid processes of the parabasisphenoid posteromedially (Figures 3b, 4b, 5b, and 6b); and the quadrate posterolaterally (Figures 3–6). In many taxa, the prefrontal also either braces the palatine dorsally (e.g., many iguanians; Figure 4) or very closely approaches this element (e.g., amphisbaenians, *Lanthanotus*, some iguanians).

Overall, the tight integration of the upper jaw elements in non-snake lizards therefore reflects an essentially akinetic palatomaxillary arch. This occurs via a completely different anatomical configuration than in leptotyphlopids (Figures 1 and 11; Section 3.6).

3.1.4 | Exceptions and variations

Given the phylogenetic, ecological, and functional diversity of non-snake lizards, it is inevitable that certain taxa present variations to the general condition described above. However, despite this variation, all taxa exhibit key features justifying their grouping with other non-snake lizards.

A particularly notable exception among non-snake lizards is *Lanthanotus* (e.g., see Evans, 2008, fig. 1.91). In this taxon, the integration between the anterior and posterior mandibular elements is reduced such that a distinct and flexible intramandibular joint occurs (Evans, 2008). This condition involves: reduced integration of the splenial with the posterior mandible (Evans, 2008); less extensive articulation of the angular with the anterior mandible and the articular with the splenial; and reduction of the anterior terminus of the coronoid and thus less distinct bracing of the intramandibular joint, including the presence of a facet anteriorly to accommodate the dentary, somewhat similar to the condition in *Cylindrophis* (Figure 7; Section 3.2). Furthermore, the palatine-pterygoid articulation in *Lanthanotus* is looser than is typical of non-snake lizards (e.g., compare Evans, 2008, fig. 1.91a to figs. 4–6 herein). Regarding these features, *Lanthanotus* could therefore be considered intermediate between typical non-snake lizards (Figures 3–6) and early-diverging alethinophidians (Figures 7 and 8).

Importantly, though, despite this looser palatine-pterygoid articulation, the overall structure of the jaws and suspensorium—especially the suspensorium and palatomaxillary arch— is otherwise consistent with the typical non-snake lizard condition. For example, the palatomaxillary arch of *Lanthanotus* lacks several other key "anilioid" features, such as a loosened maxilla-premaxilla articulation, "ball-and-socket"-like maxilla-palatine articulation, simplified ectopterygoid articulations, and the ability for unilateral movement, and the mandible lacks features such as an abutting splenial-angular contact (see Figure 7 and Section 3.2). In light of the absence of these features, and due to the otherwise similar condition of *Lanthanotus* compared to other non-snake lizards, it is therefore most reasonable to consider *Lanthanotus* as a variation of the general non-snake lizard condition.

Dibamids and amphisbaenians represent another apparent exception among non-snake lizards. As mentioned above, the lower jaw differs in these taxa compared to other non-snake lizards due to additional fusion of the posterior mandibular elements (Figures 5e,f and 6e,f). In dibamids, bipedids, and trogonophiids, this involves fusion of the articular, angular, surangular, and possibly splenial (in dibamids) to form a single articular complex (Figure 5e,f; Evans, 2008; Gans & Montero, 2008). A similar condition occurs in amphisbaenids and rhineurids, although the angular remains separate, resulting in a compound bone comparable to that of snakes (Figure 6e,f). Some iguanians also exhibit fusion of the angular and/or articular and/or surangular, again forming a "compound bone" or articular complex (Evans, 2008). These fused complexes articulate closely with the other mandibular elements, suturing dorsally or dorsomedially with the coronoid and articulating ventrally and laterally with the dentary (Figures 5e,f and 6e,f). In dibamids, this latter articulation involves a long prearticular process (sensu Evans, 2008) extending anteriorly along the medial surface of the dentary, thus bridging the intramandibular joint and bracing the dentary (Figure 5e,f).

Dibamids and amphisbaenians also differ quite distinctly from the typical condition of the non-snake lizard suspensorium. The supratemporal is highly reduced in *Trogonophis* and completely absent in *Dibamus* and most amphisbaenians (Figures 5 and 6; Evans, 2008; Gans & Montero, 2008). The squamosal is similarly absent in *Dibamus* and most amphisbaenians, though it is present but quite reduced in *Bipes* (Figures 5 and 6; Gans & Montero, 2008). *Anelytropsis* bears a small temporal element representing either a highly reduced squamosal or supratemporal (Evans, 2008). Due to this extreme reduction, the dorsal articulation of the quadrate with the skull

is therefore quite different than in other non-snake lizards (e.g., Figures 3 and 4). Ventrally, the quadrate articulates with the articular complex or compound bone (Figures 5 and 6). In amphisbaenids and rhineurids, the quadrate also articulates extensively with the pterygoid medially via a broad articulatory facet on the medial surface of the quadrate shaft (Figure 6). Finally, the quadrate itself is notable in being anteriorly displaced and angled distinctly anteroventrally (Figures 5c and 6c).

The structure of the prefrontal in dibamids further differs from other non-snake lizards. In dibamids, the prefrontal is greatly simplified and essentially plate-like (Figure 5a,c), similar to the form in leptotyphlopids (Figure 11a,c; Section 3.6). The ectopterygoid also exhibits a simpler structure and simpler articulations with the maxilla and pterygoid than in other non-snake lizards, similar to the condition in *Cylindrophis* (Figure 7; Section 3.2.3).

Finally, the lacrimal and jugal are absent in dibamids and most amphisbaenians (Figures 5 and 6), with the jugal being present but highly reduced in *Rhineura* (Gans & Montero, 2008). The lacrimal is also reduced in *Lanthanotus* and *Uranoscodon*. The palatomaxillary arch in these taxa therefore lacks these additional bracing structures as present in other non-snake lizards.

However, despite these differences, the functionality of the complexes in question remains consistent with other non-snake lizards. For example, the fused mandibular structures articulate closely with the other mandibular elements, therefore playing the same functional role as their constituent components in other non-snake lizards, that is, bracing the intramandibular joint (Figures 5e,f and 6e,f). Similarly, although the lacrimal and jugal are often absent, the palatomaxillary arch still articulates quite strongly among its constituent elements and is still braced by the vomers, premaxilla, and basipterygoid processes (Figures 5a–d and 6a–d), a configuration consistent with the general non-snake lizard condition (Figures 3 and 4). Finally, although the dibamid prefrontal is similar in form to that of leptotyphlopids, major differences include a lack of contact with the snout elements and much greater contact with the maxilla (Figures 5 and 11; see also Section 3.6 for comparison), as well as the completely different configuration of the upper jaw complex compared to any scolecophidian (Figure 1). Therefore, because the skulls of these taxa—particularly the structure and biomechanics of the palatomaxillary arch (e.g., robust, tightly interlocking, and immobile)—are otherwise consistent with the condition in other non-snake lizards, we find it reasonable to consider dibamids and amphisbaenians as variations of this general non-snake lizard condition, and the similarities between their

anatomical arrangements and those of the blindsnakes as having arisen convergently (see also Section 4.4).

3.2 | "Anilioids"—Uropeltoidea

The description of this morphotype is based on *Cylindrophis* (Figure 7). Minor variations in other uropeltoid taxa are noted where relevant, with major variations being described at the end of this section. This description of uropeltoids is largely applicable to Amerophidia (Figure 8)—the other major lineage of "anilioid" snakes—but, because Amerophidia forms a distinct phylogenetic lineage, rendering "anilioids" polyphyletic (Figures 1 and 2; Burbrink et al., 2020), this latter clade is presented separately in the next section. Previous treatments of the uropeltoid skull supplement the descriptions provided herein. Primary among these are Cundall (1995), Cundall and Irish (2008), Cundall and Rossman (1993), Olori and Bell (2012), Rieppel (1977), and Rieppel and Maisano (2007).

3.2.1 | Mandible

The uropeltoid mandible is robust and approximately equal in length to the skull (Figure 7). The dentary is large and robust (Figure 7e,f), similar to the form in non-snake lizards (Figures 1 and 3–6) and quite distinct from the reduced form in scolecophidians (Figures 1 and 9–11). The dentary tooth row is oriented anteroposteriorly (Figure 7e,f). The mandibles approach each other medially, much more so than in "macrostomatans," but slightly less so than in scolecophidians and especially non-snake lizards. A fibrocartilaginous interramal pad and collagenous intergular pad (sensu Cundall, 1995) occur at the mandibular symphysis in *Cylindrophis*, preventing lateral separation of the dentary tips (Cundall, 1995). The dentary distinctly articulates with surrounding elements, but its articulations with the compound bone and coronoid are typically quite loose compared to the tight junctions in non-snake lizards (Figures 3–6), resulting in a greater capacity for kinesis at the intramandibular joint (Figure 7e,f; Cundall, 1995). The posteroventral process of the dentary is present (Figure 7e,f).

The splenial and angular are typically well-developed (Figure 7f). These elements form low, anteriorly- and posteriorly-tapering triangles, respectively, as is typical of snakes (Figure 7f). Laterally, they articulate closely with the dentary and compound bone, respectively (Figure 7f). The splenial and angular articulate with each other via a simple abutting contact, with their articulating surfaces

exhibiting slight concavo-convexity, thus enabling intramandibular kinesis (Figure 7; Cundall, 1995).

The coronoid is robust in *Cylindrophis* (Figure 7e,f). It bears a tall coronoid process (Figure 7f), though proportionally this is not quite as tall as in scolecophidians (Figures 1 and 9–11; Sections 3.4–3.6). The coronoid articulates closely with the compound bone laterally and ventrally (Figure 7e,f). The anteromedial process of the coronoid is long and extends under the posterior extent of the dentary tooth row (Figure 7f). The coronoid-dentary articulation is relatively loose, with the coronoid being dorsoventrally flattened anteriorly with a distinct dorsal facet to accommodate the dentary, which permits intramandibular kinesis (Figure 7e,f; Cundall, 1995).

The compound bone is typically elongate and robust, comprising about 60–70% of the total skull length (Figure 7). The retroarticular process is very short, typically barely extending beyond the mandibular condyle (Figure 7e,f), though is slightly longer in *Anomochilus* (see Rieppel & Maisano, 2007).

Overall, the intramandibular joint is relatively mobile in *Cylindrophis*, particularly via lateral flexion near the angular-splenial, dentary-compound bone, and dentary-coronoid joints (Figure 7e,f; Cundall, 1995). This is presumably also the case for *Anomochilus* and *Uropeltis*, both of which exhibit similar angular-splenial and dentary-compound bone articulations. This mobility is much more extensive than the limited mandibular kinesis present in scleroglossans (Cundall, 1995).

3.2.2 | Suspensorium

The quadrate is stout and robust (Figure 7). It is oriented roughly vertically, with a large suprastapedial process posterodorsally (Figure 7c). This process is particularly elongate in *Anomochilus* and especially *Uropeltis*, to an extent unique among snakes (Olori & Bell, 2012). Dorsally, the quadrate typically articulates mainly with the prootic and supratemporal and minimally with the otoccipital (Figure 7a,c). The supratemporal is present and well-developed (Figure 7a,c). As in all snakes, the squamosal is absent.

3.2.3 | Palatomaxillary arch

The maxilla is large and robust (Figure 7a–d), similar to the robust condition in non-snake lizards (Figures 1 and 3–6), though it differs from that of non-snake lizards in the nature of its articulations with surrounding elements. The maxilla articulates posteriorly with the ectopterygoid, medially with the palatine via a "ball-and-socket"-like joint enabling rotation and minor anteroposterior movement of the maxilla (Figure 7b,d; Cundall, 1995), and dorsally with the prefrontal via a low facial process (Figure 7a–d). The maxilla approaches the septomaxilla and premaxilla medially and is attached to these elements via septomaxillo-maxillary and premaxillo-maxillary ligaments, respectively (Cundall, 1995), but does not directly contact them (Figure 7b). As such, although the maxilla articulates closely with surrounding elements, this articulation is not as tight as in non-snake lizards (Figures 3–6), resulting in less restricted palatomaxillary mobility. The maxillary tooth row is oriented anteroposteriorly (Figure 7).

The pterygoid is large, robust, and well-developed (Figure 7a–d). In this manner it is similar to non-snake lizards (Figures 3–6), but differs in bearing a more pronounced tooth row anteriorly. The pterygoid interlocks with the palatine anteriorly (Figure 7b,d), though in a slightly more flexible manner than in non-snake lizards (Figures 3–6; except *Lanthanotus*: see Section 3.1.4). As in non-snake lizards, the pterygoids are braced medially by the basipterygoid processes of the parabasisphenoid (Figures 3b, 4b, 5b, 6b, and 7b), a junction further strengthened by the basipterygoid ligaments (Cundall, 1995). The pterygoids are also braced by the ectopterygoid laterally (Figure 7a–d), though via a less complex and less extensive articulation than is typical of non-snake lizards (Figures 3–6).

The palatine is similarly large and robust (Figure 7b,d). It differs from the non-snake lizard palatine primarily in bearing teeth along the length of its main body and in bearing a distinct choanal process (Figure 7b,d). As noted above, its posterior articulation with the pterygoid is not as tight as in most non-snake lizards. The choanal processes very closely approach the palatine processes of the vomers, with these elements being linked by the vomero-palatine ligaments, such that movements of the palatine are transferred to the corresponding vomer (Cundall, 1995). Although this is superficially similar to the close palatine-vomer articulation in non-snake lizards, it lacks the extensive direct osseous contact between these elements that occurs in non-snake lizards (Figures 3–7). The palatine articulates with the maxilla via a "ball-and-socket"-like joint (Figure 7b,d).

The ectopterygoid is short and robust, articulating with the ectopterygoid process of the pterygoid posteriorly and the posterior terminus of the maxilla anteriorly (Figure 7a–d). Both articulations are less extensive and/or less complexly integrated than in non-snake lizards (e.g., compared to the broadly abutting contacts in

Physignathus or the complexly interlocking articulations in *Varanus*; Figures 3–6).

The uropeltoid prefrontal is very similar to non-snake lizards (except *Dibamus*; see Figure 5 and Section 3.1.4) in its articulations with other skull elements. For example, as in non-snake lizards (Figures 3–6), the prefrontal exhibits minimal contact with the snout, instead articulating mainly with the frontal medially and the maxilla laterally (Figure 7a,c). It also articulates ventrally with the palatine, and is further connected to the maxilla via the lateral prefronto-maxillary ligament and to the palatine via the prefronto-palatine ligament (Cundall, 1995). According to Cundall (1995), though, the integration with the maxilla and palatine is looser in alethinophidians—including "anilioids"—than in non-snake lizards. Of note, typhlopoids and leptotyphlopoids also exhibit tight integration of the prefrontal with the skull roof (Figures 9 and 11; Sections 3.4 and 3.6), though this condition differs quite distinctly from that in non-snake lizards (Figures 3–6) or "anilioids" (Figures 7 and 8).

The premaxilla is integrated into the snout more loosely than in non-snake lizards (Figures 3–6) and scolecophidians (Figures 9–11), though more tightly than in more derived alethinophidians. The prefrontal is connected to the maxilla via the premaxillo-maxillary ligament (Cundall, 1995), though, unlike non-snake lizards, it lacks direct osseous contact with the maxilla (Figure 7a,b). This configuration enables slightly more unilateral movement of the left and right palatomaxillary arches, compared to the tightly braced condition in non-snake lizards.

Overall, the palatomaxillary arch is generally similar to the condition in non-snake lizards (e.g., large, robust, interlocking elements; Figures 3–6), though its components are less tightly articulated with each other and with surrounding elements than in non-snake lizards (Figure 7a–d). The palatomaxillary arch therefore has somewhat greater kinesis than in non-snake lizards, including the ability for unilateral movement of the left and right palatomaxillary arches, albeit limited compared to more "derived" alethinophidians (Cundall, 1995). This movement is largely enabled by minor decoupling of the ventral (vomer and septomaxilla) and dorsal (nasal and premaxilla) snout elements, and the ventral snout elements from their contralaterals (Cundall, 1995). This decoupling enables slight unilateral movement within the ventral snout, which extends to the rest of the palatomaxillary arch due largely to the integration of the palatine-vomer and maxilla-septomaxilla (Figure 7; Cundall, 1995). The "ball-and-socket"-like joint between the maxilla and palatine is also essential in enabling this kinesis.

3.2.4 | Exceptions and variations

As noted above for non-snake lizards, the phylogenetic diversity among uropeltoids inevitably causes variation within this group. Much of this variation arises from miniaturization, paedomorphosis, and adaptations related to fossoriality, as explained further in the Discussion.

Representing key exceptions to the general uropeltoid condition as described above, both *Anomochilus* and *Uropeltis* (and indeed other members of the Uropeltidae such as *Plectrurus* and *Melanophidium*; Cundall & Irish, 2008) exhibit reduction of certain elements compared to *Cylindrophis*. For example: the mandible is shorter (about 70–80% of total skull length); the splenial and angular are smaller or lost altogether (*Plectrurus*; Cundall & Irish, 2008); the dentary and maxilla are robust but anteroposteriorly shorter in *Anomochilus*, and of typical length but more gracile in uropeltids; the posteroventral process of the dentary is absent in uropeltids; the coronoid is highly reduced and articulates only with the compound bone; and the compound bone is shorter in *Uropeltis* (comprising about 40–50% of the total skull length), and somewhat less robust in both taxa (see also Olori & Bell, 2012; Rieppel & Maisano, 2007). The compound bone's length varies dramatically within the Uropeltidae (Cundall & Irish, 2008). Presumably as a consequence of the drastic reduction of its posterior extent, the maxillary tooth row is angled somewhat anteromedially in *Anomochilus* (see also Rieppel & Maisano, 2007). The jaw suspension is anteriorly displaced in both *Anomochilus* and uropeltids compared to *Cylindrophis* and *Anilius*, more closely resembling the placement in scolecophidians, and the supratemporal is absent in uropeltids and *Anomochilus leonardi*, causing the quadrate to articulate dorsally with the prootic and otoccipital in *Anomochilus* and with the fused braincase in *Uropeltis* (see also Olori & Bell, 2012; Rieppel & Maisano, 2007). The pterygoid and palatine are both edentulous in these taxa, and the ectopterygoid is also reduced, to the extent that it is entirely suspended within the pterygomaxillary ligament in *Anomochilus* (see also Cundall & Rossman, 1993; Rieppel & Maisano, 2007).

Other differences involve increased robustness of the skull, such as the lateral expansion of the nasals, causing tighter integration of the prefrontal with the snout (see also Rieppel & Maisano, 2007). The premaxilla is also more tightly integrated with surrounding elements, limiting the capacity for unilateral movement of the palatomaxillary arches (see also Olori & Bell, 2012; Rieppel & Maisano, 2007). Finally, the maxilla more closely approaches the septomaxilla and premaxilla in

Anomochilus and makes extensive contact with these elements, especially the premaxilla, in *Uropeltis*.

Despite these differences, however, *Anomochilus* and *Uropeltis* still exhibit many similarities to *Cylindrophis*. For instance, although the prefrontal is more tightly integrated into the skull, it is otherwise consistent in form with the typical uropeltoid condition as described above (see also Olori & Bell, 2012; Rieppel & Maisano, 2007). Similarly, although the palatine is edentulous, the rest of its anatomy is quite similar to other uropeltoids (see also Olori & Bell, 2012; Rieppel & Maisano, 2007). Most importantly, both *Anomochilus* and *Uropeltis* appear capable of moving the ventral snout elements independently of the dorsal snout elements (Cundall, 1995; Cundall & Rossman, 1993), a key component of the functional morphology of *Cylindrophis*. Taking these similarities into account—and also recognizing that *Anomochilus* and *Uropeltis* lack the hallmark features of any of the scolecophidian morphotypes, especially regarding palatomaxillary suspension and biomechanics (see Figures 9–11 and Sections 3.4–3.6)—we ultimately consider it reasonable to classify these taxa as miniaturized variants of the general uropeltoid condition, rather than creating a different morphotype or referring them to any of the scolecophidian conditions (see also Section 4.4 for further discussion).

3.3 | "Anilioids"—Amerophidia

The clade Amerophidia is herein represented by *Anilius* (Figures 1, 2, and 8). The cranial morphology of this clade is largely consistent with the Uropeltoidea (Figure 7), as described above, especially regarding the suspensorium and palatomaxillary arch. However, amerophidians form a lineage that is phylogenetically separate from uropeltoids, creating a polyphyletic "anilioid" assemblage (Figures 1 and 2; Burbrink et al., 2020), and also exhibit a mandibular structure different from that of uropeltoids. For these reasons, these clades of early-diverging alethinophidians are treated separately. To avoid repetition, however, we here describe only the mandible of Amerophidia in detail, and refer readers to Sections 3.2.2 and 3.2.3 for a general impression of the suspensorium and palatomaxillary arch, respectively.

3.3.1 | Mandible

Anilius is notable in that the structure of its mandible differs somewhat compared to *Cylindrophis* (Figures 7 and 8). In *Anilius*, the splenial and angular may be absent or extremely reduced (Figure 8; Rieppel, 1977; Cundall &

Irish, 2008). The anterior terminus of the compound bone articulates rather extensively with the medial surface of the dentary (Figure 8f), in contrast to the interlocking configuration in *Cylindrophis* (Figure 7e,f), and the coronoid overlaps this articulation dorsally (Figure 8e,f). Altogether, this suggests a potentially lower degree of intramandibular kinesis in *Anilius* compared to *Cylindrophis*.

However, the dentary-compound bone articulation appears to still enable some degree of lateral flexion at the intramandibular joint, as the coronoid is reduced and so does not act as a medial "buttress" preventing this flexion (Figure 8e,f). This is unlike the typhlopoid mandible, for instance, in which the coronoid would prevent this movement (see Figure 9 and Section 3.4.1). Furthermore, although the intramandibular joint of *Anilius* does differ somewhat from *Cylindrophis*, the articulations and apparent mobility of this condition are much more functionally and anatomically similar to *Cylindrophis* (Figure 7) than to the tightly and pervasively interlocking condition of the non-snake lizard mandible (Figures 3–6). Combined with the consistent nature of the palatomaxillary arch in these taxa, including the suggestion that *Anilius* is also capable of unilateral movement of the palatomaxillary arches (Cundall, 1995), it is therefore reasonable to include *Anilius* under the same biomechanical category as *Cylindrophis*.

3.4 | Typhlopoidea

The clade Typhlopoidea contains three families: Gerrhopilidae, Typhlopidae, and Xenotyphlopidae (Figures 1 and 2). Our scans of gerrhopilids were not of sufficient resolution to digitally segment or figure these specimens in the same detail as the other scolecophidian families, but did allow us to assess key aspects of their anatomy. Iordansky (1997), Kley (2001), and Chretien et al. (2019) present detailed descriptions of typhlopoid jaw anatomy, with Iordansky (1997) and Kley (2001) also discussing the functional morphology of the typhlopid jaw complex. Classical studies such as Haas (1930), Mahendra (1936), Evans (1955), and List (1966) also provide descriptions of the typhlopid skull; much of the historical literature was summarized by Cundall and Irish (2008).

3.4.1 | Mandible

The typhlopoid mandible is long and slender, measuring approximately 60–75% of the total skull length (Figure 9). The dentaries are highly reduced, each typically forming

a flat crescent or slightly rod-like form curved medially toward the mandibular symphysis (Figure 9e,f), though the dentary is more straight and rod-like in some (e.g., *Acutotyphlops kunuaensis*, *A. subocularis*). The dentaries closely approach each other medially, linked by a cartilaginous nodule as in leptotyphlopids (Kley, 2001). The dentary exhibits broad contact ventrally with the splenial, also overlapping the coronoid and compound bone posteroventrally (Figure 9e,f). The interramal surface is smooth, lacking articulatory or symphyseal facets, unlike the condition in non-snake lizards (see also Kley, 2006). The posteroventral process of the dentary is absent (Figure 9e,f); Rieppel, Kley, and Maisano (2009) described this absence as uniting all scolecophidians, though see Section 3.5.1 for our interpretation in anomalepidids. The dentary is edentulous (Figure 9e,f), a condition unique to typhlopoids among snakes (Kley, 2001).

The typhlopoid splenial is proportionally quite large compared to other squamates, ranging from approximately equal in length to the dentary (e.g., *Acutotyphlops infralabialis*, among others) to approximately twice the length of the dentary (e.g., *Afrotyphlops*, *Amerotyphlops*, *Anilios*, among others; Figure 9e,f). The gerrhopilid splenial is somewhat more gracile, being slightly shorter and thinner than the dentary in *Gerrhopilus persephone*, of typical length but thin and rod-like in *G. beddomii*, and of typical length but not extending as far anteriorly in *G. ater*. The splenial typically extends anteriorly almost to the anterior terminus of the mandible in most typhlopoids (Figure 9e,f), though it terminates farther posteriorly in a few taxa (*Acutotyphlops infralabialis*, *A. kunuaensis*, *Gerrhopilus persephone*, *G. ater*). The splenial articulates extensively with all other mandibular elements, fully spanning the intramandibular joint (Figure 9e,f).

The angular is quite reduced, forming a thin splint lying between the dorsal margin of the splenial and the ventral margins of the compound bone and coronoid (Figure 9e,f). The angular directly contacts the coronoid in some taxa (e.g., *Acutotyphlops*, *Afrotyphlops*, *Typhlops*; Figure 9f) and closely approaches but does not directly contact it in others (e.g., *Antillotyphlops*, *Xenotyphlops*). The angular is absent in some typhlopoids (e.g., *Anilios*, *Indotyphlops*, *Ramphotyphlops*, *Xerotyphlops*, and potentially *Gerrhopilus*).

The coronoid is large, flat, and triangular, with a tall coronoid process (dorsal process sensu Kley, 2006; Figure 9e,f). The base of the coronoid extends well anteriorly and posteriorly, articulating closely with the dentary, splenial, and compound bone in all typhlopoids (Figure 9e,f), though it does not extend as far anteriorly in *Gerrhopilus ater* and *G. persephone* as in other

typhlopoids. Contact with the angular varies among taxa (see above).

The typhlopoid compound bone is long, measuring approximately 50–65% of the total skull length, and is distinctly anteriorly downcurved (Figure 9). This curvature is especially pronounced in xenotyphlopids, in conjunction with the distinctive ventral inflection of the anterior skull (see Chretien et al., 2019). The compound bone bears a moderate retroarticular process, typically comprising about 20–25% of the total length of the compound bone (Figure 9e,f), though this process is shorter in some taxa (about 7–10% in *Acutotyphlops*, and 16–18% in *Antillotyphlops*, *Cubatyphlops*, and *Gerrhopilus*). The retroarticular process terminates well anterior to the level of the occipital condyle (Figure 9). The compound bone articulates with all other mandibular elements (Figure 9e,f).

Altogether, the intramandibular hinge is essentially immobile, with the mandibular elements articulating tightly with each other, especially the broadly overlapping splenial, coronoid, and compound bone (see also Kley, 2001). Additionally, although the mandibles are rather fixed with respect to one another, some longitudinally rotational intermandibular mobility is possible, as indicated by the muscular attachments of the compound bone and suspensorium and the jugomandibular ligament, which permit a deeper intermandibular oral trough than would be possible were the mandibles medially linked by more tightly interlocking articulatory or symphyseal facets (Iordansky, 1997).

3.4.2 | Suspensorium

As is typical of scolecophidians, the quadrate is elongate and strongly anteroventrally angled (Figure 9c). However, it is not as elongate as in leptotyphlopids, with the long axis of the quadrate equivalent to approximately 25–30% of the total skull length in typhlopoids (Figure 9; though it is longer in some taxa, for example, 37–40% in *Indotyphlops*, *Typhlops*, and *Xerotyphlops*), compared to approximately 40–45% in leptotyphlopids (Figure 11). In typhlopids and gerrhopilids, the quadrate bears a pronounced anterior process (sensu Palci, Caldwell, Hutchinson, Konishi, & Lee, 2020) slightly posterior to the mandibular condyle (Figure 9c). This process is somewhat smaller and more posteriorly positioned in *Xenotyphlops* (see Chretien et al., 2019). The quadrate articulates dorsally with the prootic and otoccipital in most typhlopoids (Figure 9; e.g., *Afrotyphlops*, *Amerotyphlops*, *Anilios*, *Antillotyphlops*, *Cubatyphlops*, *Typhlops*, *Xerotyphlops*), though these elements are fused in xenotyphlopids, gerrhopilids, and some typhlopids

(e.g., *Acutotyphlops*, *Indotyphlops*, *Ramphotyphlops*, and *Madatyphlops*; see also Hawlitschek, Scherz, Webster, Ineich, & Glaw, 2021). The supratemporal is absent in all typhlopoids. As is typical of snakes, the squamosal is also absent.

3.4.3 | Palatomaxillary arch

The typhlopoid maxilla is highly mobile and is unique among squamates in rotating around the maxillary process of the palatine via a large foramen (in most typhlopoids; Figure 9) or deep medial excavation (e.g., *Acutotyphlops infralabialis*, *A. kunuaensis*, *A. solomonis*, *Afrotyphlops schlegelii*). The maxillary tooth row is directed roughly transversely, with the maxilla angled posteroventrally at rest (Figure 9a–d). A pronounced facial process articulates loosely alongside the lateral surface of the prefrontal (Figure 9a–d).

As is typical of scolecophidians, the pterygoid is long, rod-like, and edentulous (Figure 9a–d). Its anterior terminus, or palatine process, is forked to articulate with the palatine (Figure 9b,d). The pterygoid and palatine underlie the skull more broadly than in leptotyphlopids (Figure 11; Section 3.6.3). The parabasisphenoid lacks basipterygoid processes in most typhlopoids (Figure 9b), though rudimentary processes are present in *Xenotyphlops* (Chretien et al., 2019). However, these processes are much less prominent than in non-snake lizards and do not approach the pterygoids as closely, and the pterygoids lack corresponding articulatory facets (see Chretien et al., 2019).

The palatine is edentulous and highly reduced, essentially consisting only of its maxillary and choanal processes (Figure 9b,d). The palatine also bears a highly reduced pterygoid process and distinct ventral process (the latter of which may reflect a uniquely forked condition of the former) which articulate with the forked anterior terminus of the pterygoid (Figure 9b,d). The choanal process forms a thin and narrow arch very closely approaching the corresponding vomer (Figure 9b), though—like snakes (Figures 7–11) and unlike non-snake lizards (Figures 3–6)—there is no direct osseous contact between these elements. Most distinctively, the maxillary process of the palatine is unique among squamates in forming an elongate rod projecting laterally to articulate with a foramen and/or medial depression in the maxilla (Figure 9a–d).

The ectopterygoid is absent in all typhlopoids (see also Chretien et al., 2019). The prefrontals are expanded and immobile, being tightly integrated into the snout and skull roof via extensive articulation with the nasals, septomaxillae, and frontals in all typhlopoids (Figure 9a–

d), as well as the premaxilla in xenotyphlopids (see also Chretien et al., 2019). The premaxilla is tightly integrated with the other snout elements, but does not contact the palatomaxillary arches and therefore does not affect palatomaxillary mobility (Figure 9a–c).

Altogether, the palatomaxillary arch is highly mobile, with its functionality reliant upon a unique maxilla-palatine articulation (see also Chretien et al., 2019; Iordansky, 1997; Kley, 2001). Drastic reduction of the ligamentous connection between the pterygoid and quadrate further reflects decoupling of the upper (palatomaxillary arch) and lower (mandible and suspensorium) jaws, as in leptotyphlopids (Kley, 2001).

3.5 | Anomalepididae

Like typhlopoids, anomalepidid jaw biomechanics rely heavily on movements of the palatomaxillary arches; however, this occurs via a totally different anatomical configuration than in typhlopoids (Figures 9 and 10; Chretien et al., 2019). Unfortunately, although typhlopoid jaw anatomy has been described in detail from a functional morphological perspective (Iordansky, 1997; Kley, 2001), this system has yet to be examined in similar morphofunctional detail in anomalepidids. Rieppel et al. (2009) recently provided a detailed description of the anomalepidid skull, focusing on *Liotyphlops* and *Typhlophis*, with Santos and Reis (2019) providing detailed imaging of *Anomalepis*. Classical work was summarized by Cundall and Irish (2008). Important among historical works are those by Haas (1964, 1968) describing anomalepidid skull anatomy, although it is worth noting that these studies were based on serial sectioning and suffered greatly from the small size of these animals, leading to almost comically wavy bone shapes in Haas' illustrations. This issue has been completely overcome by micro-CT approaches.

3.5.1 | Mandible

The anomalepidid mandible is extremely long and slender, measuring approximately 85–90% of the total skull length in most anomalepidids and 100% of the total skull length in *Typhlophis* (Figure 10). The dentary is highly reduced (Figure 10e,f), with a rod-like form—rather than the more crescentic form of typhlopoids (Figure 9e,f)—and a flattened and expanded anterior terminus. The dentary is typically toothed, like leptotyphlopids (Figure 11e,f) and unlike typhlopoids (Figure 9e,f). However, the anomalepidid dentary bears only a few tooth positions at its anterior terminus (Haas, 1968; List, 1966; Rieppel

et al., 2009), and so is not as extensively or robustly toothed as in leptotyphlopids (see Figure 11e,f and Section 3.6.1). Furthermore, we found several specimens to have edentulous mandibles (a condition which Chretien et al., 2019 mistakenly generalized to all anomalepidids); among our examined specimens, teeth are only distinctly visible on specimens of *Anomalepis mexicanus*, *Liotyphlops beui*, and *Typhlophis*, though this may be an artifact of scan resolution. List (1966) and Haas (1964) found teeth on the dentary of *Liotyphlops albirostris*, Haas (1968) in *Anomalepis aspinosus*, and McDowell and Bogert (1954) in *Helminthophis flavoterminatus* and *Typhlophis squamosus*. As in other snakes, the interramal surface lacks articulatory or symphyseal facets (see also Kley, 2006). Finally, although Rieppel et al. (2009) described the posteroventral process of the dentary as being absent in all scolecophidians, we consider it present in anomalepidids: in other squamates (Figures 3 and 5–8), this process constitutes an extension of the dentary ventral to the surangular or compound bone, which is also the condition in anomalepidids (Figure 10e). In contrast, the dentary in other scolecophidians (Figures 9 and 11) extends posterodorsal to the compound bone, reflecting an absence of the posteroventral process and presence of the posterodorsal process of other squamates (Figures 3 and 5–8).

The angular is present in anomalepidids, though the splenial is absent (Figure 10e,f; see Rieppel et al., 2009 regarding the homology of this element). The angular is elongate and rod-like, extending ventrally across the intramandibular joint (Figure 10e,f), but does not bridge this joint as extensively as the splenial does in typhlopoids (see Figure 9e,f and Section 3.4.1). It is similar in overall shape and position to the typhlopoid angular (Figure 9e,f), though is typically larger and longer, extending anteriorly to around the midpoint of the dentary in most anomalepidids (Figure 10e,f; *Liotyphlops albirostris*, *L. argaleus*, *Typhlophis*, and, to a lesser extent, *Anomalepis mexicanus* and *Helminthophis*).

The coronoid is flat and boomerang-shaped, with a tall coronoid process as in typhlopoids (Figures 9e,f and 10e,f). Because the base of the anomalepidid coronoid (Figure 10e,f) typically does not project anteriorly as in typhlopoids (Figure 9e,f), this element does not bridge the intramandibular joint as extensively as in typhlopoids. However, *Anomalepis* is an exception to this, as the anteroposterior extent of the coronoid in this genus is similar to the condition in typhlopoids. The anomalepidid coronoid articulates with the dentary and compound bone, but does not articulate to an appreciable extent with the angular (Figure 10e,f).

The compound bone is elongate, measuring about 70–75% of the total skull length in most anomalepidids

(Figure 10e,f) and about 80% in *Typhlophis*, and as such is longer than in typhlopoids (Figure 9e,f) and especially leptotyphlopids (Figure 11e,f). The compound bone shows shallow sinusoidal curvature in anomalepidids (Figure 10e,f), rather than the distinct downward curvature of the typhlopoid compound bone (Figure 9e,f). The retroarticular process is typically extremely long, comprising approximately 35–40% of the total length of the compound bone (Figure 10e,f), though it is slightly shorter in *Anomalepis mexicanus*. It extends posteriorly to—or just beyond, in the case of *A. aspinosus* and *Typhlophis*—the level of the occiput (Figure 10). Near the anterior terminus of the compound bone, the prearticular and surangular laminae briefly separate medially and laterally, respectively, before re-fusing at the anterior terminus (Figure 10f; Rieppel et al., 2009). Rieppel et al. (2009) note this separation in anomalepidids and describe it as uniquely shared with leptotyphlopids among snakes; however, leptotyphlopids differ in that these laminae remain completely separate, rather than re-fusing anteriorly as occurs in anomalepidids (see Figure 11e,f and Section 3.6.1).

Although functional studies of the anomalepidid mandible are lacking, the structure and articulations of the mandibular elements suggest that the intramandibular joint is relatively immobile, with the angular and coronoid both bridging this gap via their articulations with the dentary and compound bone (Figure 10e,f). This condition is therefore more similar to the akinetic typhlopoid mandible (Figure 9e,f; Section 3.4.1) than to the highly mobile intramandibular joint of leptotyphlopids (Figure 11e,f; Section 3.6.1). However, the integration between the anterior—dentary and splenial—and posterior—compound bone and angular—mandibular subunits is less extensive than in typhlopoids (Figure 9e,f), suggesting a less rigid condition in anomalepidids (Figure 10e,f).

3.5.2 | Suspensorium

The quadrate is elongate and anteroventrally oriented so as to be nearly horizontal (Figure 10), as is typical of scolecophidians (Figures 9–11). The quadrate is similar in length to typhlopoids (i.e., long axis equivalent to approximately 20–30% of the total skull length; Figures 9c and 10c) and shorter than in leptotyphlopids (in which the long axis of the quadrate is equivalent to approximately 40–45% of the total skull length; Figure 11c). The anterior process of the quadrate typically occurs near the same location as in typhlopids and gerrhopilids (Figures 9c and 10c)—that is, between the mandibular condyle and the midpoint of the quadrate shaft—but is

similar to or smaller than the size in xenotyphlopids (see Section 3.4.2). The dorsal terminus of the quadrate is broadly forked in most anomalepidids—except *Anomalepis*—where it meets the supratemporal (Figure 10a,c). The quadrate articulates dorsally with the fused prootic-otoccipital and the extremely reduced supratemporal in *Helminthophis*, *Liotyphlops*, and *Typhlophis* (Figure 10a, c); in *Anomalepis*, it articulates only with the fused prootic-otoccipital as the supratemporal is absent (see also Haas, 1968; Rieppel et al., 2009). The former taxa are unique among scolecophidians in retaining a supratemporal, albeit as a highly reduced splint of bone (see also Haas, 1968; Rieppel et al., 2009). As is typical of snakes, the squamosal is absent.

The overall mandibular and suspensorial structure of anomalepidids is therefore similar to that of typhlopoids (e.g., elongate mandible, immobile intramandibular joint, and similar length of the quadrate), but with several key differences (e.g., intramandibular structure and articulation, compound bone structure, presence of the supratemporal, absence of the splenial, specific structure of the quadrate, and general presence of teeth on the dentary).

3.5.3 │ Palatomaxillary arch

The anomalepidid maxilla is similar to that of typhlopoids (Figure 9a–d) in being toothed and highly mobile, bearing a pronounced facial process and transversely-to-anteromedially directed tooth row, and being angled posteroventrally at rest (Figure 10a–d). However, the suspension of the maxilla is fundamentally different from typhlopoids: in anomalepidids, the maxilla articulates posteriorly with the ectopterygoid and anterodorsally with the highly reduced prefrontal (Figure 10a–d), rather than pivoting around the palatine as in typhlopoids (Figure 9a–d). This configuration is unique to anomalepidids among squamates.

The pterygoid is elongate and edentulous (Figure 10a–d), as is typical of scolecophidians (Figures 9–11). Unlike typhlopoids (Figure 9), the anterior terminus of the pterygoid is not forked, instead tapering to a simple point as in leptotyphlopids (Figure 11), ventromedial to the pterygoid process of the palatine (Figure 10). The pterygoid does not articulate with the ventral surface of the skull (Figure 10a–d), as in typhlopoids (Figure 9a–d) and unlike leptotyphlopids (Figure 11a–d; Section 3.6.3).

As in typhlopoids (Figure 9b,d), the palatine is highly reduced, with the choanal process forming a spindly arch closely approaching the corresponding vomer (Figure 10b,d). However, unlike typhlopoids, the maxillary process in anomalepidids is quite stubby, extending toward

but still quite broadly distant from the maxilla (Figure 10a–d; see also Rieppel et al., 2009). The palatine instead bears an elongate pterygoid process deflected posterolaterally toward the space between the pterygoid and ectopterygoid (Figure 10b–d). The palatine is therefore not in distinct contact with any other element; this differs greatly from the typhlopoid condition, in which the palatine is an integral component of palatomaxillary biomechanics (Figure 9a–d; Section 3.4.3). A variation of this condition occurs in *Anomalepis*, in which the maxillary process is absent.

The ectopterygoid is present in anomalepidids (Figure 10b–d), a condition unique among scolecophidians (as also noted by for example, Rieppel et al., 2009). The ectopterygoid articulates with the pterygoid posteriorly and braces the maxilla anteriorly (Figure 10b–d). It has the same general shape as in other snakes—that is, comprising a forked maxillary process anteriorly and rod-like pterygoid process posteriorly (Figure 10b–d)—but is markedly reduced compared to other squamates (Figure 1).

The anomalepidid prefrontal is quite distinct from other squamates, including other scolecophidians. It is heavily reduced, forming a thin arch connecting the frontal posteriorly to the maxilla anteroventrally (Figure 10a–c). Its posterior terminus is forked to articulate loosely with the frontal (Figure 10a,b). The prefrontal is thus highly mobile, playing a key role in upper jaw mobility; this is notably distinct from the condition in other scolecophidians, in which the prefrontal is firmly integrated into the lateral snout and skull roof (Figures 9 and 11). The premaxilla is tightly integrated with the rest of the snout, but does not contact the palatomaxillary arches and therefore does not affect palatomaxillary mobility (Figure 10a–c).

Altogether, the palatomaxillary arch is distinctly mobile, as in typhlopoids (Figure 9a–d). However, the configuration and connectivity of the palatomaxillary arch is quite different than in typhlopoids, particularly regarding the presence of the ectopterygoid, the suspension of the maxilla, and the structure, role, and articulation of the prefrontal (Figures 9 and 10). Therefore, although both groups rely on upper jaw mobility and maxillary rotation, the unique palatomaxillary configuration of anomalepidids justifies the classification of this system as a biomechanically distinct version of microstomy.

3.6 │ Leptotyphlopidae

A thorough description of the leptotyphlopid mandible is provided by Kley (2006), who describes in detail many of

the unique features noted in this section. Detailed analyses of the functional morphology of the leptotyphlopid jaws are provided by Kley and Brainerd (1999) and Kley (2001). Earlier studies such as Brock (1932) and List (1966) also describe leptotyphlopid skull anatomy (work summarized in Cundall & Irish, 2008), with micro-CT imagery of various leptotyphlopids available in Rieppel et al. (2009), Pinto, Martins, Curcio, and Ramos (2015), and Martins et al. (2019).

3.6.1 | Mandible

The leptotyphlopid mandible is short and robust, typically measuring approximately 45% of the total skull length (Figure 11), although it measures approximately 35% in *Myriopholis tanae* and 40% in *M. macrorhyncha* and *Namibiana*. The dentary is large and robust relative to other scolecophidians (Figure 11e,f), with the tooth row angled roughly transversely and the teeth sitting on an expanded dental concha (sensu Kley, 2006). Each dentary also bears a prominent symphyseal process (sensu Kley, 2006) anteromedially, extending toward the mental symphysis (Figure 11e,f). As in other snakes, the interramal surface lacks symphyseal facets (see also Kley, 2006). As in typhlopoids—but not anomalepidids, *contra* Rieppel et al. (2009)—the dentary does not bear a posteroventral process (Figure 11e,f).

The splenial and angular are both quite reduced, but are similar in shape to those of other snakes, forming low, anteriorly- and posteriorly-tapering triangles, respectively (Figure 11e,f). The angular and splenial abut against each other; the angular is slightly concave and the splenial slightly convex in the specimens observed herein (Figure 11f), though Kley (2001, 2006) notes the splenial-angular articulation in *Leptotyphlops* (=*Rena*) as being strongly concavoconvex.

The coronoid is smaller than in typhlopoids and anomalepidids (Figures 9–11). Primarily, it is anteroposteriorly shorter, such that it closely approaches the dentary anteroventrally but only directly contacts the compound bone (Figure 11e,f), thus lacking the more extensive articulation with other mandibular elements as present in other scolecophidians (Figures 9e,f and 10e,f). However, it is also much more robust and complex in structure than in other scolecophidians, bearing distinct coronoid, surangular (= posterodorsomedial), and prearticular (= posteroventromedial; present in *Leptotyphlops*) processes (Figure 11e,f; Kley, 2006).

Similarly, the compound bone is greatly shortened relative to other scolecophidians, measuring only 20–25% of the total skull length in most leptotyphlopids and only approximately 15% in *Myriopholis tanae*, though is more

robust and complex (Figure 11e,f). The compound bone articulates posteriorly with the quadrate, dorsally with the coronoid, ventrolaterally with the angular, and anteriorly with the dentary via a loosely overlapping intramandibular hinge (Figure 11e,f). The retroarticular process barely extends beyond the mandibular condyle (Figure 11e,f). Uniquely among snakes, the prearticular and surangular laminae are separate anteriorly (Figure 11f); this condition was noted by Rieppel et al. (2009) as being uniquely shared with anomalepidids among snakes, though see Section 3.5.1 for a comparison of these conditions. Kley (2006) also notes the leptotyphlopid compound bone as being unique among snakes in the presence of a supracotylar process and a horizontal shelf extending along the surangular lamina from this process toward the anterior surangular foramen (Figure 11e,f).

Overall, the intramandibular joint is loosely articulated and quite flexible (Kley, 2001, 2006; Kley & Brainerd, 1999): the splenial abuts against the angular, the dentary and compound bone overlap loosely, and the coronoid approaches but does not directly contact the dentary anteriorly (Figure 11e,f). In contrast, the mandibles of typhlopoids (Figure 9e,f) and anomalepidids (Figure 10e,f) show more extensive integration between the anterior and posterior mandibular elements. This looser articulation in leptotyphlopids is essential in enabling retraction and flexion of the mandible during feeding (Kley, 2006; Kley & Brainerd, 1999).

3.6.2 | Suspensorium

The leptotyphlopid quadrate is oriented at the same anteroventral angle as other scolecophidians, but is comparatively much longer, with its long axis typically equivalent to about 40–45% of the total skull length (Figure 11c), compared to 20–30% in typhlopoids (Figure 9c) and anomalepidids (Figure 10c). Dorsally, the quadrate typically bears a broad, paddle-like cephalic condyle, which is confluent with the quadrate shaft and pierced by a large foramen (Figure 11c; see also Palci et al., 2020), though in some leptotyphlopids the cephalic condyle is simpler and not as expanded (e.g., *Myriopholis tanae*, *Namibiana*, *Rena*, *Tricheilostoma*). The supratemporal and squamosal are both absent, so the quadrate articulates with the braincase: typically the prootic and otoccipital (Figure 11b,c), though the braincase elements may be fused in some taxa (e.g., *Tricheilostoma*).

Altogether, leptotyphlopids therefore exhibit an overall mandibular and suspensorial structure that is quite distinct from other scolecophidians (Figures 9 and 10), consisting of short, robust, and complex mandibular elements (especially the dentary and compound bone),

bearing a flexible intramandibular joint, and being suspended from the skull via an extremely elongate quadrate (Figure 11).

3.6.3 | Palatomaxillary arch

Most distinctively, the palatomaxillary arch is completely edentulous in leptotyphlopids, a condition unique to leptotyphlopids among snakes (see also Kley, 2001). The maxilla is immobile, articulating broadly with the premaxilla, septomaxilla, and prefrontal and closely approaching the palatine (Figure 11a–d), with contact occurring with the latter in some taxa (e.g., *Trilepida*). Extensive ligamentous connections between the maxilla and snout further impede movement of the maxilla, and thus the palatomaxillary arch (Kley, 2001).

The pterygoid is elongate, rod-like, and edentulous (Figure 11b–d), like other scolecophidians (Figures 9 and 10), but underlies the skull much more closely than in other scolecophidians. Uniquely among squamates, the frontal bears a shallow ventral facet posteriorly to accommodate the palatine and the anterior terminus of the pterygoid (Figure 11b). This palatine process of the pterygoid lies alongside the pterygoid process of the palatine in a structurally quite simple articulation (Figure 11b–d).

The palatine is rather robust relative to other scolecophidians (Figures 9 and 10; Sections 3.4.3 and 3.5.3), though is still quite reduced compared to other squamates (Figures 3–7). Similar to the pterygoid, the palatine is more integrated into the skull than in other scolecophidians (Figures 9 and 10), articulating extensively with the frontal dorsally—which bears a corresponding ventral facet—and vomer ventromedially, and very closely approaching the prefrontal, septomaxilla, and maxilla anteriorly (Figure 11b,c). The choanal process is particularly well-developed, articulating broadly with the vomer and frontal (Figure 11b–d).

The ectopterygoid is absent in all leptotyphlopids (see also Chretien et al., 2019). The prefrontal is broad and plate-like (Figure 11a,c), superficially similar in structure to that of dibamids (Figure 5a,c), though see Section 3.1.4 for a comparison to the dibamid condition. The prefrontal is closely integrated with several elements—including the nasal, septomaxilla, maxilla, frontal, and palatine (Figure 11a–c)—though this integration is not as extensive and the prefrontal not as expanded as in typhlopoids (Figure 10a–c). The premaxilla is tightly integrated with the rest of the snout (Figure 11b,c). It briefly contacts the maxilla, but to a much lesser extent and in a different configuration than in non-snake lizards (Figures 3–6). Therefore, whereas the non-snake lizard premaxilla plays a direct role in bracing the palatomaxillary arches and

preventing unilateral movement (see Section 3.1.3), this condition is quite different in leptotyphlopids.

Altogether, the palatomaxillary arches are essentially immobile in leptotyphlopids, with feeding being performed entirely by the mandibles (Kley, 2001, 2006; Kley & Brainerd, 1999). Decoupling of the upper and lower jaws is also evident from the extensive reduction of the ligamentous connection between the pterygoid and quadrate, as in typhlopoids (Kley, 2001). However, in typhlopoids, the palatomaxillary arch is highly mobile and the mandible is relatively rigid (Figure 9; Section 3.4), whereas the opposite is true of leptotyphlopids (Figure 11).

3.7 | Ancestral state reconstruction

The "basic," "detailed microstomy," and "detailed microstomy and macrostomy" scoring methods produced different ASRs, especially at key nodes representing the origins of major clades.

Under the "basic" scoring method (Figure 12), microstomy is the most parsimonious state for the origin of snakes and of alethinophidians, though the evolution of macrostomy was reconstructed equivocally, with microstomy and macrostomy being equally parsimonious in the nodes separating booid-pythonoids and caenophidians (Figure 12a). In contrast, under the "detailed microstomy" scoring method (Figure 13), all states are equally parsimonious for the origins of snakes and of alethinophidians, as well as the origins of Scolecophidia sensu stricto (i.e., Typhlopoidea and Leptotyphlopidae; sensu Miralles et al., 2018) and of all other snakes (i.e., Anomalepididae and Alethinophidia). As in the "basic" scoring method, the reconstruction of macrostomy is equivocal (Figure 13a). Finally, under the "detailed microstomy and macrostomy" scoring method (Figure 14), all versions of microstomy are again equally parsimonious for the origin of snakes, the origin of Scolecophidia sensu stricto, and the origin of all other snakes. However, in contrast to previous scoring methods, the reconstruction of macrostomy is definitive: booid-type and caenophidian-type macrostomy are reconstructed as evolving independently, with "snout-shifting" being most parsimonious for the intervening nodes (Figure 14a).

A similar trend of increasing complexity and decreasing certainty occurs in the ML reconstructions (Figures 12b, 13b, and 14b). Under the "basic" scoring method (Figure 12), microstomy is definitively reconstructed at the origin of snakes (99.996%) and is also the most likely state for the origin of alethinophidians (77.459%), consistent with the MP reconstruction. Unlike the MP
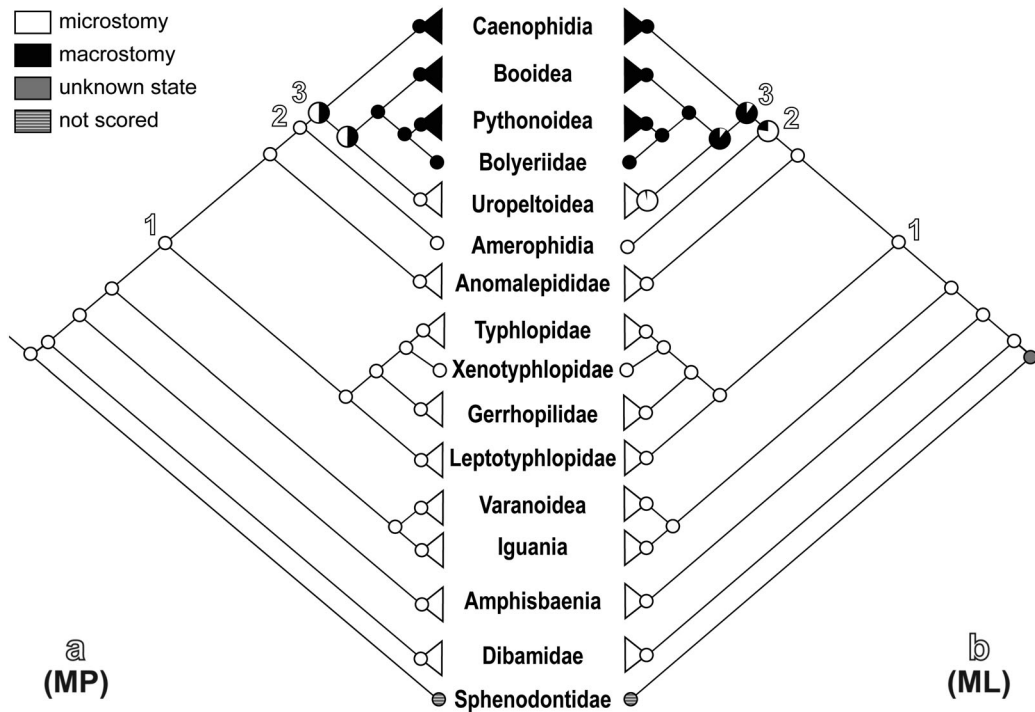
FIGURE 12 Ancestral state reconstruction (ASR) of feeding mechanisms in squamates, using a "basic" character scoring scheme with two states: microstomy and macrostomy. (a) Maximum parsimony (MP)-based ASR; (b) maximum likelihood (ML)-based ASR. Key nodes are numbered: 1, origin of snakes; 2, origin of Alethinophidia; 3, origin of "Macrostomata." See text for details regarding results, including the impact of different character scoring approaches

reconstruction, however, macrostomy is definitively reconstructed (90.059–90.121%) for the nodes connecting booid-pythonoids and caenophidians (Figure 12b). Microstomy is thus reconstructed as having evolved independently in Uropeltoidea compared to Amerophidia (Figure 12b). Under the "detailed microstomy" scoring method (Figure 13), reconstructions at the origin of snakes, of Scolecophidia sensu stricto, and of the ancestor of Anomalepididae and Alethinophidia become equivocal (Figure 13b), as in the MP reconstruction (Figure 13a). In contrast to the MP analysis, though, macrostomy is reconstructed as by far the most likely ancestral alethinophidian state (88.466%; Figure 13b), again reflecting an independent evolution of microstomy in Uropeltoidea and Amerophidia as in the "basic" ML scoring method (Figure 12b). Finally, under the "detailed microstomy and macrostomy" scoring method (Figure 14), the ancestral nodes for snakes, for Scolecophidia sensu stricto, and for all other snakes (Anomalepididae + Alethinophidia) are again equivocal (Figure 14b). "Snout-shifting" is reconstructed as the most likely ancestral state for alethinophidians (58.225%) and at the nodes connecting booid-pythonoids and caenophidians (just over 57% at both nodes). Thus, as in the MP reconstruction for this scoring method (Figure 14a), booid- and caenophidian-type macrostomy are reconstructed as

evolving independently from an ancestral "snout-shifting" condition (Figure 14b).

4 | DISCUSSION

4.1 | Homology

As this discussion centers around homology, a complex topic accompanied by a vast literature, it is important to first define our approach to homology and homology assessment.

Homology can be divided into two sequential concepts: primary homology followed by secondary homology (Brower & Schawaroch, 1996; de Pinna, 1991; Hawkins, Hughes, & Scotland, 1997). Primary homology is essentially a conjecture of homology, in which an anatomical or molecular feature in a taxon is proposed—based on various criteria but prior to any test of phylogenetic congruence—to be homologous to a similar feature in different taxa (Brower & Schawaroch, 1996; de Pinna, 1991; Rieppel & Kearney, 2002; Simões, Caldwell, Palci, & Nydam, 2017). Principal among these criteria is "topological equivalence," that is, articulations with the same surrounding elements, which allow morphological structures in different taxa to be recognized as
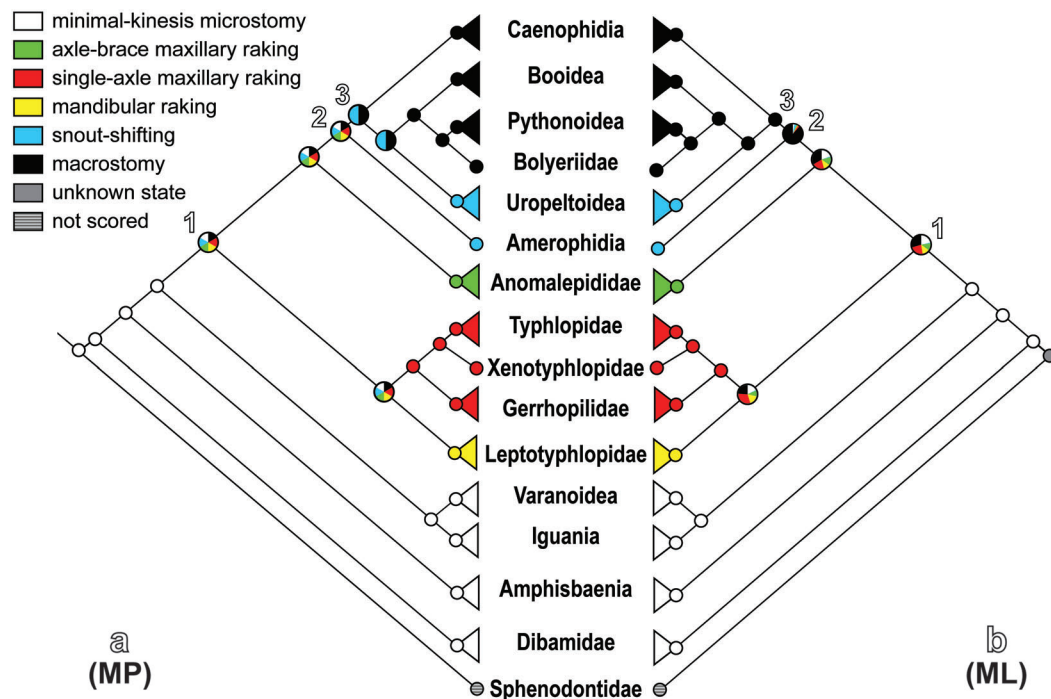
FIGURE 13 Ancestral state reconstruction (ASR) of feeding mechanisms in squamates, using a "detailed microstomy" character scoring scheme dividing microstomy into the five morphotypes described herein: "axle-brace maxillary raking," "mandibular raking," "minimal-kinesis microstomy," "single-axle maxillary raking," and "snout-shifting." Macrostomy is scored under a single state. (a) Maximum parsimony (MP)-based ASR; (b) maximum likelihood (ML)-based ASR. Key nodes are numbered: 1, origin of snakes; 2, origin of Alethinophidia; 3, origin of "Macrostomata." See text for details regarding results, including anatomical descriptions and the impact of different character scoring approaches

evolutionarily equivalent (Rieppel & Kearney, 2002; Simões et al., 2017). Ancillary to topological correspondence are the criteria of "special similarity or quality" of structures and "intermediate forms" (Rieppel & Kearney, 2002). The former refers to specific anatomical similarities among the structures in question, whereas the latter encapsulates ontogeny, fossils, and morphoclines as evidence for "intermediacy" and thus anatomical correspondence of a structure across taxa (Rieppel & Kearney, 2002). These criteria together constitute the "test of similarity" by which a hypothesis of primary homology is either refuted or supported (Patterson, 1982; Rieppel & Kearney, 2002).

Secondary homology is the corroboration of this hypothesis via recovery of the feature in question as synapomorphic across the relevant taxa (de Pinna, 1991; Patterson, 1982; Rieppel, 1994; Rieppel & Kearney, 2002). Just as the "test of similarity" forms the basis for primary homology, this "test of congruence" constitutes the test of secondary homology, and it is only by passing these tests of similarity and congruence that features can be considered homologous or synapomorphic (de Pinna, 1991; Patterson, 1982; Rieppel, 1994; Rieppel & Kearney, 2002). Because a

feature must pass this test of secondary homology to be homologous, and because it can only reach this stage by first being accepted as a primary homolog, it is therefore clear that a hypothesis of primary homology is the most fundamental step in the recognition of homology among taxa and their traits (de Pinna, 1991; Rieppel & Kearney, 2002; Simões et al., 2017).

Beyond the "test of congruence," a final test of homology in extant taxa can also be performed in the form of genetic and/or developmental confirmation, that is, determining whether secondary homologs are consistent at an underlying genetic or developmental level. However, this, too, requires primary homology to even be considered, and then requires substantial resources, not least of which are financial. Furthermore, ontogeny has been debated as a sufficient indicator of homology (e.g., Mabee et al., 2020; Rieppel, 1994; Simões et al., 2017), and this approach would also require far greater knowledge of the connection between genotype and phenotype than generally currently exists. Thus, for now, such assessment of absolute homology is of tertiary relevance from the perspective of researchers interested in trait evolution; assessments of primary and secondary homology remain paramount.
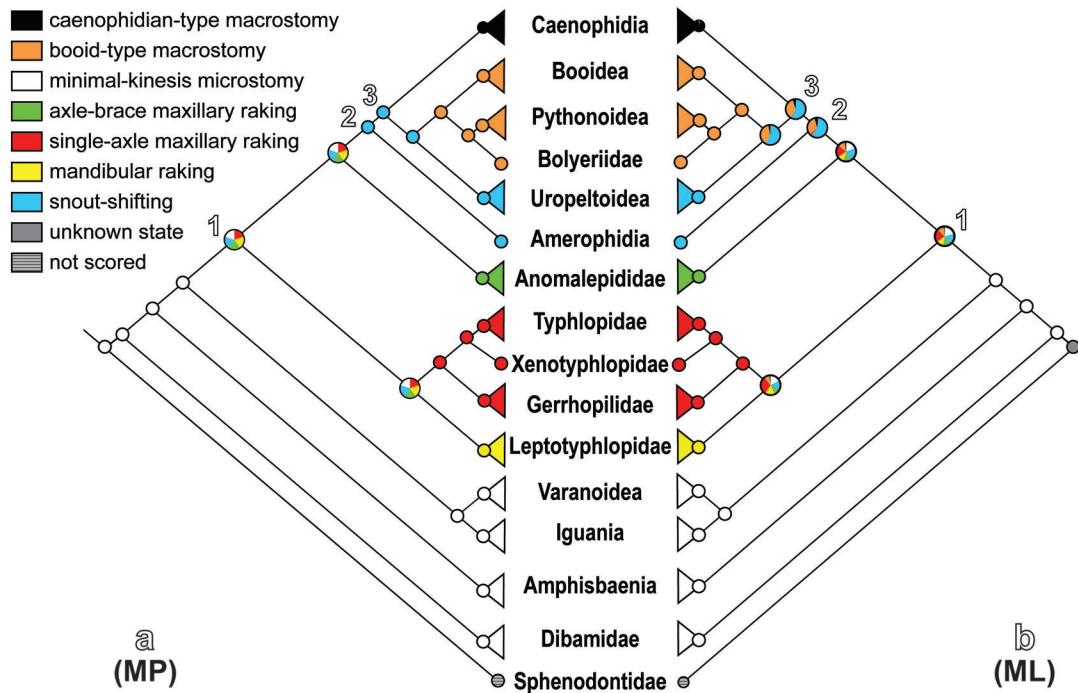
FIGURE 14 Ancestral state reconstruction (ASR) of feeding mechanisms in squamates, using a "detailed microstomy and macrostomy" character scoring scheme. This scheme divides microstomy into the five morphotypes described herein ("axle-brace maxillary raking," "mandibular raking," "minimal-kinesis microstomy," "single-axle maxillary raking," and "snout-shifting") and divides macrostomy into separate morphotypes ("booid-type" and "caenophidian-type" macrostomy) as proposed in recent literature (e.g., Burbrink et al., 2020; Palci, Lee, & Hutchinson, 2016; Strong, Simões, Caldwell, & Doschak, 2019). (a) Maximum parsimony (MP)-based ASR; (b) maximum likelihood (ML)-based ASR. Key nodes are numbered: 1, origin of snakes; 2, origin of Alethinophidia; 3, origin of "Macrostomata." See text for details regarding results, including anatomical descriptions and the impact of different character scoring approaches

However, an important distinction must be drawn between the homology of characters and the homology of character states. Although Patterson (1982, 1988) considered characters and character states to both be "characters," just at more or less inclusive levels, we agree with several other authors (e.g., Brower & Schawaroch, 1996; Hawkins et al., 1997; Sereno, 2007; Simões et al., 2017) that this distinction is not trivial. Characters and character states are indeed similar in that they are both a type of homolog, but differ in that characters are comparable categories which must first be established and tested before character states can be assessed (Brower & Schawaroch, 1996; Hawkins et al., 1997). For example, a modern bird and an extinct non-avian theropod may both bear feathers on the forelimb. However, before attempting to create states reflecting the conditions of these feathers, we must first determine whether the feathers themselves are homologous across these taxa. Only once we have established the homology of these feathers—that is, the existence of the "feather" as a character—can we parse this anatomical structure into meaningful states. In other words, character states are conditioned on the fundamental existence of the character itself, in this example the feather. Thus, just as

primary and secondary homology are inherently sequential subdivisions of homology as a whole, character and character state homology are inherently sequential subdivisions of primary homology.

Brower and Schawaroch (1996) addressed this distinction by considering primary homology at two levels: "topographical identity" (i.e., primary homology of characters) and "character state identity" (i.e., primary homology of character states). Essentially, topographical identity concerns the homology of structures, whereas character state identity concerns the homology of conditions of those structures. Sereno (2007) presented a similar argument for distinguishing between characters as independent variables and character states as mutually exclusive conditions of that character, though specifically eschewed the subject of homology in his treatment of this logical distinction. Unfortunately, despite the significant attention directed toward the identification and testing of topographical identity or character homology (Patterson, 1982, 1988; Rieppel, 1994), the concept of character state identity or homology has been comparatively neglected (Brower & Schawaroch, 1996; Hawkins et al., 1997). Yet, it is this latter concept which is central to answering the

questions at the core of this study, as it is character states which ultimately reflect synapomorphies.

Most importantly, the question of how to test proposed character state homologs has not been explicitly addressed. Previous discussions of the "test of similarity" have focused on primary homology at the level of topographical identity, with this test's major criterion—topological correspondence—being particularly well-suited for testing the homology of characters (e.g., whether two bones are homologous). However, as an organism's anatomy becomes more and more atomized—that is, considered at finer and finer levels of constituent elements, as is necessary to identify homology (Rieppel, 1994; Wilkinson, 1995)—this criterion eventually becomes inadequate. Consider, for example, the squamate quadrate. The observation that this element consistently connects the mandible ventrally with the skull dorsally allows this element to be considered a primary character homolog across squamates. When considering how to test the homology of its character states (e.g., quadrate orientation), though, this criterion is not useful, as the proposed states often differ in some manner unrelated to topology. Indeed, apart from character states dealing with presence/absence of an element or structure or dealing specifically with how a structure articulates with surrounding components, the criterion of topology is often entirely uninformative. How, then, can character state homology be effectively tested?

Given the uninformative nature of the criterion of connectivity, the subsidiary criteria of "special similarity or quality" and "intermediate forms" must be employed (Rieppel & Kearney, 2002). Herein lies another important difference between the primary homology of characters and character states: for characters, anatomical topology is the main arbiter of primary homology, with the specific shape and function of structures being largely disregarded (Rieppel, 1994; Rieppel & Kearney, 2002; Zaher & Rieppel, 2002); in contrast, testing the primary homology of character states requires the consideration almost exclusively of "special quality" of the shape and size of the character in question, with topological relations serving only to identify the structure in question. This approach is often employed operationally, such as Simões et al.'s (2017) proposal that states for continuous characters should only be delimited when there are breaks in the distribution of that character, that is, distinct subdivisions of size and shape that justify consideration of these subdivisions as distinct conditions. Admittedly, "special similarity" may seem rather nebulous compared to the more concrete process of testing character homology by assessing topological relations and connectivity. However, by comparing characters using a combination of shape, size, and function, and by employing operational

criteria such as that described above, it is possible to establish and test hypotheses of character state homology in a manner that is replicable and logically consistent, as exemplified below and as is necessary to establish a "meaningful" character (Rieppel & Kearney, 2002; Simões et al., 2017).

Assessing the homology or identity of character states is in turn necessary to assess the homology of overall character complexes, such as microstomy. This concept of "character complex homology" differs from, and is essentially an expansion upon, the concept of secondary homology. Whereas secondary homology focuses on identifying a single character and its states as synapomorphic, the identification of an integrated set of characters as "homologous" is an inherently more holistic process, requiring the simultaneous consideration of several characters so as to compare entire morphofunctional systems across taxa. Although such an undertaking may seem quite subjective, this is exactly the implication of hypotheses such as whether scolecophidians retain and share an ancestral "microstomatan" feeding mechanism (e.g., Bellairs & Underwood, 1951; Miralles et al., 2018). Such hypotheses of entire morphofunctional systems as homologous are common, yet typically not explicitly assessed or justified. Thus, through this discussion of squamate feeding mechanisms, we aim to explain and enact a more transparent, replicable, and theoretically consistent approach to this broader conceptualization of homology. This more explicit approach is essential in rendering subsequent hypotheses of character evolution replicable, testable, and falsifiable (Rieppel & Kearney, 2002), as well as in avoiding the pitfalls of either under- or over-atomizing complex anatomies (e.g., as discussed by Wilkinson, 1995 for "composite" versus "reductive" character construction).

Despite the differences between the homology of individual characters and of overall character complexes, the fundamental question underlying the search for homology remains the same: did these structures (or complexes) evolve once, thus uniting these taxa as a monophyletic group bearing a synapomorphic condition, or did these structures (or complexes) evolve independently? Of course, for character complexes there is no single "test of congruence" which can instantly characterize the entire complex as synapomorphic. Rather, a different benchmark for considering such conditions as "homologous" or "synapomorphic" is necessary.

Most critically, such an approach must be able to recognize shared common ancestry while also allowing for variation among taxa. To this end, we propose a guideline based on Patterson's (1982, p. 35) definition of a morphotype as "a list of the homologies (synapomorphies) of

a group." We herein use the term "morphotype" to refer to homologous character complexes, defined by the possession of key synapomorphies (i.e., secondarily homologous character states). Similar to a taxonomic diagnosis, a character complex can be considered homologous among taxa—that is, considered to belong to the same morphotype—if it possesses the key synapomorphies of that morphotype and does not possess the features "diagnosing" other morphotypes. Character complexes can only be considered homologous if their constituent characters and character states pass the tests of primary and secondary homology, as well as the guideline described above; as such, this approach to morphotype homology allows such a hypothesis to be tested and falsified. This rigorous assessment is essential for proper identification of homology (Rieppel & Kearney, 2002), which is in turn critical for higher-level evolutionary analyses, such as ASRs (see below) or recent computational advances related to homology (e.g., Mabee et al., 2020 and the Phenoscape project).

4.2 | Is the jaw complex homologous among scolecophidians?

An intriguing hypothesis proposed in recent works suggests that the jaw structures in anomalepidids, leptotyphlopids, and typhlopoids may have evolved independently (Caldwell, 2019; Chretien et al., 2019; Harrington & Reeder, 2017). This is of course in distinct contrast to characterizations of the scolecophidian condition as more-or-less homogenous and as reflecting the ancestral snake condition (e.g., Miralles et al., 2018). Even in previous acknowledgments of the autapomorphic nature of the scolecophidian skull (e.g., Hsiang et al., 2015; Kley & Brainerd, 1999; Rieppel, 1988), the uniqueness of this morphology is typically emphasized for scolecophidians as a whole in comparison to other squamates, rather than scolecophidians in comparison to each other (though see Bellairs & Underwood, 1951; Cundall & Irish, 2008; Kley, 2001; List, 1966 for preliminary discussions of this hypothesis).

The results of this study provide strong support for the independent evolution of microstomy in each major scolecophidian clade. We propose that each clade exhibits a unique morphotype of microstomy (Figure 1)—"single-axle maxillary raking" in typhlopoids, "axle-brace maxillary raking" in anomalepidids, and "mandibular raking" (sensu Kley & Brainerd, 1999) in leptotyphlopids—each of which is distinguished by several features that are universal within and entirely unique to each morphotype (Tables 3 and 4; see also Caldwell, 2019; Chretien et al., 2019; Kley, 2001).

In the "single-axle maxillary raking" morphotype (Figure 9; Tables 3 and 4), prey ingestion and transport occurs exclusively via asynchronous unilateral movements of the maxillae, which rotate about the elongate maxillary process of the palatine (Chretien et al., 2019; Kley, 2001). The palatines and pterygoids are highly reduced; these elements contribute to rotation of the maxillae, but only the maxillae bear teeth and thus only the maxillae are directly responsible for prey transport (Figure 9a–d; Caldwell, 2019; Chretien et al., 2019; Kley, 2001). The mandibles are highly reduced and rigidly integrated, so as to also not contribute to prey transport (Figure 9e–f; Kley, 2001; Caldwell, 2019).

In the "axle-brace maxillary raking" morphotype (Figure 10; Tables 3 and 4), the maxilla is suspended from the reduced and mobile prefrontal and braced posteriorly by the ectopterygoid (Chretien et al., 2019). The pterygoids and palatines are highly reduced, similar to "single-axle maxillary raking," and the mandibles are reduced and immobile, though to a lesser extent than in the "single-axle" morphotype (Figures 9 and 10). The highly reduced teeth on the mandible at most help to hold the prey in the mouth during maxillary raking.

In the "mandibular raking" morphotype (Figure 11; Tables 3 and 4), the palatomaxillary arch is immobile and edentulous, thus not contributing at all to prey transport (Chretien et al., 2019; Kley, 2001, 2006; Kley & Brainerd, 1999). Rather, it is the highly mobile mandible—including a flexible intramandibular joint—that drives feeding, bearing a quite robust and complex structure in comparison to the conditions in "single-axle" and "axle-brace" microstomy (Figures 1 and 9–11; List, 1966; Kley & Brainerd, 1999; Kley, 2001, 2006; Caldwell, 2019; Chretien et al., 2019). The mandibles move in a bilaterally synchronous manner, being joined at the symphysis via a cartilaginous nodule (Kley, 2006) which enables rotation between the left and right mandibles, but prevents lateral and anteroposterior separation of the mandibular tips (Kley, 2001, 2006).

These morphotypes are distinct and non-homologous because they each comprise key features that are not homologous with the corresponding conditions in other taxa (Figures 9–11; Tables 3 and 4). Consider, for example, the maxillary process of the palatine as a character, and its degree of elongation as the character states in question. At the level of topographical identity, the maxillary process passes the "test of similarity" among squamates, as it occurs in a consistent topographic location and so can be considered a primary homolog. However, when considering its character states, the elongate condition of the maxillary process is consistent among typhlopoids (Figure 9), but is both anatomically and functionally unique compared to the condition of this

TABLE 3 Summary of morphotypes of "microstomy," including select key synapomorphies of each morphotype

Morphotype and taxa	Key biomechanics	Key synapomorphies
Axle-brace maxillary raking (Anomalepididae)	• Suspension of maxilla from prefrontal • Bracing of maxilla by ectopterygoid • No contribution of mandible to feeding	• Reduced, arch-like, and mobile prefrontal • Reduced ectopterygoid • Highly reduced palatine, including stubby maxillary process • Inflexible mandible, with elongate angular and reduced dentition • Elongate and anteroventrally oriented quadrate
Mandibular raking (Leptotyphlopidae)	• Bilaterally synchronous retraction of mandibles • No contribution of palatomaxillary arch to feeding	• Edentulous and fixed palatomaxillary arch • Reduced mandible with flexible intramandibular joint • Robust dentary, including dental concha and symphyseal process • Structurally complex coronoid and compound bone • Extremely elongate and anteroventrally oriented quadrate
Minimal-kinesis microstomy (Non-snake lizards)	• No unilateral movement of jaws • Minimal kinesis due to tight integration and strong bracing of jaw elements	• Robust and tightly integrated palatomaxillary arch elements • Tight bracing at ectopterygoid-maxilla and -pterygoid articulations • Osseous contact between premaxilla and maxilla • Well-developed basipterygoid processes • Robust mandibular elements tightly integrated, including across intramandibular joint • Symphyseal facets on mandibular symphysis • Stout and upright quadrate, with squamosal present
Single-axle maxillary raking (Typhlopoidea)	• Rotation of maxilla about maxillary process of palatine • No contribution of mandible to feeding	• Elongate and rod-like maxillary process of palatine • Deep medial excavation or foramen in maxilla • Edentulous and inflexible mandible, including elongate splenial and reduced angular • Elongate and anteroventrally oriented quadrate
Snout-shifting (Uropeltoidea and Amerophidia)	• Minor unilateral movement of palatomaxillary arches • Flexion of mandibles	• "Ball-and-socket"-like maxilla-palatine joint • Loose palatine-pterygoid joint • Robust palatine, though lacking osseous contact with vomer • Moderate basipterygoid processes • Robust mandible with flexible intramandibular joint, including abutting splenial-angular contact • Stout and upright quadrate, bearing large suprastapedial process

Note: See text for details, including anatomical descriptions and additional synapomorphies. See Table 4 for key features summarized in taxon-character matrix format.

TABLE 4 Key features of each morphotype of "microstomy," presented in taxon-character matrix format

	Axle-brace maxillary raking (Anomalepididae)	Mandibular raking (Leptotyphlopidae)	Minimal-kinesis microstomy (Non-snake lizards)	Single-axle maxillary raking (Typhlopoidea)	Snout-shifting (Uropeltoidea and Amerophidia)
Dentary teeth: present (0); absent (1).	0/1	0	0	1	0
***Dentary*, *tooth row*, *orientation*: roughly anteroposterior (0); transverse (1).	0	1	0	–	0
***Maxillary teeth*: present (0); absent (1).	0	1	0	0	0
Maxilla, *tooth row*, *orientation*: roughly anteroposterior (0); transverse (1).	1	–	0	1	0
Pterygoid teeth: absent (0); present (1).	0	0	0	0	1
Palatine teeth: absent (0); present (1).	0	0	0	0	1
***Premaxilla*, *articulation with maxilla*, *extent of integration*: broad osseous contact (0); loosely articulated (1); broadly separate (2).	2	1	0	2	1
***Frontal*, *articulation with prefrontal*, *complexity*: extensive, abutting, or overlapping (0); reduced, clasping (1).	1	0	0	0	0
***Frontal*, *ventral facet accommodating palatine and pterygoid*: absent (0); present (1).	0	1	0	0	0
***Prefrontal*, *articulation with maxilla*, *configuration*: abutting or overlapping (0); interlocking along facial process of maxilla in "peg-and-socket"-like joint (1); forked/bifurcating (2); broadly swivelling (3).	2	0	0	3	1
***Palatine*, *articulation with pterygoid*, *configuration*: broadly abutting or overlapping (0); interlocking, complex	3	3	0/1	2	1

T A B L E   4   (Continued)

	Axle-brace maxillary raking (Anomalepididae)	Mandibular raking (Leptotyphlopidae)	Minimal-kinesis microstomy (Non-snake lizards)	Single-axle maxillary raking (Typhlopoidea)	Snout-shifting (Uropeltoidea and Amerophidia)
but mobile (1); interlocking, simple forking (2); simple flap-overlap (3).					
Palatine, medial (=choanal, vomerine) process, osseous contact with vomer: present (0); absent (1).	1	0	0	1	1
***Palatine, medial (=choanal, vomerine) process, form*: flat process extending horizontally (0); broad arch (1); narrow arch (2).	2	1	0	2	1
***Palatine, maxillary process*: present (0); highly reduced or absent (1).	1	0	0	0	0
***Palatine, maxillary process, articulation with maxilla, configuration*: broad osseous contact (0); articulating via "ball-and-socket"-like joint accommodating palatine process of maxilla (1); articulating with large medial excavation or foramen on maxilla (2); articulation minimal (3).	–	3	0	2	1
Pterygoid, posterior process (=quadrate ramus), form: robust (0); simple, rod-like (1).	1	1	0	1	0
Ectopterygoid: present (0); absent (1).	0	1	0	1	0
****Ectopterygoid, form*: robust (0); distinctly reduced, rod-like (1).	1	–	0	–	0
Quadrate, orientation in lateral view: roughly vertical (0); slanted clearly anteriorly, nearly horizontal (1).	1	1	0	1	0

(Continues)

TABLE 4 (Continued)

	Axle-brace maxillary raking (Anomalepididae)	Mandibular raking (Leptotyphlopidae)	Minimal-kinesis microstomy (Non-snake lizards)	Single-axle maxillary raking (Typhlopoidea)	Snout-shifting (Uropeltoidea and Amerophidia)
***Quadrate, shaft, length*: short/stout (0); elongate (1); extremely elongate (2).	1	2	0	1	0
Supratemporal: present (0); highly reduced or absent (1).	1	1	0	1	0
Squamosal: present (0); absent (1).	1	1	0	1	1
Parabasisphenoid, basipterygoid processes: present (0); absent (1).	1	1	0	1	0
***Parabasisphenoid, basipterygoid processes, size*: large, forming distinct projections (0); moderate, forming low ridges (1).	–	–	0	–	1
***Dentary, dental concha*: absent (0); present (1).	0	1	0	0	0
***Dentary, symphysis, articular facet*: present (0); absent (1).	1	1	0	1	1
***Dentary, symphysis, symphyseal process*: absent (0); present (1).	0	1	0	0	0
Dentary, symphysis, cartilaginous inter-ramal nodule: absent (0); present (1).	?	1	0	1	0
Angular, form: robust (0); simple, rod-like (1).	1	0	0	1	0
Splenial: present (0); absent (1).	1	0	0	0	0
Splenial, articulation with angular, configuration: overlapping (0); abutting (1).	–	1	0	0	1
***Splenial, length relative to dentary*: shorter than (0); subequal to or longer than (1).	–	0	0	1	0

T A B L E 4 (Continued)

	Axle-brace maxillary raking (Anomalepididae)	Mandibular raking (Leptotyphlopidae)	Minimal-kinesis microstomy (Non-snake lizards)	Single-axle maxillary raking (Typhlopoidea)	Snout-shifting (Uropeltoidea and Amerophidia)
Surangular-articular, fusion: unfused (0); fused to form compound bone (1).	1	1	0	1	1
***Compound bone, surangular and prearticular laminae, fusion*: fully fused (0); briefly separate (1); fully separate (2).	1	2	–	0	0
***Compound bone/ surangular, anterior terminus, orientation*: not downcurved (0); distinctly downcurved (1); slightly downcurved, resulting in gentle sinusoidal shape (2).	2	0	0	1	0
***Surangular, supracotylar process*: absent (0); present (1).	0	1	0	0	0

Note: Each morphotype comprises a distinct suite of character states, with many features being entirely unique to and consistent within each morphotype (indicated by ***). Scorings are based on the exemplar taxa in Figures 3–4 for non-snake lizards, Figure 7 for "anilioids," and Figures 9–11 for scolecophidians; see main text for variations within these broader groups, as well as for anatomical descriptions and additional synapomorphies.

process in any other squamate (Figures 3–8, 10, and 11). Thus, this character state passes the "test of similarity" among typhlopoids but fails this test in comparison to other squamates, and so cannot be considered synapomorphic between typhlopoids and other squamates.

This same process of rejecting homology at the level of character state identity also applies to other key typhlopoid features, such as the medially excavated maxilla, the downcurved compound bone, and the enlarged splenial, among many other features (Figure 9; Section 3.4; Tables 3 and 4). These unique primary homologs, alongside a unique combination of other distinct features, ultimately result in a feeding mechanism that is fundamentally different from the condition in any other squamate—including other scolecophidians—and so represents a morphotype functionally and evolutionarily unique to typhlopoids: "single-axle maxillary raking."

This process can also be applied to the key features of anomalepidids (Figure 10; Tables 3 and 4; Section 3.5), such as the structure of the prefrontal and ectopterygoid, and those of leptotyphlopids (Figure 11; Tables 3 and 4;

Section 3.6), such as the edentulous maxilla, fixed palatine and pterygoid, uniquely structured dentary, and extremely elongate quadrate. Again, because the character states in question are anatomically consistent within each clade but distinct from the condition in any other taxon, each state passes the "test of similarity" within each clade but fails across clades. Thus, "axle-brace maxillary raking" and "mandibular raking" each comprise their own set of unique character states that cannot be synapomorphic with any other squamate, just as in "single-axle maxillary raking," and so are also distinct morphotypes not representative of an ancestral snake condition (see also Kley, 2001, 2006; Kley & Brainerd, 1999).

Of course, there are certain features of the jaws and suspensorium that are consistent across scolecophidians, such as the anteriorly oriented quadrate, absent or heavily reduced supratemporal and ectopterygoid, tall coronoid, and, at least in typhlopoids and leptotyphlopids, the cartilaginous interramal nodule (Figures 9–11; Kley, 2001, 2006; Rieppel et al., 2009). The presence of these shared conditions would appear to undermine our hypothesis of the independent evolution

of microstomy: each of these conditions passes the "test of similarity" across scolecophidians and, according to morphology-based phylogenies in which scolecophidians are monophyletic (e.g., Garberoglio, Apesteguía, et al., 2019; Gauthier et al., 2012; Hsiang et al., 2015), also passes the "test of congruence." Thus, based on these criteria, these character states can be accepted as synapomorphic for scolecophidians.

However, an important counterpoint to this "undermining" is the extensive paedomorphosis exhibited by scolecophidians relative to other squamates (Caldwell, 2019; Da Silva et al., 2018; Kley, 2006; Palci et al., 2016; Strong et al., 2021). Paedomorphosis is the retention of features typical of embryonic or juvenile individuals of an ancestral taxon into adults of a descendant taxon (McNamara, 1986). In scolecophidians, as noted by other authors (e.g., Caldwell, 2019; Kley, 2006; Strong et al., 2021), this paedomorphosis occurs throughout the skull, but is particularly prevalent in the mandible, palatomaxillary arch, and suspensorium.

This includes the anteroventral orientation of the quadrate (Figures 9–11), a condition typical of embryonic squamates (Caldwell, 2019; Kamal, 1966; Kley, 2006; Rieppel & Zaher, 2000; Scanferla, 2016). The cartilaginous interramal nodule is likely also paedomorphic: although Kley (2006) interpreted this feature as a fibrocartilaginous elaboration of the midline raphe in *Leptotyphlops* (=*Rena*), he also noted that the midline raphe is universally absent in other scolecophidians, causing us to consider this hypothesis unlikely. We instead agree with other interpretations of this nodule as an extension of the Meckelian cartilages anterior to the dentary tips (e.g., Caldwell, 2019; Kley, 2001), a phenomenon that is known to occur throughout the embryonic development of the mandible in snakes (e.g., Al-Mohammadi, Khannoon, & Evans, 2020) and that therefore renders the scolecophidian interramal nodule paedomorphic. Features related to the reduction and simplification of elements (e.g., pterygoid, palatine, supratemporal; Figures 9–11) are also tied to paedomorphosis, with the reduction or absence of these structures reflecting early developmental stages in other squamates (e.g., see Ollonen, Silva, Mahlow, & Di-Poï, 2018; Polachowski & Werneburg, 2013; Werneburg et al., 2015). Finally, a disproportionately tall coronoid (Figures 9e,f, 10e,f, and 11e,f) aids in increasing mechanical advantage of the lower jaw musculature (Rieppel, 1984), an adaptation important in compensating for the reorganization of the lower jaw as occurs in miniaturized and paedomorphic vertebrates (Hanken & Wake, 1993; Olori & Bell, 2012).

Given that scolecophidians are highly miniaturized, that miniaturization often co-occurs with fossoriality (Olori & Bell, 2012), and that miniaturization has been hypothesized as being caused by—or at least strongly correlated with—paedomorphosis (Fröbisch & Schoch, 2009; Hanken, 1984; Wake, 1986), these shared features thus all relate to miniaturization. Importantly, miniaturization, fossoriality, and paedomorphosis are all strongly associated with homoplasy (Fröbisch & Schoch, 2009; Hanken & Wake, 1993; Maddin, Olori, & Anderson, 2011; Olori & Bell, 2012; Wiens, Bonett, & Chippindale, 2005). In other words, the only major features of the scolecophidian jaw complex which fully pass the test of primary homology—and which potentially unite scolecophidians to the exclusion of other snakes—are highly homoplastic. It is therefore quite possible that the aforementioned conditions apparently shared among scolecophidians in fact arose independently, as the result of the independent evolution of fossoriality and miniaturization in each scolecophidian clade (Caldwell, 2019; Chretien et al., 2019).

Indeed, such a hypothesis is consistent with the separate morphotypes of "microstomy" present in scolecophidians. This proposed scenario of independent excursions into fossoriality and miniaturization presents a logical explanation for why the jaws and suspensorium reflect so many entirely unique and non-homologous conditions across the scolecophidian clades (see also Caldwell, 2019; Chretien et al., 2019). This degree of variation is consistent with the morphological novelty typical of miniaturized vertebrates (Hanken, 1984; Hanken & Wake, 1993). Occurring simultaneously along these independent paths of miniaturization and fossoriality, we propose that other elements—such as the supratemporal, pterygoid, and quadrate—converged upon conditions that are known to have frequently evolved independently throughout Squamata (e.g., dibamids: see Figure 5 and Rieppel, 1984; amphisbaenians: see Figure 6 and Gans & Montero, 2008; uropeltids: see Olori & Bell, 2012; colubroids: see Strong et al., 2021).

Although such a hypothesis clearly contradicts the morphology-based phylogenetic placement of scolecophidians as a single clade (e.g., Garberoglio, Apesteguía, et al., 2019; Gauthier et al., 2012; Hsiang et al., 2015), it is important to recognize the potential role of homoplasy in biasing phylogenies, especially as associated with paedomorphosis and/or fossoriality (Hanken & Wake, 1993; Pinto et al., 2015; Struck, 2007; Wiens et al., 2005). As examined previously for paedomorphic salamanders, morphology-based phylogenies can be misled by the shared presence of paedomorphic traits, causing the affected taxa to be artificially grouped together (Wiens et al., 2005). The distinct incongruence between molecular and morphological phylogenies of scolecophidians (e.g., Gauthier et al., 2012; Hsiang et al.,

2015; versus Figueroa et al., 2016; Zheng & Wiens, 2016) further supports the possibility that confounding factors may be at play. It is thus clear that, in order to resolve longstanding questions regarding scolecophidian phylogeny and further assess the evolutionary hypotheses presented herein, a robust morphological and molecular framework for scolecophidians is crucial. Although such an undertaking is beyond the scope of this study, morphological analyses similar to the present study represent a key component in laying the foundation for such a framework.

Ultimately, we definitively reject the contention that scolecophidians are "morphologically and ecologically consistent" (Miralles et al., 2018, p. 1785). From a biomechanical perspective, the jaws of each scolecophidian clade function in a completely different manner, as outlined in the Section 3. This lack of consistency also occurs from an evolutionary perspective, on the basis of primary homology, as argued above. Beyond superficially similar reduction of the jaw complex in each scolecophidian clade, almost every element of the upper and lower jaws shows fundamental anatomical and functional differences (Figures 9–11; Tables 3 and 4), and those elements that do remain consistent (e.g., pterygoid, suspensorium) are highly susceptible to homoplasy.

Importantly, because microstomy occurs via a distinct, non-homologous, and thus independently evolving morphotype in each scolecophidian clade, we can therefore logically reject the hypothesis that scolecophidians as a whole represent a morphologically homogenous remnant of the ancestral snake condition, as per Caldwell (2019), Chretien et al. (2019), and Strong et al. (2021), and contra, for example, Rieppel (2012) and Miralles et al. (2018). Indeed, scolecophidians are so strongly influenced by the constraints of ecology and heterochrony (see also Section 4.4)—and thus so highly modified relative to other squamates and to each other—that for this group to have given rise to the morphology of all other snakes is in our view highly unlikely (see also Caldwell, 2019; Chretien et al., 2019; Strong et al., 2021). Rather than a plesiomorphic condition, the various scolecophidian lineages instead reflect convergence upon a miniaturized, fossorial, and myrmecophagous ecomorph, superficially similar to each other but in reality highly autapomorphic (Caldwell, 2019; Chretien et al., 2019; Harrington & Reeder, 2017). The combination of strongly homoplastic and strikingly divergent features across scolecophidians highlights the complicated interplay between determinism and contingency in organismal evolution, especially in the context of phenomena such as fossoriality, myrmecophagy, miniaturization, and paedomorphosis.

4.3 | Is the scolecophidian jaw complex homologous to the condition in non-snake lizards?

The hypothesis that scolecophidians are retaining the same version of microstomy as in non-snake lizards—that is, that these conditions are homologous—is an implicit though inherent assumption of how these taxa are scored in ASRs of this feature (e.g., Harrington & Reeder, 2017; Miralles et al., 2018). This assumption of homology is more broadly reflected in the traditional division of squamates into "Macrostomata" and non-macrostomatans (reviewed in Rieppel, 1988), with the corresponding assumption that, because scolecophidians, early-diverging alethinophidians, and non-snake lizards all lack macrostomy, this lack of macrostomy—as characterized in this simplistic manner (on the complexities of macrostomy, see Palci et al., 2016; Caldwell, 2019)—is a fundamentally plesiomorphic retention from non-snake lizards (e.g., Bellairs & Underwood, 1951; Rieppel, 2012). However, we argue that these groups exhibit distinct morphotypes of microstomy (Tables 3 and 4), rendering the evolution of this feeding mechanism much more complex than the aforementioned perspective.

From one line of reasoning, if we accept the hypothesis that microstomy is not homologous across scolecophidians and instead evolved independently in each clade (as argued above), then logically we must reject the hypothesis that "microstomy" as present in scolecophidians is "primitive" or homologous to that of non-snake lizards. Recent discussions arguing that the scolecophidian skull could quite reasonably be derived from an alethinophidian or even "macrostomatan" ancestor (Caldwell, 2019; Harrington & Reeder, 2017; Kley, 2006; Strong et al., 2021) further indicate that the presence of a scolecophidian morphotype—including the presence of microstomy—does not in and of itself indicate a "microstomatan" ancestral condition of snakes. Even if we accept the proposition from several authors—problematic as these hypotheses may be (Caldwell, 2019; Kley, 2006)—that scolecophidians retain certain plesiomorphic features of non-snake lizards (e.g., multipennate jaw adductor musculature, tall coronoid; Kley, 2006; Rieppel, 2012), the presence of many non-homologous features indicates that microstomy cannot be considered a homogenous or consistent condition across these taxa.

A particularly important feature is the mandibular symphysis, which in non-snake lizards bears distinct symphyseal facets but which in snakes—including scolecophidians—is smooth and more widely separated (see also Kley, 2006). As discussed by Kley (2006), this observation suggests that scolecophidians in fact evolved

from a more "snake-like" ancestor, in which the mandibles were already capable of independent movement and possibly macrostomy. This of course contradicts the hypothesis of scolecophidians retaining a non-snake lizard-like version of this component of "microstomy." Similarly, although the tightly-linked interramal symphysis in scolecophidians may superficially evoke the condition in non-snake lizards, the robust cartilaginous nodule in scolecophidians is entirely different from other squamates (Kley, 2006) and, as noted above, is most likely a distinctly paedomorphic—not plesiomorphic—condition. Finally, Kley (2006) also notes the *M. retractor pterygoidei* and *M. protractor pterygoidei* in leptotyphlopids as suggesting derivation from an ancestral condition in which the palatomaxillary arch was quite mobile. This in turn implicates a possibly "macrostomatan" ancestral condition and contradicts Rieppel's (2012) conclusion that the scolecophidian jaw adductor musculature reflects a plesiomorphic non-snake lizard anatomy (see also Caldwell, 2019).

Several other key conditions of the jaws and suspensorium are also not homologous among scolecophidians, "anilioids," and non-snake lizards. The maxillary process of the palatine was discussed above in the context of "single-axle maxillary raking," though is also important when considering "anilioids" and non-snake lizards (Table 4). In non-snake lizards, this process is quite broad, articulating extensively with the maxilla (Figures 3b,d, 4b,d, 5b,d, and 6b,d); in uropeltoids and amerophidians, however, this process is reduced and the maxilla-palatine articulation is instead a "ball-and-socket"-like joint formed mainly by the palatine process of the maxilla (Figures 7b,d and 8b,d). Thus, although the maxillary process of the palatine passes the "test of similarity" at the level of topographical identity (i.e., primary character homology), it fails at the level of character state identity, as it exhibits anatomically and functionally distinct forms across these taxa. The condition of this character in uropeltoids and amerophidians is further notable in that, although these lineages are not closely related (Figures 1 and 2), they exhibit primary homology or character state identity of the "ball-and-socket"-like joint. This is a key innovation of the feeding mechanism in these taxa, distinct from any other "microstomatan" squamate. The shared presence of this feature in these distinct lineages suggests it to better reflect the ancestral snake condition than any state exhibited by scolecophidians for this character.

The vomerine process of the palatine also differs among these taxa (Table 4), with non-snake lizards bearing a broad vomerine process in extensive osseous contact with the vomer (Figures 3b,d, 4b,d, 5b,d, and 6b,d), uropeltoids and amerophidians bearing a broad choanal

process lacking this sutural contact (Figures 7b,d and 8b,d), and scolecophidians bearing a highly reduced and likely paedomorphic choanal process (Figures 9b,d, 10b,d, and 11b,d). Other characters with states that differ across non-snake lizards, "anilioids," and scolecophidians include: the basipterygoid processes and their size and extent of articulation with the pterygoids; the presence and extent of the premaxilla-maxilla articulation; the integration and extent of mobility between the ventral and dorsal snout elements; and the suspension of the quadrate (Figures 1 and 3–11; Tables 3 and 4).

All of these characters exhibit character states which differ distinctly and consistently among the taxa in question (Tables 3 and 4; as described in the Results), which bear distinct functional consequences, and which altogether reflect a lack of primary and thus secondary homology across these taxa. As a result, because so many of these key features are nonhomologous, the overall jaw complex cannot be considered consistent across these taxa. Rather, non-snake lizards, "anilioids," and the scolecophidian clades each exhibit distinct morphotypes of microstomy, characterized by their own unique sets of character states (Figures 1 and 3–11; Tables 3 and 4).

The morphotype exhibited by non-snake lizards (Figures 3–6; Tables 3 and 4) is characterized by robust and tightly integrated jaw elements compared to the condition in snakes, particularly at the intramandibular joint and mandibular symphysis. We herein term this morphotype "minimal-kinesis microstomy," in recognition of the numerous robustness-related character states of this morphotype, as well as previous discussions of the minimally kinetic nature of the non-snake lizard skull relative to that of snakes (e.g., Cundall, 1995).

The uropeltoid and amerophidian morphotype (Figures 7 and 8; Tables 3 and 4) is similar to non-snake lizards in terms of general robustness, though it differs in certain key aspects (see also Cundall, 1995). This includes greater kinesis of the intramandibular joint and, perhaps most importantly, the capacity for unilateral movement of the palatomaxillary arches (Section 3.2; Cundall, 1995). Because decoupling of the snout elements is integral to the jaw biomechanics of *Cylindrophis* (see Section 3.2.3; analyzed in greater detail by Cundall, 1995), and has further been proposed to occur throughout Uropeltoidea and Amerophidia (Cundall, 1995), we retain Cundall's (1995) use of the term "snout-shifting" to describe this biomechanical morphotype (Tables 3 and 4).

However, despite its capacity for unilateral palatomaxillary movement, the "snout-shifting" jaw complex is still more closely integrated than the condition in "macrostomatan" snakes, indicating a much more limited degree of kinesis in uropeltoids and amerophidians

relative to these more derived alethinophidians (Cundall, 1995). The "snout-shifting" morphotype is therefore intermediate between the "minimally-kinetic microstomatan" and "macrostomatan" conditions in terms of both anatomy and function (Cundall, 1995; Cundall & Rossman, 1993; Kley, 2001).

Due to this intermediacy, it is tempting to hypothesize the "anilioid" skull as representing the ancestral snake condition. Indeed, the presence of a highly consistent jaw morphotype in uropeltoids and amerophidians—two basally-diverging but phylogenetically distinct alethinophidian lineages (Figures 1 and 2)—provides compelling evidence for this morphotype as ancestral for alethinophidians, if not all snakes. However, attempts to reconstruct the ancestral condition for snakes should not rest solely on extant taxa (see also Caldwell, 2019). Given that millions of years have elapsed since the origin of snakes (e.g., 166.76 Ma; Garberoglio, Apesteguía, et al., 2019), a more logical approach would be to give precedence to the fossil record, using morphological information from taxa temporally—and thus likely morphologically—much closer to the origin of Ophidia (Caldwell, 2019). This is especially true as extinct taxa can provide character state information not present in modern taxa, thus providing a necessary supplement to the neontological record (Betancur-R, Ortí, & Pyron, 2015; Caldwell, 2019; Finarelli & Flynn, 2006; Finarelli & Goswami, 2013; Mongiardino Koch & Parry, 2020; Puttick, 2016).

This is not to say that extant taxa are altogether uninformative in hypothesizing the ancestral snake morphology. Indeed, recently discovered and exceptionally preserved specimens of the extinct *Najash* (Garberoglio et al., 2019; Garberoglio, Apesteguía, et al., 2019) reveal a morphology similar to "anilioids," suggesting uropeltoids and amerophidians to be the extant taxa most representative of this ancestral condition (Caldwell, 2019; Garberoglio, Gómez, et al., 2019). However, an important logical distinction must be emphasized: uropeltoids and amerophidians are not representative of this ancestral morphology because they are the most "lizard-like" groups of snakes; rather, they are representative of this ancestral condition because they are the extant groups most morphologically similar to early-evolving fossil snakes (Garberoglio, Gómez, et al., 2019). The primacy of the fossil record in hypothesizing ancestral conditions is paramount (Caldwell, 2019), as reflected by the key role of fossils in fuelling phylogenetic debates regarding the origin of snakes (e.g., Apesteguía & Zaher, 2006; Caldwell, 2000; Caldwell, 2007; Harrington & Reeder, 2017; Lee & Caldwell, 1998; Zaher, 1998; Zaher & Rieppel, 1999; Zaher & Rieppel, 2002).

On a similar note, this intermediate status of "anilioids" may suggest that their jaw complex ought to be considered homologous to the non-snake lizard condition, that is, grouped under the same morphotype due to the shared presence of robust features. However, as outlined above, a number of key character states do differ between non-snake lizards and "anilioids," in turn reflecting the distinct functional nature of the uropeltoid and amerophidian jaw complex (e.g., the ability for "snout-shifting") compared to that of non-snake lizards (Figures 3–8; Tables 3 and 4). Because of these consistent homological and functional differences between the non-snake lizard and early-diverging alethinophidian jaw mechanisms, these conditions therefore cannot be considered directly homologous; although hypotheses of the "anilioid" condition as representing an evolutionarily intermediate stage between non-snake lizards and "macrostomatan" snakes are possible, any such hypothesis must recognize the distinct nature of the "anilioid" skull. Other studies have similarly cautioned against drawing direct parallels between "anilioids" and non-snake lizards (e.g., Harrington & Reeder, 2017).

Finally, an important clarification to this discussion of homology is that synapomorphies can only be fully corroborated by the "test of congruence" sensu Patterson (1982, 1988), a test requiring rigorous phylogenetic analysis and thus falling beyond the scope of the current study. Although we do not perform this test herein, the rejection of homology at the level of character state identity for several key features means that we *can* definitively deem these conditions—and, by extension, their morphotypes of "microstomy"—as nonhomologous and nonsynapomorphic. Essentially, our perspective that the jaw complexes in non-snake lizards, early-diverging alethinophidians, and the scolecophidian lineages are not primary homologs by definition precludes them from being secondary homologs, that is, synapomorphic.

A related caveat applies to "snout-shifting" snakes. Amerophidians and uropeltoids both possess the character states comprising this morphotype, thus satisfying the test of primary homology. However, under the current phylogenetic framework (Figures 1 and 2), two evolutionary scenarios for this morphotype are equally possible: either each constituent character state—and thus the overall "snout-shifting" morphotype—arose once at the base of Alethinophidia and was subsequently lost in caenophidians and booid-pythonoids, meaning that "snout-shifting" is indeed a synapomorphy of uropeltoids and amerophidians and the plesiomorphic state for Alethinophidia (e.g., Figure 14a); or "snout-shifting" arose independently in Amerophidia and Uropeltoidea, and is in fact convergent (e.g., Figure 13b). It is therefore currently ambiguous as to whether this morphotype

would pass the test of congruence. However, the fossil evidence presented above, combined with the presence of numerous consistent character states in such distantly-related lineages—not least of which is an unusual morphological innovation, the "ball-and-socket"-like maxilla-palatine joint—in our view favors the interpretation of this morphotype as indeed homologous across these early-diverging alethinophidian clades, reflecting an ancestral snake morphology.

4.4 | Variation within morphotypes

As a final note when considering the homology of "microstomy" across squamates, the anatomical variants discussed in Sections 3.1.4 and 3.2.4 raise the question of whether it is appropriate to include the taxa in question (dibamids and amphisbaenians, and *Anomochilus* and *Uropeltis*) under the same morphotype as other non-snake lizards and other early-diverging alethinophidians, respectively. As mentioned in Section 4.1, when considering the homology of entire morphofunctional complexes, it is inevitable that some variation will arise due to the taxonomic breadth of each morphotype and thus must be allowed and accounted for. For the taxa mentioned above, although certain features may vary relative to their respective morphotypes, ultimately these taxa do remain consistent with these overall morphotypes.

For all of these taxa, many of the differences they exhibit compared to other non-snake lizards or "anilioids" are paedomorphic. In this case, these paedomorphic features mainly include the absence or drastic reduction of elements (e.g., supratemporal, squamosal, ectopterygoid; Figures 5 and 6), which can be recognized as paedomorphic by comparison to the typical, well-developed condition of these elements in other squamates (e.g., see Ollonen et al., 2018; Polachowski & Werneburg, 2013; Werneburg et al., 2015). Anterior displacement of the jaw suspension and anteroventral orientation of the quadrate (Figures 5 and 6) are also paedomorphic traits, common among miniaturized vertebrates (Olori & Bell, 2012; Strong et al., 2021) and reflecting retention of the embryonic condition of the suspensorium in squamates (Kamal, 1966; Kley, 2006; Rieppel & Zaher, 2000; Scanferla, 2016). This paedomorphosis is likely tied to miniaturization (Maddin et al., 2011; Olori & Bell, 2012; Rieppel, 1984; Rieppel & Maisano, 2007), as dibamids, *Anomochilus*, and uropeltids have all been recognized as miniaturized (e.g., Olori & Bell, 2012; Rieppel, 1984), and developmental truncation has been hypothesized as one of the main processes by which such drastic size reduction occurs (Hanken, 1984).

Other features, such as the structure of the suspensorium (Figures 5 and 6), are also common among miniaturized and fossorial taxa (see also Evans, 2008; Maddin et al., 2011; Rieppel, 1984). Similarly, features such as the more tightly integrated premaxilla and prefrontal in *Anomochilus* and *Uropeltis*, as well as the laterally enclosed braincase in dibamids and amphisbaenians, are logical consequences of fossoriality in these taxa (Cundall & Rossman, 1993). Miniaturization may also play a role, as elements must be more compactly arranged in a smaller skull, resulting in tighter integration relative to nonminiaturized taxa.

In light of these phenomena, it is reasonable to hypothesize the derivation of the dibamid or amphisbaenian skull from a more "typical" non-snake lizard morphotype via miniaturization- and/or fossoriality-related paedomorphosis, or the derivation of the skull of *Anomochilus* or *Uropeltis* from a more "typical" uropeltoid condition in a similar manner. As in scolecophidians, features susceptible to homoplasy—such as those related to fossoriality, miniaturization, and paedomorphosis—must be taken into account and recognized as superimposing potentially misleading features upon the morphology in question. For scolecophidians, this means recognizing these potentially homoplastic features as quite weak evidence for synapomorphy or homology (see Section 4.2); for dibamids, amphisbaenians, and paedomorphic uropeltoids, this means recognizing this homoplasy as a likely independent superimposition overtop the core morphotype in question. After accounting for such phenomena as miniaturization and fossoriality, the dibamid and amphisbaenian skulls otherwise share several conditions with other non-snake lizards, and the same is true for *Anomochilus* and *Uropeltis* in comparison to other "anilioids" (see Sections 3.1.4 and 3.2.4). In contrast, after taking these phenomena into account for scolecophidians, the jaw complexes are still fundamentally different, justifying separate morphotypes. Accounting for these phenomena is therefore essential in recognizing and accounting for homoplasy when evaluating the homology of character complexes.

Of these taxa, *Anomochilus* most prominently displays a unique skull structure that is not easily referable to any of the main morphotypes. As described by Cundall and Rossman (1993), the skull of *Anomochilus* is unique among snakes, having been proposed as an intermediate between scolecophidians and alethinophidians. One of the most unique features of *Anomochilus* is its palatomaxillary structure: the maxilla is reduced compared to other "anilioids," especially in anteroposterior length, and does not contact the reduced ectopterygoid (Cundall & Rossman, 1993; Rieppel & Maisano, 2007). This would suggest different palatomaxillary

biomechanics, as movement of the maxilla would presumably be driven only by the palatine, with which it articulates medially (Cundall & Rossman, 1993). This is reminiscent of "maxillary raking" as occurs in some scolecophidians.

However, the rest of the jaws and suspensorium differ sufficiently from scolecophidians—and molecular evidence places *Anomochilus* firmly within the Uropeltoidea, possibly as sister to Cylindrophiidae (Pyron et al., 2013)—such that we consider this similarity convergent, driven by paedomorphosis affecting the ectopterygoid and maxilla in *Anomochilus*, rather than modification from a "maxillary raking" scolecophidian ancestor. Cundall and Rossman (1993) similarly reject the possibility that *Anomochilus* and scolecophidians (in their discussion, specifically typhlopids) share a homologous feeding mechanism. Ultimately, the exact nature and phylogenetic position of *Anomochilus* requires its own detailed treatment, beyond the scope of the current paper. However, following the effects of paedomorphosis and fossoriality as discussed above, and in light of previous morphological analyses supporting the uropeltoid affinities of *Anomochilus* (e.g., Rieppel & Maisano, 2007) and genetic evidence affirming this conclusion (e.g., Pyron et al., 2013), we consider it most reasonable to classify *Anomochilus* as a modified "snout-shifting" taxon.

Finally, many morphological phylogenies often recover dibamids, amphisbaenians, and snakes as part of a clade of fossorial and/or limb-reduced taxa (e.g., the Scincophidia of Conrad, 2008). Indeed, certain features are consistent among these taxa; for example, the suspensorium in dibamids and amphisbaenians (Figures 5 and 6; Section 3.1) is quite similar to the condition in scolecophidians (Figures 9–11; Sections 3.4–3.6), particularly regarding the extreme reduction of the supratemporal and anterior orientation of the quadrate. However, as noted above, these features likely result from miniaturization-driven paedomorphosis (Maddin et al., 2011; Olori & Bell, 2012; Rieppel, 1984). Given that miniaturization, paedomorphosis, and fossoriality are often associated with homoplasy (Fröbisch & Schoch, 2009; Hanken & Wake, 1993; Maddin et al., 2011; Rieppel, 1984, 1988; Wiens et al., 2005), and the fact that amphisbaenians, dibamids, and scolecophidians are not considered to be closely related in most recent phylogenies (e.g., Burbrink et al., 2020; Reeder et al., 2015; Simões et al., 2018; Wiens et al., 2010), these similarities are therefore almost certainly driven by the independent evolution of miniaturization and fossoriality in these groups. This conclusion is consistent with previous arguments that the recovery of a "fossorial clade" is simply the result of a homoplastic fossorial ecomorph evolving convergently in these taxa (e.g., Lee, 1998; Rieppel, 1988). The numerous ways in which the amphisbaenian or dibamid skull differs from that of scolecophidians—especially regarding the robustness and degree of integration of the jaw elements (Figures 5, 6, and 9–11)—support the hypothesis that these similarities are convergent, rather than reflecting that the scolecophidian jaw condition is strictly homologous to, or a retention of, the dibamid or amphisbaenian condition.

4.5 | Ancestral state reconstruction

The overarching outcome of our ASRs is that different hypotheses of homology result in very different reconstructions of key nodes (Figures 12–14). For example, the ancestral snake node is definitively reconstructed as "microstomy" under the simplest scoring scheme (Figure 12), but is equivocal under both other schemes (Figures 13 and 14) under both ML and MP algorithms. Similarly, the ancestral alethinophidian node is variably reconstructed as definitively "microstomy" (Figure 12a) or "snout-shifting" (Figure 14a), very likely "macrostomy" (Figure 13b), or ambiguous (Figures 12b, 13a, and 14b).

Although it may seem a foregone conclusion that increasing the number of character states increases the uncertainty of reconstruction, such an outcome is not trivial. Simple approaches to reconstruction tend to produce correspondingly straightforward hypotheses of character evolution, such as "microstomy" as the definitive ancestral condition for snakes. However, scoring "microstomy" under a single state reflects an implicit assumption that this condition is directly comparable—that is, homologous—across the taxa in question. Once homology is explicitly assessed and character scoring adjusted to reflect this homology (or lack thereof), ASRs become more complicated, more ambiguous, and therefore less apparently informative. However, most importantly, these reconstructions also become more accurate, as they more closely reflect the biological reality of the conditions in question and thus provide a more realistic reconstruction of their evolution.

Arguably, to provide the most realistic reconstruction of ancestral nodes, any semblance of morphotypes or overarching character complexes should be eliminated altogether, and each character should instead be reconstructed separately (e.g., the "reductive coding" approach of Wilkinson, 1995). Indeed, such an approach is essential in reconstructing hypothetical transitional taxa, that is, nodes bearing novel combinations of character states (Wilkinson, 1995). However, this method is not without flaws. For example, how much atomization is

enough, or is too much (Wilkinson, 1995)? Are these novel trait combinations plausible, or even biologically possible? Focusing on morphotypes—rather than individual characters—avoids these issues, as this concept involves accurately conceptualizing morphofunctional systems without sacrificing their inherent integration and complexity. Ultimately, both approaches to ASR have merit, with the morphotype concept in particular avoiding both the under-atomization (e.g., treating "microstomy" as homogenous) and over-atomization (e.g., as may occur in "reductive coding") of complex morphofunctional systems.

Conversely, one could instead argue that our more complex scoring methods essentially "over-separate" microstomy into so many states as to be uninformative. For example, what if the purpose of the analysis is simply to determine if the ancestral snake was "some kind of microstomatan" versus "some kind of macrostomatan," regardless of the specific morphology of this condition? In this case, would it not be acceptable to simply score taxa as "microstomy" versus "macrostomy"? Such an approach, however, is untenable, and would be similar to the problems created, for example, by using the term "big wing" versus "small wing" in systematizing birds using wing size. In any examination of the evolution of a character and its states, the anatomy in all of its details must take primacy (Rieppel & Kearney, 2002; Simões et al., 2017; Wilkinson, 1995). Hypotheses regarding character evolution must be constructed using a "bottom-up" approach, that is, starting with assessments of fundamental homology and building from this starting point. "Top-down" approaches—that is, lumping various conditions together from the outset, and only later considering nonhomology—represent a theoretically "backward" approach to the study of character evolution.

The fallacy of this approach is especially true when it results in hypotheses that taxa such as scolecophidians are plesiomorphically "retaining" ancestral conditions (e.g., Miralles et al., 2018). Of note, Harrington and Reeder (2017) also scored all taxa as simply "macrostomy" or "nonmacrostomy" in their analysis of snake morphotype evolution. However, following their ASR, they did critically examine the relevant morphologies in a manner similar to that recommended by Griffith et al. (2015), ultimately concluding that the scolecophidian morphotype is not representative of the ancestral snake condition and in fact may have evolved convergently (Harrington & Reeder, 2017). We commend this comparative anatomical perspective, with our results supporting these authors' conclusions. However, in order to be fully theoretically sound, this assessment of homology should be performed prior to the analysis—that is, when delimiting character states—rather than afterward.

Critical examination of primary homology prior to reconstructing ancestral states is indeed crucial: non-homologous conditions cannot be included under the same character or state in a phylogenetic analysis (Rieppel & Kearney, 2002; Simões et al., 2017), a principle which logically must also apply to ASRs. To do otherwise is to equate conditions which are fundamentally incomparable, creating an artificial category—in this case, of uniform "microstomy"—without reflecting the morphological nuance associated with this condition. Just as Simões et al. (2017:200) caution against "naïve connectivity" in the employment of the "test of similarity," we caution against the issue of "naïve homology" when comparing character complexes across taxa. Admittedly, for certain conditions (e.g., diel activity pattern, biome, aquatic habits, prey preference: Hsiang et al., 2015; limb reduction: Harrington & Reeder, 2017), primary homology is difficult or impossible to assess; as such, it is often unavoidable to group each of these conditions under the same overarching character state. However, for a condition such as microstomy, for which homology can be thoroughly assessed, conflating non-homologous conditions introduces substantive, not to mention unnecessary, logical error into the analysis. We therefore advocate the importance of a thorough comparative anatomical approach when formulating hypotheses regarding evolution (see also Rieppel & Kearney, 2002; Simões et al., 2017). This echoes recent discussions that ASRs should not be an analytical endpoint, but rather should be treated as hypotheses to be rigorously assessed in their own right (Griffith et al., 2015).

Although the present study focuses on "microstomy," the concept of "macrostomy" is equally in need of re-examination. Recent authors have suggested that the versions of "macrostomy" present in booid-pythonoids and caenophidians may have evolved independently, based on both molecular (Burbrink et al., 2020) and ontogenetic (Palci et al., 2016) evidence. Furthermore, even within each of these groups, different variations of macrostomy may have arisen convergently (Caldwell, 2019; Strong et al., 2019). Similarly, although specimens of tropidophiids were not available for the present study, this family is particularly worthy of attention: recent phylogenies (e.g., Burbrink et al., 2020) have recovered these "macrostomatans" as the sister group to Aniliidae within the Amerophidia, an early-diverging placement in turn suggesting that macrostomy may have evolved earlier among snakes than is often recognized, including within our own ASRs (Figures 12–14). Therefore, much like the conflation of "microstomy" as a uniform character state is inaccurate, as presented herein, the conflation of "macrostomy" in a similar manner may also be incorrect. Our scoring methods include "macrostomy" as both single

and separate morphotypes in order to recognize this uncertainty; however, a detailed re-examination of macrostomy very much requires its own treatment, so as to better understand the complexity of this feeding mechanism and its evolution.

Finally, this ASR is not an attempt to definitively determine the ancestral snake morphology. Indeed, certain aspects of our analysis—particularly regarding limited sampling of "macrostomatans" (given our focus on microstomy) and no sampling of extinct taxa (given our chosen phylogenetic framework)—largely preclude such a definitive determination of such a complex problem. Rather, our aim was to assess the impact that different perspectives on homology and morphology might have in shaping higher-level hypotheses of character and taxon evolution, as examined above.

As for future studies which do aim to definitively reconstruct the "ancestral snake morphology," the inclusion of extinct taxa is a particularly crucial component. Data from fossils have consistently been shown to improve ASRs by providing critical information not reflected by extant taxa, such as taxonomic diversity, character state distributions, unique character states or state combinations, and impact upon the phylogeny itself on which the ASR is based (Betancur-R et al., 2015; Caldwell, 2019; Finarelli & Flynn, 2006; Finarelli & Goswami, 2013; Mongiardino Koch & Parry, 2020; Puttick, 2016). Exceptionally preserved snake fossils, such as recently described specimens of *Najash* (Garberoglio, Apesteguía, et al., 2019; Garberoglio, Gómez, et al., 2019), are particularly promising in allowing the detailed anatomical analysis necessary for accurate reconstructions. We therefore encourage the inclusion of extinct taxa alongside thorough comparative anatomical analysis in future attempts at reconstructing the "ancestral snake morphology."

ORCID
Catherine R. C. Strong https://orcid.org/0000-0002-6080-9245
Mark D. Scherz https://orcid.org/0000-0002-4613-7761
Michael W. Caldwell https://orcid.org/0000-0002-2377-3925

REFERENCES
Al-Mohammadi, A. G. A., Khannoon, E. R., & Evans, S. E. (2020). The development of the osteocranium in the snake *Psammophis sibilans* (Serpentes: Lamprophiidae). *Journal of Anatomy*, *236*, 117–131.

Apesteguía, S., & Zaher, H. (2006). A cretaceous terrestrial snake with robust hindlimbs and a sacrum. *Nature*, *440*, 1037–1040.

Asplen, M. K., Whitfield, J. B., de Boer, J. G., & Heimpel, G. E. (2009). Ancestral state reconstruction analysis of hymenopteran sex determination mechanisms. *Journal of Evolutionary Biology*, *22*, 1762–1769.

Bellairs, A. D., & Underwood, G. (1951). The origin of snakes. *Biological Reviews*, *26*, 193–237.

Betancur-R, R., Ortí, G., & Pyron, R. A. (2015). Fossil-based comparative analyses reveal ancient marine ancestry erased by extinction in ray-finned fishes. *Ecology Letters*, *18*, 441–450.

Brock, G. T. (1932). The skull of *Leptotyphlops* (*Glauconia nigricans*). *Anatomischer Anzeiger*, *73*, 199–204.

Brower, A. V. Z., & Schawaroch, V. (1996). Three steps of homology assessment. *Cladistics*, *12*, 265–272.

Burbrink, F. T., Grazziotin, F. G., Pyron, R. A., Cundall, D., Donnellan, S., Irish, F., … Zaher, H. (2020). Interrogating genomic-scale data for Squamata (lizards, snakes, and amphisbaenians) shows no support for key traditional morphological relationships. *Systematic Biology*, *69*, 502–520.

Caldwell, M. W. (2000). On the phylogenetic relationships of *Pachyrhachis* within snakes: A response to Zaher (1998). *Journal of Vertebrate Paleontology*, *20*, 187–190.

Caldwell, M. W. (2007). The role, impact, and importance of fossils: Snake phylogeny, origins, and evolution (1869–2006). In J. Anderson & H.-D. Sues (Eds.), *Major transitions in vertebrate evolution* (pp. 253–302). Bloomington, Indiana: Indiana University Press.

Caldwell, M. W. (2019). *The origin of snakes: Morphology and the fossil record*. Boca Raton, FL: Taylor & Francis.

Campbell, J. A., Smith, E. N., & Hall, A. S. (2018). Caudals and calyces: The curious case of a consumed Chiapan colubroid. *Journal of Herpetology*, *52*, 459–472.

Chretien, J., Wang-Claypool, C. Y., Glaw, F., & Scherz, M. D. (2019). The bizarre skull of *Xenotyphlops* sheds light on synapomorphies of Typhlopoidea. *Journal of Anatomy*, *234*, 637–655.

Conrad, J. L. (2008). Phylogeny and systematics of Squamata (Reptilia) based on morphology. *Bulletin of the American Museum of Natural History*, *310*, 1–182.

Cundall, D. (1995). Feeding behaviour in *Cylindrophis* and its bearing on the evolution of alethinophidian snakes. *Journal of Zoology*, *237*, 353–376.

Cundall, D., & Irish, F. (2008). The snake skull. In C. Gans, A. S. Gaunt, & K. Adler (Eds.), *Biology of the reptilia: Morphology H, the skull of lepidosauria* (pp. 349–692). Ithaca, New York: Society for the Study of Amphibian and Reptiles.

Cundall, D., & Rossman, D. A. (1993). Cephalic anatomy of the rare Indonesian snake *Anomochilus weberi*. *Zoological Journal of the Linnean Society*, *109*, 235–273.

Da Silva, F. O., Fabre, A.-C., Savriama, Y., Ollonen, J., Mahlow, K., Herrel, A., … Di-Poï, N. (2018). The ecological origins of snakes as revealed by skull evolution. *Nature Communications*, *9*, 376.

de Pinna, M. G. G. (1991). Concepts and tests of homology in the cladistic paradigm. *Cladistics*, *7*, 367–394.

Dragonfly 4.0. 2019. http://www.theobjects.com/dragonfly

Evans, H. E. (1955). The osteology of a worm snake, *Typhlops jamaicensis* (Shaw). *The Anatomical Record*, *122*, 381–396.

Evans, S. E. (2008). The skull of lizards and tuatara. In C. Gans, A. S. Gaunt, & K. Adler (Eds.), *Biology of the reptilia. The skull of lepidosauria* (Vol. 20, pp. 1–347). Ithaca: Society for the Study of Amphibians and Reptiles.

Figueroa, A., McKelvy, A. D., Grismer, L. L., Bell, C. D., & Lailvaux, S. P. (2016). A species-level phylogeny of extant snakes with description of a new colubrid subfamily and genus. *PLoS One*, *11*, e0161070.

Finarelli, J. A., & Flynn, J. J. (2006). Ancestral state reconstruction of body size in the Caniformia (Carnivora, Mammalia): The effects of incorporating data from the fossil record. *Systematic Biology*, *55*, 301–313.

Finarelli, J. A., & Goswami, A. (2013). Potential pitfalls of reconstructing deep time evolutionary history with only extant data, a case study using the Canidae (Mammalia, Carnivora). *Evolution*, *67*, 3678–3685.

Frazzetta, T. H. (1962). A functional consideration of cranial kinesis in lizards. *Journal of Morphology*, *111*, 287–319.

Fröbisch, N. B., & Schoch, R. R. (2009). Testing the impact of miniaturization on phylogeny: Paleozoic dissorophoid amphibians. *Systematic Biology*, *58*, 312–327.

Gans, C., & Montero, R. (2008). An atlas of amphisbaenian skull anatomy. In C. Gans, A. S. Gaunt, & K. Adler (Eds.), *Biology of the Reptilia. Morphology I. The skull and appendicular locomotor apparatus of lepidosauria* (Vol. 21, pp. 621–738). Ithaca, New York: Society for the Study of Amphibians and Reptiles.

Garberoglio, F. F., Apesteguía, S., Simões, T. R., Palci, A., Gómez, R. O., Nydam, R. L., ... Caldwell, M. W. (2019). New skulls and skeletons of the cretaceous legged snake *Najash*, and the evolution of the modern snake body plan. *Science Advances*, *5*, eaax5833.

Garberoglio, F. F., Gómez, R. O., Apesteguía, S., Caldwell, M. W., Sánchez, M. L., & Veiga, G. (2019). A new specimen with skull and vertebrae of *Najash rionegrina* (Lepidosauria: Ophidia) from the early late cretaceous of Patagonia. *Journal of Systematic Palaeontology*, *17*, 1533–1550.

Gauthier, J. A., Kearney, M., Maisano, J. A., Rieppel, O., & Behlke, A. D. B. (2012). Assembling the squamate tree of life: Perspectives from the phenotype and the fossil record. *Bulletin of the Peabody Museum of Natural History*, *53*, 3–308.

Greer, A. E. (1985). The relationships of the lizard genera *Anelytropsis* and *Dibamus*. *Journal of Herpetology*, *19*, 116–156.

Griffith, O. W., Blackburn, D. G., Brandley, M. C., van Dyke, J. U., Whittington, C. M., & Thompson, M. B. (2015). Ancestral state reconstructions require biological evidence to test evolutionary hypotheses: A case study examining the evolution of reproductive mode in squamate reptiles. *Journal of Experimental Zoology. Part B, Molecular and Developmental Evolution*, *324B*, 493–503.

Haas, G. (1930). Über das Kopfskelett und die Kaumuskulatur der Typhlopiden und Glauconiiden. *Zoologische Jahrbücher Abteilung für Anatomie*, *52*, 1–94.

Haas, G. (1964). Anatomical observations on the head of *Liotyphlops albirostris* (Typhlopidae, Ophidia). *Acta Zoologica*, *1964*, 1–62.

Haas, G. (1968). Anatomical observations on the head of *Anomalepis aspinosus* (Typhlopidae, Ophidia). *Acta Zoologica*, *48*, 63–139.

Hanken, J. (1984). Miniaturization and its effects on cranial morphology in plethodontid salamanders, genus *Thorius* (Amphibia: Plethodontidae). I. Osteological variation. *Biological Journal of the Linnean Society*, *23*, 55–75.

Hanken, J., & Wake, D. B. (1993). Miniaturization of body size: Organismal consequences and evolutionary significance. *Annual Review of Ecology and Systematics*, *24*, 501–519.

Harrington, S. M., & Reeder, T. W. (2017). Phylogenetic inference and divergence dating of snakes using molecules, morphology and fossils: New insights into convergent evolution of feeding morphology and limb reduction. *Biological Journal of the Linnean Society*, *121*, 379–394.

Hawkins, J. A., Hughes, C. E., & Scotland, R. W. (1997). Primary homology assessment, characters and character states. *Cladistics*, *13*, 275–283.

Hawlitschek, O., Scherz, M. D., Webster, K. C., Ineich, I., & Glaw, F. (2021). Morphological, osteological, and genetic data support a new species of *Madatyphlops* (Serpentes: Typhlopidae) endemic to Mayotte Island, Comoros archipelago. *The Anatomical Record*, *2021*, 1–15.

Hsiang, A. Y., Field, D. J., Webster, T. H., Behlke, A. D. B., Davis, M. B., Racicot, R. A., & Gauthier, J. A. (2015). The origin of snakes: Revealing the ecology, behavior, and evolutionary history of early snakes using genomics, phenomics, and the fossil record. *BMC Evolutionary Biology*, *15*, 87.

Iordansky, N. N. (1997). Jaw apparatus and feeding mechanics of *Typhlops* (Ophidia: Typhlopidae): A reconsideration. *Russian Journal of Herpetology*, *4*, 120–127.

Kamal, A. M. (1966). On the process of rotation of the quadrate cartilage in Ophidia. *Anatomischer Anzeiger*, *118*, 87–90.

Kearney, M., & Stuart, B. L. (2004). Repeated evolution of limblessness and digging heads in worm lizards revealed by DNA from old bones. *Proceedings of the Royal Society of London. Series B, Biological sciences*, *271*, 1677–1683.

Kley, N. J. (2001). Prey transport mechanisms in blindsnakes and the evolution of unilateral feeding systems in snakes. *American Zoologist*, *41*, 1321–1337.

Kley, N. J. (2006). Morphology of the lower jaw and suspensorium in the Texas blindsnake, *Leptotyphlops dulcis* (Scolecophidia: Leptotyphlopidae). *Journal of Morphology*, *267*, 494–515.

Kley, N. J., & Brainerd, E. L. (1999). Feeding by mandibular raking in a snake. *Nature*, *402*, 369–370.

Kraus, F. (2017). New species of blindsnakes (Squamata: Gerrhopilidae) from the offshore islands of Papua New Guinea. *Zootaxa*, *4299*, 75–94.

Lee, M. S. Y. (1998). Convergent evolution and character correlation in burrowing reptiles: Towards a resolution of squamate relationships. *Biological Journal of the Linnean Society*, *65*, 369–453.

Lee, M. S. Y., & Caldwell, M. W. (1998). Anatomy and relationships of *Pachyrhachis problematicus*, a primitive snake with hindlimbs. *Philosophical Transactions of the Royal Society, Series B: Biological Sciences*, *353*, 1521–1552.

Lewis, P. O. (2001). A likelihood approach to estimating phylogeny from discrete morphological character data. *Systematic Biology*, *50*, 913–925.

List, J. C. (1966). Comparative osteology of the snake families typhlopidae and leptotyphlopidae. *Illinois Biological Monographs*, *36*, 1–112.

Mabee, P. M., Balhoff, J. P., Dahdul, W. M., Lapp, H., Mungall, C. J., & Vision, T. J. (2020). A logical model of homology for comparative biology. *Systematic Biology*, *69*, 345–362.

Maddin, H. C., Olori, J. C., & Anderson, J. S. (2011). A redescription of *Carrolla craddocki* (Lepospondyli: Brachystelechidae) based on high-resolution CT, and the impacts of miniaturization and fossoriality on morphology. *Journal of Morphology*, *272*, 722–743.

Maddison, W. P., Maddison, D. R. (2006). StochChar: a package of Mesquite modules for stochastic models of character evolution. Version 1.1.

Maddison, W. P., Maddison, D. R. (2019). Mesquite: a modular system for evolutionary analysis. Version 3.61. http://mesquite project.org

Mahendra, B. C. (1936). Contributions to the osteology of the Ophidia. I. the endoskeleton of the so-called 'blind-snake', *Typhlops braminus* Daud. *Proceedings of the Indian Academy of Sciences*, *3*, 128–142.

Martins, A., Koch, C., Pinto, R., Folly, M., Fouquet, A., & Passos, P. (2019). From the inside out: Discovery of a new genus of threadsnakes based on anatomical and molecular data, with discussion of the leptotyphlopid hemipenial morphology. *Journal of Zoological Systematics and Evolutionary Research*, *57*, 840–863.

McDowell, S. B., & Bogert, C. M. (1954). The systematic position of *Lanthanotus* and the affinities of the anguimorphan lizards. *Bulletin of the American Museum of Natural History*, *105*, 1–142.

McNamara, K. J. (1986). A guide to the nomenclature of heterochrony. *Journal of Paleontology*, *60*, 4–13.

Miralles, A., Marin, J., Markus, D., Herrel, A., Hedges, S. B., & Vidal, N. (2018). Molecular evidence for the paraphyly of Scolecophidia and its evolutionary implications. *Journal of Evolutionary Biology*, *31*, 1782–1793.

Mongiardino Koch, N., & Parry, L. A. (2020). Death is on our side: Paleontological data drastically modify phylogenetic hypotheses. *Systematic Biology*, *69*, 1052–1067.

Nagy, Z. T., Marion, A. B., Glaw, F., Miralles, A., Nopper, J., Vences, M., & Hedges, S. B. (2015). Molecular systematics and undescribed diversity of Madagascan scolecophidian snakes (Squamata: Serpentes). *Zootaxa*, *4040*, 31–47.

Ollonen, J., Silva, F. O. D., Mahlow, K., & Di-Poï, N. (2018). Skull development, ossification pattern, and adult shape in the emerging lizard model organism *Pogona vitticeps*: A comparative analysis with other squamates. *Frontiers in Physiology*, *9*, 278.

Olori, J. C., & Bell, C. J. (2012). Comparative skull morphology of uropeltid snakes (Alethinophidia: Uropeltidae) with special reference to disarticulated elements and variation. *PLoS One*, *7*, e32450.

Palci, A., Caldwell, M. W., Hutchinson, M. N., Konishi, T., & Lee, M. S. Y. (2020). The morphological diversity of the quadrate bone in squamate reptiles as revealed by high-resolution computed tomography and geometric morphometrics. *Journal of Anatomy*, *236*, 210–227.

Palci, A., Lee, M. S. Y., & Hutchinson, M. N. (2016). Patterns of postnatal ontogeny of the skull and lower jaw of snakes as revealed by micro-CT scan data and three-dimensional geometric morphometrics. *Journal of Anatomy*, *229*, 723–754.

Patterson, C. (1982). Morphological characters and homology. In K. A. Joysey & A. E. Friday (Eds.), *Problems of phylogenetic reconstruction* (pp. 21–74). London and New York: Academic Press.

Patterson, C. (1988). Homology in classical and molecular biology. *Molecular Biology and Evolution*, *5*, 603–625.

Pinto, R. R., Martins, A. R., Curcio, F., & Ramos, L. O. (2015). Osteology and cartilaginous elements of *Trilepida salgueiroi* (Amaral, 1954) (Scolecophidia: Leptotyphlopidae). *The Anatomical Record*, *298*, 1722–1747.

Polachowski, K. M., & Werneburg, I. (2013). Late embryos and bony skull development in *Bothropoides jararaca* (Serpentes, Viperidae). *Zoology*, *116*, 36–63.

Puttick, M. N. (2016). Partially incorrect fossil data augment analyses of discrete trait evolution in living species. *Biology Letters*, *12*, 20160392.

Pyron, R. A., Burbrink, F. T., & Wiens, J. J. (2013). A phylogeny and revised classification of Squamata, including 4161 species of lizards and snakes. *BMC Evolutionary Biology*, *13*, 93.

Reeder, T. W., Townsend, T. M., Mulcahy, D. G., Noonan, B. P., Wood, P. L., Sites, J. W., & Wiens, J. J. (2015). Integrated analyses resolve conflicts over squamate reptile phylogeny and reveal unexpected placements for fossil taxa. *PLoS One*, *10*, e0118199.

Rieppel, O. (1977). Studies on the skull of the Henophidia (Reptilia: Serpentes). *Journal of Zoology*, *181*, 145–173.

Rieppel, O. (1984). The cranial morphology of the fossorial lizard genus *Dibamus* with a consideration of its phylogenetic relationships. *Journal of Zoology*, *204*, 289–327.

Rieppel, O. (1988). A review of the origin of snakes. In M. K. Hecht, B. Wallace, & G. T. Prance (Eds.), *Evolutionary biology* (pp. 37–130). Boston, MA: Springer.

Rieppel, O. (1994). Homology, topology, and typology: The history of modern debates. In B. K. Hall (Ed.), *Homology: The hierarchical basis of comparative biology* (pp. 63–100). San Diego: Academic Press.

Rieppel, O. (2012). "Regressed" macrostomatan snakes. *Fieldiana Life and Earth Sciences*, *2012*, 99–103.

Rieppel, O., & Kearney, M. (2002). Similarity. *Biological Journal of the Linnean Society*, *75*, 59–82.

Rieppel, O., Kley, N. J., & Maisano, J. A. (2009). Morphology of the skull of the white-nosed blindsnake, *Liotyphlops albirostris* (Scolecophidia: Anomalepididae). *Journal of Morphology*, *270*, 536–557.

Rieppel, O., & Maisano, J. A. (2007). The skull of the rare Malaysian snake *Anomochilus leonardi* Smith, based on high-resolution X-ray computed tomography. *Zoological Journal of the Linnean Society*, *149*, 671–685.

Rieppel, O., & Zaher, H. (2000). The intramandibular joint in squamates, and the phylogenetic relationships of the fossil snake *Pachyrhachis problematicus* Haas. *Fieldiana Geology*, *43*, 1–69.

Santos, F. J. M., & Reis, R. E. (2019). Redescription of the blind snake *Anomalepis Colombia* (Serpentes: Anomalepididae) using high-resolution X-ray computed tomography. *Copeia*, *107*, 239–243.

Scanferla, A. (2016). Postnatal ontogeny and the evolution of macrostomy in snakes. *Royal Society Open Science*, *3*, 160612.

Sereno, P. C. (2007). Logical basis for morphological characters in phylogenetics. *Cladistics*, *23*, 565–587.

Simões, T. R., Caldwell, M. W., Palci, A., & Nydam, R. L. (2017). Giant taxon-character matrices: Quality of character constructions remains critical regardless of size. *Cladistics*, *33*, 198–219.

Simões, T. R., Caldwell, M. W., Tałanda, M., Bernardi, M., Palci, A., Vernygora, O., ... Nydam, R. L. (2018). The origin of squamates revealed by a middle Triassic lizard from the Italian Alps. *Nature*, *557*, 706–709.

Strong, C. R. C., Palci, A., & Caldwell, M. W. (2021). Insights into skull evolution in fossorial snakes, as revealed by the cranial morphology of *Atractaspis irregularis* (Serpentes: Colubroidea). *Journal of Anatomy*, *238*, 146–172.

Strong, C. R. C., Simões, T. R., Caldwell, M. W., & Doschak, M. R. (2019). Cranial ontogeny of *Thamnophis radix* (Serpentes: Colubroidea) with a re-evaluation of current paradigms of snake skull evolution. *Royal Society Open Science*, *6*, 182228.

Struck, T. H. (2007). Data congruence, paedomorphosis and salamanders. *Frontiers in Zoology*, *4*, 22.

Wake, M. H. (1986). The morphology of *ldiocranium russeli* (Amphibia: Gymnophiona), with comments on miniaturization through heterochrony. *Journal of Morphology*, *189*, 1–16.

Werneburg, I., Polachowski, K. M., & Hutchinson, M. N. (2015). Bony skull development in the Argus monitor (Squamata, Varanidae, *Varanus panoptes*) with comments on developmental timing and adult anatomy. *Zoology*, *118*, 255–280.

Wiens, J. J., Bonett, R. M., & Chippindale, P. T. (2005). Ontogeny discombobulates phylogeny: Paedomorphosis and higher-level salamander relationships. *Systematic Biology*, *54*, 91–110.

Wiens, J. J., Kuczynski, C. A., Townsend, T. M., Reeder, T. W., Mulcahy, D. G., & Sites, J. W. J. (2010). Combining

phylogenomics and fossils in higher-level squamate reptile phylogeny: Molecular data change the placement of fossil taxa. *Systematic Biology*, 59, 674–688.

Wilkinson, M. (1995). A comparison of two methods of character construction. *Cladistics*, 11, 297–308.

Zaher, H. (1998). The phylogenetic position of *Pachyrhachis* within snakes (Squamata, Lepidosauria). *Journal of Vertebrate Paleontology*, 18, 1–3.

Zaher, H., & Rieppel, O. (1999). The phylogenetic relationships of *Pachyrhachis problematicus*, and the evolution of limblessness in snakes (Lepidosauria, Squamata). *Comptes Rendus de l'Académie des Sciences - Series IIA - Earth and Planetary Science*, 329, 831–837.

Zaher, H., & Rieppel, O. (2002). On the phylogenetic relationships of the cretaceous snakes with legs, with special reference to *Pachyrhachis problematicus* (Squamata, Serpentes). *Journal of Vertebrate Paleontology*, 22, 104–109.

Zheng, Y., & Wiens, J. J. (2016). Combining phylogenomic and supermatrix approaches, and a time-calibrated phylogeny for squamate reptiles (lizards and snakes) based on 52 genes and 4162 species. *Molecular Phylogenetics and Evolution*, 94, 537–547.

SUPPORTING INFORMATION

Additional supporting information may be found online in the Supporting Information section at the end of this article.